

**NEAR-REAL TIME RAINFALL ESTIMATION
USING APT DATA FROM NOAA SATELLITES
AND METEOROLOGICAL DATA**

Chonmapat Torasa

**A Thesis Submitted in Partial Fulfillment of the Requirements for the
Degree of Doctor of Philosophy in Geoinformatics**

Suranaree University of Technology

Academic Year 2009

การประมาณการฝนตกแบบใกล้เวลาจริงโดยใช้ข้อมูล APT
จากดาวเทียม NOAA และข้อมูลอุตุนิยมวิทยา

นายชนมภัทร โตรระสะ

วิทยานิพนธ์นี้เป็นส่วนหนึ่งของการศึกษาตามหลักสูตรปริญญาวิทยาศาสตรดุษฎีบัณฑิต
สาขาวิชาภูมิสารสนเทศ
มหาวิทยาลัยเทคโนโลยีสุรนารี
ปีการศึกษา 2552

**NEAR-REAL TIME RAINFALL ESTIMATION
USING APT DATA FROM NOAA SATELLITES
AND METEOROLOGICAL DATA**

Suranaree University of Technology has approved this thesis submitted in partial fulfillment of the requirements for the Degree of Doctor of Philosophy.

Thesis Examining Committee

(Asst. Prof. Dr. Suwit Ongsomwang)

Chairperson

(Asst. Prof. Dr. Sunya Sarapirome)

Member (Thesis Advisor)

(Asst. Prof. Dr. Songkot Dasananda)

Member

(Assoc. Prof. Dr. Kaew Nualchawee)

Member

(Dr. Dusadee Sukawat)

Member

(Prof. Dr. Sukit Limpijumnong)

Vice Rector for Academic Affairs

(Assoc. Prof. Dr. Prapan Manyum)

Dean of Institute of Science

ชนมภัทร โตรระสะ : การประมาณการฝนตกแบบใกล้เวลาจริงโดยใช้ข้อมูล APT จากดาวเทียม NOAA และข้อมูลอุตุนิยมวิทยา (NEAR-REAL TIME RAINFALL ESTIMATION USING APT DATA FROM NOAA SATELLITES AND METEOROLOGICAL DATA) อาจารย์ที่ปรึกษา : ผู้ช่วยศาสตราจารย์ ดร.สัญญา สราภิรมย์, 145 หน้า

งานวิจัยนี้มีวัตถุประสงค์เพื่อสร้างและติดตั้งระบบรับสัญญาณจากระบบส่งสัญญาณภาพอัตโนมัติ (Automatic Picture Transmission : APT) จากดาวเทียม NOAA และพัฒนาแบบจำลองการประมาณการฝนตกแบบใกล้เวลาจริงโดยใช้ข้อมูล APT ที่รับได้จากระบบรับสัญญาณที่สร้างขึ้นร่วมกับข้อมูลอุตุนิยมวิทยา

ระบบรับสัญญาณ APT ที่สร้างขึ้นประกอบด้วยสายอากาศแบบ Cross-dipole ตัวขยายสัญญาณวิทยุ (RF Pre-amplifier) เครื่องรับสัญญาณวิทยุ และคอมพิวเตอร์พีซีพร้อมโปรแกรมสำหรับถอดสัญญาณ APT ระบบรับสัญญาณ APT ติดตั้งที่กรุงเทพมหานคร ตั้งแต่ปี ค.ศ. 2004 สามารถรับสัญญาณ APT ได้อย่างถูกต้องในขณะที่ดาวเทียม NOAA โคจรผ่านประเทศไทย

แบบจำลองการประมาณการฝนตกแบบใกล้เวลาจริงนั้น ได้รับการพัฒนาขึ้นโดยใช้ข้อมูล brightness temperature (T_b) ที่ผ่านการแปลงรูป (reformat) จากค่า digital number (DN) ของภาพ APT ที่รับได้จากระบบรับสัญญาณที่สร้างขึ้น ร่วมกับข้อมูลความชื้นสัมพัทธ์ (relative humidity) และความกดอากาศ (air pressure) จากข้อมูล METAR ซึ่งสามารถประมาณการตำแหน่งฝนตก/ไม่ตกได้ และประมาณการปริมาณฝนตกที่สัมพันธ์กับพื้นที่โดยใช้ความสัมพันธ์ระหว่างค่า T_b กับปริมาณน้ำฝนจากสถานีตรวจอากาศกรมอุตุนิยมวิทยา ในปี ค.ศ. 2005 ค.ศ. 2006 และ ค.ศ. 2007 ทำการพัฒนา 4 แบบจำลองที่ได้ให้เป็นซอฟต์แวร์โมดูล และตรวจสอบแบบจำลองที่สร้างขึ้นกับข้อมูลฝนในพื้นที่กรุงเทพมหานครโดยใช้ภาพ APT ในปี ค.ศ. 2006 ค.ศ. 2007 และ ค.ศ. 2008 จำนวน 33 ภาพ ผลการตรวจสอบพบว่า แบบจำลองปี ค.ศ. 2006 ที่ใช้ค่าช่วงเวลา (time interval) แบบอัตราส่วน (Ratio) ในการหาปริมาณน้ำฝนจากเครื่องตรวจวัดแสงแดดได้ตั้งสมการ $Rainrate = 61887.18365 \exp^{(-x/19.17829)} + 0.9992$ เมื่อ x คืออุณหภูมิความสว่างมีหน่วยเป็นเคลวิน จะให้ผลดีที่สุดคือมีค่าผิดพลาดจากการประมาณการฝนตก/ไม่ตกเท่ากับ 11.270 เปอร์เซ็นต์ และค่าผิดพลาดของการประมาณการปริมาณฝน (RMSE) เท่ากับ 0.525 มิลลิเมตรต่อ 15 นาที

สาขาวิชาการรับรู้จากระยะไกล
ปีการศึกษา 2552

ลายมือชื่อนักศึกษา _____
ลายมือชื่ออาจารย์ที่ปรึกษา _____

CHONMAPAT TORASA : NEAR-REAL TIME RAINFALL ESTIMATION
USING APT DATA FROM NOAA SATELLITES AND
METEOROLOGICAL DATA. THESIS ADVISOR : ASST. PROF. SUNYA
SARAPIROME, Ph.D. 145 PP.

APT RECEIVING SYSTEM / APT DATA / NEAR-REAL TIME RAINFALL
ESTIMATION

The main objectives of this study were to assemble and construct Automatic Picture Transmission (APT) receiving system from NOAA satellite and develop near-real time rainfall model using APT data from the receiving system together with meteorological data.

The APT receiving system includes cross-dipole antenna, RF pre-amplifier, radio receiver and PC computer with APT decoding software. The APT receiving system has been installed at Bangkok since 2004. The system can receive APT signals properly while NOAA satellites are orbiting pass over Thailand.

Near-real time rainfall models were developed using brightness temperature (T_b) from reformatted Digital Number (DN) of APT data together with relative humidity and air pressure from METAR data. The models can be applied to determining raining condition (rain/no rain) and to rain rate estimation by using the relationships between T_b and rain rate recorded in years 2005, 2006, and 2007 from the Thai Meteorological Department stations. The 4 rainfall models were developed to be software module. The models were validated using rain data recorded within Bangkok area and 33 APT images in years 2006, 2007, and 2008. The result revealed

that the 2006 model with ratio time interval, which can be expressed as Rain rate = $61887.18365 \exp^{(-x/19.17829)} + 0.9992$, where x is brightness temperature in Kelvin, is the best. It shows 11.270 % rain condition error and 0.525 mm/15 minutes of rain rate RMSE.

School of Remote Sensing

Academic Year 2009

Student's Signature _____

Advisor's Signature _____

ACKNOWLEDGEMENT

This work is the result of study which takes many years to complete. By that time, I have worked with a great number of people whose contribution in many ways to the research. It is a pleasure to convey my gratitude to them all.

In the first place I would like to express profound gratitude to my advisor, Asst. Prof. Dr. Sunya Sarapirome for his supervision, advice, and guidance from the very early stage of this research. He provided me his precious time to discuss, continued encouragement and invaluable suggestions during this work. He is also helping me with the editing of the thesis. I am indebted to him more than he knows.

I would also like to thank all the thesis examination committee, Dr. Suwit Ongsomwang, Assoc. Prof. Dr. Kaew Nualchawee, Asst. Prof. Dr. Songkot Dasananda, and Dr. Dusadee Sukawat for their guidance and excellent suggestions during the thesis examination.

I would also like to thank the Department of Drainage and Sewerage, Bangkok Metropolitan and Thai Metrological Department, who support for rainfall data.

I would like to thank Mr. Piyorot Khongchuay, who helped me develop the MATLAB module.

A very special word of thanks goes for my family and Ms. Nichanant Sermsri, who have given me the extra strength and motivation to get things done. This thesis is dedicated to them.

Chonmapat Torasa

CONTENTS

	Page
ABSTRACT IN THAI.....	I
ABSTRACT IN ENGLISH.....	II
ACKNOWLEDGEMENT.....	IV
CONTENTS.....	V
LIST OF TABLES.....	X
LIST OF FIGURES.....	XIV
LIST OF ABBREVIATIONS.....	XVIII
LIST OF SYMBOLS.....	XX
CHAPTER	
I INTRODUCTION.....	1
1.1 Background problem and significance of the study.....	1
1.2 Objectives of the study.....	3
1.3 Scope and limitations of the study.....	3
1.4 Study area.....	4
II LITERATURE REVIEW.....	6
2.1 APT system.....	6
2.2 APT receiving system.....	7
2.3 APT data applications.....	11
2.4 Rainfall estimation researches.....	12

CONTENTS (Continued)

	Page
III RESEARCH METHODOLOGY	21
3.1 APT receiving system construction.....	21
3.1.1 APT receiving system assembly.....	21
3.1.2 APT receiving system installation.....	23
3.2 Data selection and preparation.....	24
3.2.1 APT data selection.....	24
3.2.2 APT data reformatting process.....	26
3.2.2.1 Data geo-referencing.....	27
3.2.2.2 Brightness temperature (T_b) determination.....	28
3.2.3 METAR data processing.....	29
3.2.4 Input data preparation for near-real time rainfall model.....	31
3.3 Near-real time rainfall model development.....	31
3.3.1 Climatic data analysis for raining condition.....	31
3.3.2 Rain rate estimation models formulation.....	32
3.3.3 MATLAB module development of near-real time rainfall models.....	33
3.4 Near-real time rainfall model validations.....	33
3.5 Equipments and data.....	35
IV RESULTS AND DISCUSSION	36
4.1 Installed APT receiving system.....	36
4.1.1 Assembled APT receiving system.....	36
4.1.2 Installed APT receiving system.....	38

CONTENTS (Continued)

	Page
4.2 Processed APT and METAR data	40
4.2.1 Selected APT data	40
4.2.2 Processed APT data	41
4.2.2.1 Geo-referenced APT images	41
4.2.2.2 Results of T_b determination	42
4.2.3 Processed METAR data	43
4.2.4 Input data for near-real time rainfall model	45
4.3 The developed near-real time rainfall model	45
4.3.1 Decision tree for raining condition analysis	45
4.3.2 Regression models for rain rate estimation	50
4.3.3 The developed MATLAB module for near-real time rainfall model	53
4.4 Results of near-real time rainfall model validation	57
4.4.1 Without wind involvement	58
4.4.1.1 Comparison of raining condition	58
4.4.1.2 Comparison of rain rate	59
4.4.2 With wind involvement	61
4.4.2.1 Comparison of raining condition	61
4.4.2.2 Comparison of rain rate	62
4.5 Discussion on validation results	64
4.5.1 Raining condition error discussion	64
4.5.2 Rain rate RMSE discussion	66

CONTENTS (Continued)

	Page
V CONCLUSION AND RECOMMENDATION	70
5.1 Conclusions	70
5.2 Recommendation and further improvement	72
REFERENCES	74
APPENDICES	81
APPENDIX A APT SYSTEM	82
APPENDIX B TYPES OF ANTENNA	86
a) TURNSTILE ANTENNA	86
b) QUADRIFILAR HELIX ANTENNA	87
c) LINDENBLAD ANTENNA	88
APPENDIX C PARAMETERS OF RAINFALL CONDITION	89
APPENDIX D NOAA SATELLITE ORBITING TIME SCHEDULE	94
APPENDIX E LIST OF 12 AIRPORT STATIONS	96
APPENDIX F RAINING CONDITION DATA FOR CLIMATIC ANALYSIS	97
APPENDIX G DATA OF DECISION TREE ANALYSIS	106
APPENDIX H EXAMPLES OF MATLAB SOURCE CODE	107
a) BRIGHTNESS TEMPERATURE DETERMINATE FUNCTION	107
b) RAIN CONDITION ESTIMATE FUNCTION	108
c) RAIN RATE ESTIMATE FUNCTION	109

CONTENTS (Continued)

	Page
APPENDIX I TABLE OF VALIDATION DATA	110
APPENDIX J VALIDATION RESULTS	126
APPENDIX K EXAMPLES OF APT IMAGE AND THEIR ANALYTICAL RESULTS	129
APPENDIX L LIST OF 71 STATIONS OF DEPARTMENT OF DRAINAGE AND SEWERAGE IN BANGKOK	135
APPENDIX M FM RECEIVER	138
CURRICULUM VITAE	145

LIST OF TABLES

Table	Page
4.1 Regression equations showing relationships between T_b and rain rates recorded in year 2005, 2006, 2007, and 2005-2007.....	53
4.2 Near-real time raining condition error resulted from the models of the years 2005, 2006, 2007, and 2005-2007.....	59
4.3 Near-real time raining condition error resulted from the models of the years 2005, 2006, 2007, and 2005-2007 which assume that rain rate < 0.5 is equal to 0 mm.....	60
4.4 Near-real time rain rate RMSEs resulted from the models of the year 2005, 2006, 2007, and 2005-2007.....	60
4.5 Near-real time rain rate RMSEs resulted from the models of the year 2005, 2006, 2007, and 2005-2007 which assumes that rain rate < 0.5 is equal to 0 mm.....	61
4.6 After 15 minutes received APT data, raining condition error resulted from the models of the years 2005, 2006, 2007, and 2005-2007.....	62
4.7 After 15 minutes received APT data, raining condition error resulted from the models of the years 2005, 2006, 2007, and 2005-2007 which assume that rain rate < 0.5 is equal to 0 mm.....	63
4.8 After 15 minutes received APT data, rain rate RMSEs resulted from the models of the years 2005, 2006, 2007, and 2005-2007.....	63

LIST OF TABLES (Continued)

Table	Page
4.9 After 15 minutes received APT data, rain rate RMSEs resulted from the models of the years 2005, 2006, 2007, and 2005-2007 which assume that rain rate < 0.5 is equal to 0 mm.....	64
A.1 Carrier frequency of APT signal form NOAA satellite.....	83
A.2 APT Characteristics.....	83
C.1 Cloud classification, base on altitude level.....	91
C.2 Criteria appropriate climate for a day.....	92
D.1 NOAA satellites orbit time schedule pass over Thailand.....	95
E.1 The position of 12 airport stations.....	96
F.1 Raining condition data for climatic analysis.....	97
I.1 Near-real time raining condition error data from the models of the years 2005, 2006, 2007, and 2005-2007.....	110
I.2 After 15 minutes received APT data, raining condition error data from the models of the years 2005, 2006, 2007, and 2005-2007.....	112
I.3 Near-real time raining condition error data from the models of the years 2005, 2006, 2007, and 2005-2007 which assumes that rain rate < 0.5 is equal to 0 mm.....	114
I.4 After 15 minutes received APT data, raining condition error data from the models of the years 2005, 2006, 2007, and 2005-2007 which assumes that rain rate < 0.5 is equal to 0 mm.....	116
I.5 Near-real time rain rate RMSE data from the models of the years 2005, 2006, 2007, and 2005-2007.....	118

LIST OF TABLES (Continued)

Table	Page
I.6 After 15 minutes received APT data, rain rate RMSE data from the models of the years 2005, 2006, 2007, and 2005-2007	120
I.7 Near-real time rain rate RMSE data from the models of the years 2005, 2006, 2007, and 2005-2007 which assumes that rain rate < 0.5 is equal to 0 mm	122
I.8 After 15 minutes received APT data, rain rate RMSE data from the models of the years 2005, 2006, 2007, and 2005-2007 which assumes that rain rate < 0.5 is equal to 0 mm	124
J.1 Comparison of raining condition errors between the actual rain rates estimated from the models and when measurement ability of rain gauge is involved	126
J.2 Comparison of raining condition errors when wind and without wind are considered	126
J.3 Comparison of raining condition errors when wind and measurement ability of rain gauge are considered simultaneously	127
J.4 Comparison of rain rate RMSEs with and without measurement ability of rain gauge involved	127
J.5 Comparison of rain rate RMSEs when wind and without wind are considered	128
J.6 Comparison of rain rate RMSEs when wind, and measurement ability of rain gauge are considered simultaneously	128

LIST OF TABLES (Continued)

Table	Page
L.1 The position of 71 stations of Department of Drainage and Sewerage, Bangkok Metropolitan.....	135

LIST OF FIGURES

Figure	Page
1.1 Bangkok, the study area	4
1.2 The SCADA system of The Department of Drainage and Sewerage	5
2.1 APT signal receiving system block diagram	7
3.1 Diagram of research processes	22
3.2 APT receiving system components	23
3.3 Positions of rainfall measurement stations of the Department of Drainage and Sewerage of Bangkok Metropolitan Administration	25
3.4 APT images reformatting process flow chart	26
3.5 Code in METAR data	30
3.6 Readable format of METAR data after decoding	30
4.1 The crossed-dipole antenna of the receiving system	37
4.2 The RF pre-amplifier	37
4.3 The FM receiver	38
4.4 The installed APT receiving system at Bangkok	39
4.5 APT data from the receiving system constructed	40
4.6 An example of geo-referenced APT image with overlay of Thailand administrative boundary	41
4.7 T_b determination interface of the module developed using MATLAB	42
4.8 Data table of determined T_b values of the subset of an APT image	43
4.9 T_b and METAR data set for raining condition analysis	44

LIST OF FIGURES (Continued)

Figure	Page
4.10 RH and P data table derived from METAR data of Suvarnabhumi airport and Donmuang airport.....	44
4.11 An example of input data for near-real time rainfall model.....	45
4.12 Relationship between T_b and raining condition.....	46
4.13 Relationship between RH and raining condition.....	47
4.14 Relationship between P and raining condition.....	48
4.15 Decision tree for rain conditioning analysis.....	49
4.16 Fit curve of T_b and rain rate records in year 2005.....	50
4.17 Fit curve of T_b and rain rate records in year 2006.....	51
4.18 Fit curve of T_b and rain rate records in year 2007.....	52
4.19 Fit curve of T_b and rain rate records in year 2005-2007.....	52
4.20 Flow diagram of the near-real time rainfall model.....	54
4.21 Module interface of the near-real time rainfall model, developed using MATLAB.....	55
4.22 An example of output data table from the module of near-real time rainfall model.....	56
4.23 GIS grid point data with attributes of raining condition and rain rates.....	56
4.24 Grid point data showing raining (yellow) and no-raining (blue).....	57
4.25 Comparison of raining condition errors between the actual rain rates estimated from the models and when measurement ability of rain gauge is involved.....	65

LIST OF FIGURES (Continued)

Figure	Page
4.26 Comparison of raining condition errors when wind and without wind are considered.....	66
4.27 Comparison of raining condition errors when wind and measurement ability of rain gauge are considered simultaneously.....	67
4.28 Comparison of rain rate RMSEs with and without measurement ability of rain gauge involved.....	67
4.29 Comparison of rain rate RMSEs when wind and without wind are considered.....	68
4.30 Comparison of rain rate RMSEs when wind, and measurement ability of rain gauge are considered simultaneously.....	69
A.1 APT frame format.....	84
A.2 APT ground station receiving system.....	85
B.1 Tunenstile antenna.....	86
B.2 QFA antenna.....	87
B.3 Lindenblad antenna.....	88
D.1 Sample of NOAA satellite pass list over receiving station.....	94
G.1 Data of decision tree analysis.....	106
K.1 APT image of NOAA 17, date 03/06/2008, 22:07 form APT receiving system.....	129
K.2 Grid point data result from APT image, date 03/06/2008 showing raining (yellow) and no-raining (blue).....	130
K.3 Rainfall measurement stations showing raining on 03/06/2008, 22:00.....	130

LIST OF FIGURES (Continued)

Figure	Page
K.4 Near-real time rainfall estimated result from APT image, date 03/06/2008.....	131
K.5 After 15 minutes received, rainfall estimated result from APT image, date 03/06/2008.....	131
K.6 APT image of NOAA 17, date 19/10/2008, 22:08 form APT receiving system.....	132
K.7 Grid point data result from APT image, date 19/10/2008 showing raining (yellow) and no-raining (blue).....	132
K.8 Rainfall measurement stations showing raining on 19/10/2008, 22:00.....	133
K.9 Near-real time rainfall estimated result from APT image, date 19/10/2008.....	133
K.10 After 15 minutes received, rainfall estimated result from APT image, date 19/10/2008.....	134
M.1 FM receiver kits.....	138
M.2 FM receiver print circuit broad kits.....	138
M.3 List of FM receiver assembling components.....	139
M.4 FM receiver schematic.....	141
M.5 FM receiver assembling print circuit broad layout.....	142
M.6 FM receiver connecting and control button layout.....	143
M.7 FM receiver assembled.....	143
M.8 FM receiver to computer interface cable assembling and schematic.....	144

LIST OF ABBREVIATIONS

AM	Amplitude Modulation
APT	Automatic Picture Transmission
AVHRR	Advance Very High Resolution Radiometer
CTT	Cloud Top Temperature
DC	Direct Current
DMSP	Defense Meteorological Satellite Programs
DN	Digital Number
FM	Frequency Modulation
FRQH	Folding Resonant Quadrifilar Helical
GIS	Geographic Information System
GMS	Geostationary Meteorological Satellite
GPS	Global Positioning System
GOES	Geostationary Operational Environmental Satellite
HRPT	High Resolution Picture Transmission
IR	Infrared
LST	Land Surface Temperature
METAR	Meteorological Aviation Report
MTSAT	Multi-function Transport Satellite
NOAA	National Oceanic and Atmospheric Administration
P	Pressure

LIST OF ABBREVIATIONS (Continued)

QFH	Quadrifilar Helix
RF	Radio Frequency
RH	Relative Humidity
RMSE	Root Mean Square Error
RQFH	Resonant Quadrifilar Helix
SCADA	Supervisory Control and Data Acquisition
TMD	Thai Meteorological Department
VHF	Very High Frequency
VIS	Visible
WEFAX	Weather Facsimile

LIST OF SYMBOLS

dB	Decibel
Hz	Hertz
k	Kilo
K	Kelvin
M	Mega
MB	Millibar
T_b	Brightness temperature
V	Volt
$^{\circ}\text{C}$	Degree Celsius
$^{\circ}\text{E}$	Degree East
$^{\circ}\text{N}$	Degree North

CHAPTER I

INTRODUCTION

1.1 Background problem and significance of the study

Rainfall is the most important climatic element especially in the tropics because it determines many agricultural and hydrological activities, which are dominant in the economies of the developing countries. Most of the rainfall data in the region is derived from rain gauge records. The present network for rainfall monitoring around the world by conventional means is deficient in many areas, especially if rainfall data are required in near-real time. Important near-real time or real time uses of rainfall data are found in weather forecasting, water supply management and flood control because they complement conventional data in space and time. Rain gauge is direct measurement of rain but no coverage over oceans or remote regions. Rain gauge supports temporal resolution on the other hand it is weakness in the quality of spatial resolution. In the problem of collecting more data, many studies have been undertaken in search of alternative methods of collecting data. The methods are now available in the form of satellite remote sensing system to help overcome the deficiency of rain gauge networks by means of remote sensing. The satellite remote sensing system is to use images from satellite because it offers wider area, temporal resolution of 1-3 hours and spatial resolution about 1-5 kilometers, real-time data and great importance in meteorology, hydrology, climatology and agriculture applications. Some data from satellite can be achieved

free of charge. Normally, one drawback is that the ground receiving signal system is extremely complicated. However, there are free satellites which uncomplicated and low cost economical receiving system can be easily constructed and installed. Automatic Picture Transmission (APT) from National Oceanic and Atmospheric Administration (NOAA) satellite is one of them. The APT system is an analog image transmission system developed for use on weather satellites. It was over four decades has provided image data to relatively low-cost user stations at locations in most countries of the world. A user station anywhere in the world can receive local data at least twice a day from each satellite as it passes nearly overhead. The APT data compose of two images are 4 km per pixel smoothed 8-bit images derived from two channels of the Advanced Very High Resolution Radiometer (AVHRR) sensor. Of the two images, one is typically thermal infrared (10.8 micrometers) with the second switching between near infrared (0.86 micrometers) and mid infrared (3.75 micrometers). However, NOAA can configure the satellite to transmit any two of the AVHRR's image channels. The APT data can apply to many applications such as, Land Surface Temperature (LST) and Cloud Top Temperature (CTT) analysis, cloud classification, and rainfall estimation.

Therefore, the researcher intends to construct low cost economical NOAA/APT receiving system, which are composed of cross dipole antenna, Very High Frequency (VHF) pre-amplifier, VHF receiver and APT decoder software. The APT receiving system is low cost, easy self-construction and installation, providing free and reliable data anytime when required. The research requires near-real time georeferenced and brightness temperature (T_b) data to incorporate with meteorological data such as rainfall, relative humidity, and pressure from ground stations for develop

rainfall estimation model.

1.2 Objectives of the study

1. To construct and install NOAA/APT receiving system.
2. To develop near-real time rainfall models for rain condition determination and rain rate estimation using NOAA/APT data from a self-made low cost receiving system.

1.3 Scope and limitations of the study

1. Data of years 2005-2007 used for model development were from Thai Meteorological Department (TMD) stations distributed all over Thailand.
2. The data during rainy season (May-October) of year 2006-2008 from total 71 stations of the Department of Drainage and Sewerage, distributed in Bangkok area, were used to validate the models.
3. Only 2 airport stations, Don Muang Airport and Suvarnabhumi Airport, were used to provide wind data which are one of the Meteorological Aviation Report (METAR) data. These data were applied to relocate point data from the selected images.
4. Only channel B (TIR) of NOAA/APT data will be used in the rainfall models.
5. The rainfall modules will be developed using MATLAB.

1.4 Study area

The study area herein, Bangkok, is where the data for model validation are gathered to use. The city covering area approximately 1,570 square kilometers from latitude $13^{\circ} 29' 48.24''$ N to $13^{\circ} 56' 46.80''$ N and longitude $100^{\circ} 21' 41.76''$ E to $100^{\circ} 56' 50.64''$ E, is located on the low plain with 1.50-2 m above the sea level (Figure 1.1). The climate is tropical zone with average temperature 29.2°C . The maximum average temperature is 38°C while the minimum average temperature is 19.2°C . The relative humidity is high through the year because Bangkok is located near the Gulf of Thailand where the vapor always blows. The average relative humidity is 73%. Moreover, there are 3 seasons, namely, summer during February-April, rainy season during May-October, and winter during November-January.

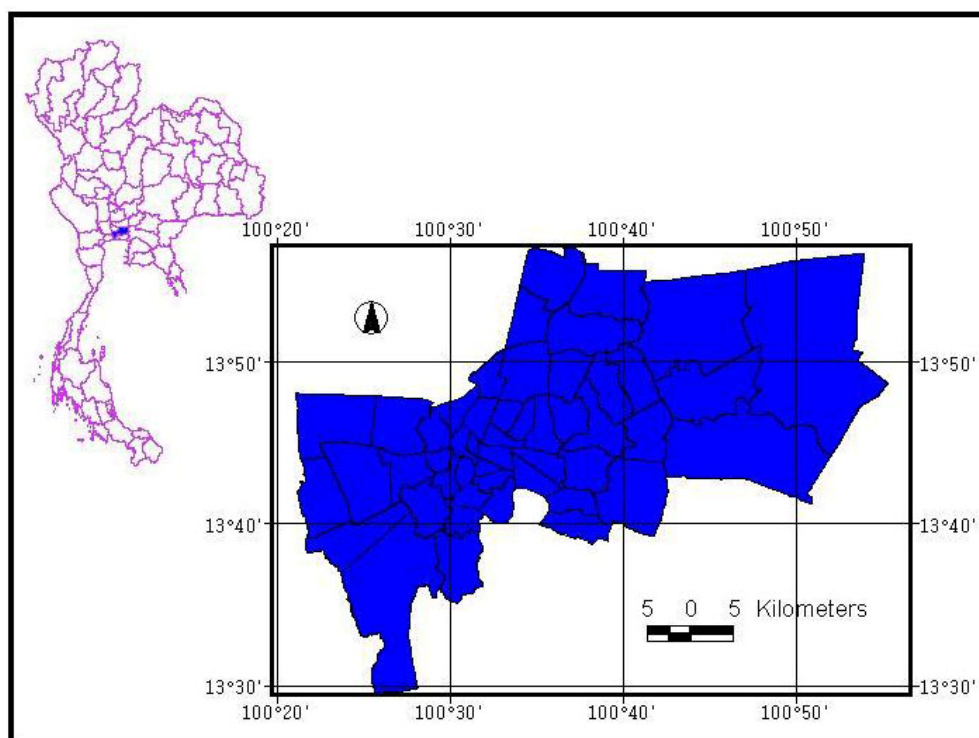


Figure 1.1 Bangkok, the study area.

During the rainy season, it is plenty of rain in Bangkok. It is easy to be flooded because Bangkok land is quite low, flat, and poor drainage system. Thus, 71 rainfall measurement stations in SCADA system were established cover in Bangkok as shown the Figure 1.2. They were designed to focus on automatic updating rainfall data in every 15 minutes. Therefore, data from these stations are spatially and temporally adequate and very effective for validation rain condition and rain rate received from the models.

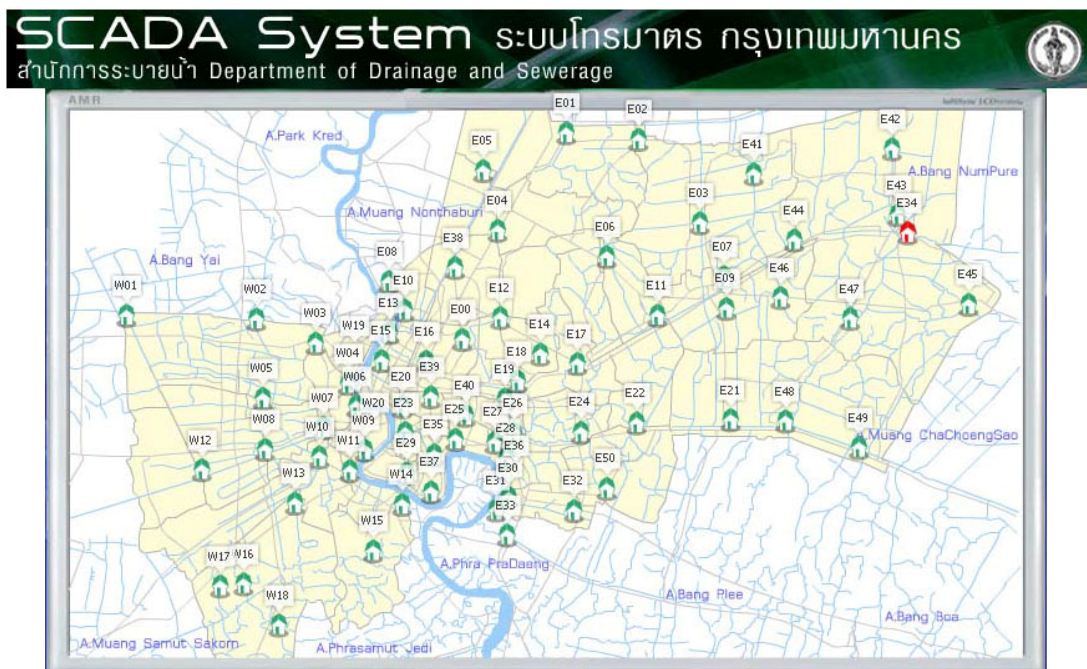


Figure 1.2 The SCADA system of The Department of Drainage and Sewerage. (Department of Drainage and Sewerage, 2009)

CHAPTER II

LITERATURE REVIEW

The review of the literatures for near-real time rainfall estimation using Automatic Picture Transmission (APT) data from NOAA satellite and meteorological data research have 4 parts; the first part is APT system, the second part is APT receiving system, the third part is APT data applications, the final part is rainfall estimation researches.

2.1 APT system

The APT system on the NOAA satellites of the USA provides a reduced resolution data stream from two of the Advanced Very High Resolution Radiometer (AVHRR) sensors, the two spectral channels are determined by NOAA ground command control station and are not selectable by the user. A visible channel is used to provide visible APT image during daylight, and one infrared (IR) channel is used constantly (day and night). A second IR channel can be scheduled for replacing to visible channel during the night time portion of the orbit. APT data has a resolution of approximately 4 km. It transmits the data continuously as an analogue broadcast in form of radio wave with 137 MHz frequency band that can be received in real-time, inexpensive ground station equipment while the satellite is within radio range (National Aeronautics and Space Administration, 2000). It has provided image data for relatively low-cost user stations at locations in most countries of the world, free

signal satellite imagery, gives many professional and other users their first introduction to real-time satellite imagery (more detail see Appendix A).

2.2 APT receiving system

The basic component of APT receiving system consists of omni-directional antenna, RF pre-amplifier, receiver, computer with sound card and APT decoder software, as seen in Figure 2.1.

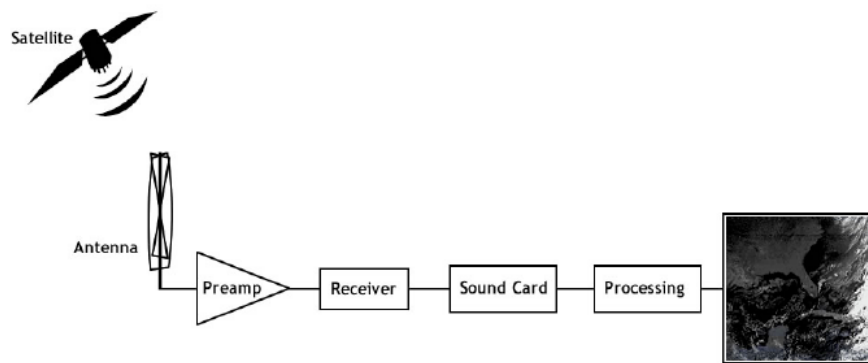


Figure 2.1 APT signal receiving system block diagram. (Eric, K. S. *et al.*, 2006)

The weak APT signals from the satellite are captured by a circular omni-direction antenna and amplified by a preamplifier. The data is then retrieved from these signals by a receiver. The receiver demodulates the FM signals and then sends data with the 2,400 Hz AM as a sub-carrier to the sound card in a PC computer which performs the analog-to-digital conversion of signals and recorded them as a wave file (.wav). Using a computer sound card for this process is very inexpensive compared with other analog-to-digital conversion methods. The wave file is then decoded by APT decoder software to generate APT images. There are many different types of antenna suitable for receiving APT signal from polar orbiting satellites. The popular

designs omni-direction antenna for APT reception include Crossed dipole or Turnstile antenna and Quadrifilar antenna (more detail see Appendix B). Of these, the Quadrifilar antenna probably gives the best performance but is not easy to build because it is essentially a truncated double helix. The only common design criterion is that they should detect circularly polarized radio waves in the 137 MHz to 138 MHz range. Many users developed and constructed antenna to receive APT signal, such as:

Hayes (2000) developed and constructed QFH antenna, the antenna element made by RG-58 coaxial cable and antenna support made by wood.

Jansen (2000) developed and constructed Folding Resonant Quadrifilar Helical (FRQH) antenna. He used Stanley measuring tape made to antenna element.

Hollander and Jansen (1999) developed Resonant Quadrifilar Helix (RQFH) antenna.

Thorp (1998) and Sykes and Cobey (1997) used copper tube construct QFH antenna element.

Taylor (1997) constructed Lindenblad antenna (more detail see appendix B), consists of four copper wire folded dipoles, equally spaced around the circumference of a horizontal circle.

Vanlint (1996) designed and constructed portable Quadrifilar Helix (QFH) antenna, the antenna element made by coaxial cable and the support mast made by PVC tube.

Jansen (1995) and Pepper (1994) constructed Quadrifilar antenna. The antenna element made by copper tube.

The antennas for receiving APT signal that have the many types as exemplify above. But, there are 2 basics in design and construction, the antenna can receive a

signal in omni-direction and has the circular polarization radiation pattern, because of, the APT signal broadcasting from NOAA satellite is right circular polarization. Copper which is the material with good conductivity is always applied to antenna element. However, oxide is easily formed on its surface when installed for the long time and that can cause receiving efficiency reduction. This problem can be solved by using copper wires with sheath insulator. Another popular material to be antenna element is aluminum because it has high conductivity, lightweight, cheapness and is not easily reacted to form oxide. For this study, the researcher uses aluminum tubes to be antenna elements confided as the cross-dipole antenna for the APT receiving system.

The APT receivers and decoder software have many types, for APT receiver example, R2FX model manufactured by Holger Eckardt of Hohenbrunn, Germany (www.df2fq.de), ProScan model manufactured by Timestep, England (www.timestep.com), RX137-141 model developed by Ing. Miroslav Gola (www.emgola.cz) and R139 model manufactured by Hamtronics Inc., USA (www.hamtronics.com), etc. APT decoder software has freeware, shareware and commercial software, the example, the freeware is APTDecoder by Thierry Leconte (www.poes-weather.com). The sharewares are Wxsat by Christian Bock (www.hffax.de), WxtoImg by Abstract Technologies New Zealand Limited (www.wxtoimg.com) and SatSignal by David & Cecilia Taylor's (www.david-taylor.myby.co.uk). The commercial software is WinsatPro by Dartcom, England (www.dartcom.co.uk), etc.

The user station everywhere in the world can receive local data from up to four satellites overpasses twice a day from each satellite. Thus there are many users received APT image around the world, for example;

The School of Remote Sensing of Suranaree University of Technology (SUT) in Thailand used APT receiver, Quadrifilar helix (QFH) antenna and WinsatPro decoder software from Dartcom in remote sensing lab.

Learning Center for Earth Science and Astronomy of Thailand received APT image in Center for research-based learning on Global Environment Observation (CGEO) project (<http://www.chanwittaya-cgeo.net/>).

Gola (2008) received APT image by hand made EMGO receiver and Wxtoimg software in Czech.

Tsander Space Research Lab in University of Latvia (2008) used receiver model MF-R1, Turnstile-reflector antenna model APT-2, Demodulator and MFMAP7 software from Multifax (www.qsl.net/n2zde).

Benabadji *et al.* (2004) constructed APT receiver system, composed of, Omnidirectional aerial turnstile and Quadrifilar helix antenna, 32 dB gain RF pre-amplifier fixed under the antenna, APT receiver and WXSAT software for decode and process the APT image in the laboratory.

Loh (2001) constructed APT receiver system, composed of, Quadrifilar helix antenna, RX2 receiver and ProSat software in Malaysia.

John (1992) and Steven (1995) integrated APT, High Resolution Picture Transmission (HRPT) reception system from NOAA satellite and Weather Facsimile (WEFAX) reception system from Geostationary Operational Environmental Satellite (GOES) satellite used in the classroom.

2.3 APT data applications

APT data received from NOAA satellite can receive themselves by using the signal reception equipment which is cheap. Moreover, it is easy to install in every location. So researchers take those data to apply for their works such as;

Gower *et al.* (1989) used near infrared and thermal infrared from APT data demonstrated real time mapping of weather patterns and sea surface temperature.

Heinzmann (1993) used APT data and ground observation analysis cloud types and distribution in the region of the upper Rhine valley in central Europe.

Islam and Exell (1996) used visible and far infrared APT image to calculate the clouds in the sky for solar radiation mapping in Thailand. The empirical coefficients obtained by correlating cloudiness with ground measured solar radiation are used to estimate solar radiation at a target on the ground knowing the cloud in the sky from a APT image.

Gjertsen (1997) used the visible and thermal infrared APT image to classify cloud layers over central Europe.

Pestemalci *et al.* (2004) used APT image estimate the land surface temperature of the Cukurova region in Turkey. These rectified APT image on April and July 1998 were used to estimate the surface temperature and compared with the meteorological ground base measurements.

In addition, the software used for processing APT image in freeware, shareware and commercial software is functioned to process composite image in order to show land surface temperature, sea surface temperature, vegetation, and precipitation etc.

2.4 Rainfall estimation researches

There are many different methods of rainfall estimations. Recently the most interesting methods to estimate rainfall using satellite-based sensors have been developed because the methods have high spatial and temporal resolution. However, direct measurement of rainfall from satellites for operational purposes has not been generally feasible because the capacity of the clouds prevents direct observation of the precipitation with visible, near-infrared and thermal infrared sensors. But improved analysis of rainfall can be achieved by using both the satellite and the conventional ground-based data. Satellite data is most useful in providing information on the spatial distribution of cloud brightness, cloud top temperatures, cloud types, cloud areas, and the duration of cold convective clouds over an area as a parameter in calculating the rainfall (Ouma *et al.*, 2005). Useful data can be derived from the satellites that are used primarily for meteorological purposes. They are polar orbits such as the NOAA, the Feng-Yun (FY-1), Defense Meteorological Satellite Programs (DMSP), and geostationary satellites such as GOES, Geostationary Meteorological Satellite (GMS), Feng-Yun (FY-2) the Multi-functional Transport Satellite (MTSAT). Their visible and infrared images can only provide information about the cloud tops. However, since these satellites do provide frequent observations, even at night with the thermal sensors. The characteristics of the potentially precipitating clouds and the rates of changes in the cloud areas and shapes can be observed. From those observations, the estimates of rainfall can be made which relate to the cloud characteristics from the rain rates and rainfall area. The Visible (VIS) and IR satellite image rainfall estimation methods. VIS and IR image are grouped together because they share common characteristics. The methods are based on radiation coming from the top or

inside of the clouds. All visible and infrared rainfall estimation schemes are indirect. The cloud brightness or equivalent blackbody temperature may be related to the rainfall. But the rainfall is not directly sensed. So the is brightness characteristics of the clouds in visible images and temperature characteristics of the clouds in infrared images are the basic of precipitation estimate from the satellite data. The physical basis of rainfall estimation from visible and infrared satellite images may be stated as follows: clouds that are bright in visible images are more likely to precipitate than dark clouds because the brightness is related to the optical depth and thus to cloud thickness. Clouds that are cold in infrared images are more likely to precipitate than warm clouds because cold clouds have higher tops than the warm clouds. This is called high brightness which is a large thick cloud. This implies greater probability of rain and low temperature. Therefore, the precipitating clouds can be distinguished from all others on the basis of, their brightness characteristics in visible images or temperature characteristics in the infrared images. The brightness or temperature of a precipitating cloud is a measure of the precipitation intensity (Kidder and Vonder Haar, 1995). The sample of precipitation and rainfall estimations are as follows;

Barrett (1970) developed a cloud indexing method. The method assigns a rain rate over a given area which is related to the amount and the type of cloud that is present in the satellite imagery over this area. He used a daily cloud chart produced by NOAA's predecessor and the Environmental Science Service Administration (ESSA) to estimate precipitation over Australia and adjacent area. The rain rate at a particular location is presented by Equation 2.1.

$$Rr = \sum_i r_i f_i \quad (2.1)$$

Where Rr is the rain rate

r_i is the rain rate assigned to cloud type i

f_i is the fraction of area covered by cloud type i

Arkin and Meisner (1987) estimated precipitation by the cloud indexing method. They call their precipitation estimate the GOES Precipitation Index (GPI). They use a 235 K in the IR threshold and a constant rain rate of 3 mm./h, which are appropriate for estimating tropical precipitation in areas approximately $2.5^\circ \times 2.5^\circ$ of latitude. GPI presented by Equation 2.2.

$$GPI = 3f\Delta t \quad (2.2)$$

Where GPI is an estimate of the mean rain depth in the area

f is the fraction of area colder than the threshold

Δt is the time in hours for which f applies

Bayasgalan and Erdenetuya (1992) developed methods for estimation the amounts of cloud, cloud types and delineation of precipitation area used AVHRR/NOAA and ground meteorological observation data over territory of Mongolia. They used channels 3 and 4 of AVHRR data to analyze cloud amounts by discriminating function, $Dcl = 0.054 * T_3 - 0.174 * T_4 - 1.46$, while T_3 and T_4 are radiance temperature values of channel 3 and 4 which supervised classification. The training area was selected interactively such area where has ground observation of cloud data. They used statistical value of cloud top temperature, albedo variations and cloud amounts to classify types of cloud. The strato-cumulus (Sc), strong

cumulonimbus (Cb) and stratus (St) cloud types have accuracy 83.7%. However cirrus (Ci), cumulus (Cu) and very low clouds are not good. Precipitation area was analyzed the relationship between rainfall and cloud type, rainfall and cloud amount. The precipitation probability increased with cloud amount and cumulonimbus cloud type.

Inoue (1993) estimated rainfall from AVHRR/NOAA data on July-September, 1990 in Japan. He used split window data (11 μm and 12 μm band) to compare with hourly radar rainfall data, the split window technique is effective method in delineation for rain area from low level clouds. However, the technique is not still effective for the rainfall rate estimation.

Csiszar and Kerenyi (1996) used satellite cloud parameters; cloud optical depth (τ), effective radius (r_e) and cloud top temperature from AVHRR/NOAA data estimate ground precipitation in Hungary. Cloud optical depth and effective radius were derived from channel 1 and 3 reflectivity and cloud top temperature from channel 4. They derived an empirical relationship between satellite cloud parameters and ground precipitation. The regression equation estimate ground precipitation amount in mm./hour from satellite cloud parameters is $I = -0.071 * \tau * r_e + 0.735\tau + 1.212r_e - 0.122T_c + 23.333$. The ground precipitation estimation has correlation accuracy 0.51.

Hilario (1998) studied estimation of rainfall from tropical cyclones by using 3 hr. interval of infrared and visible images from GMS satellite and rainfall data from weather observation stations in Philippine. The regression models involving the linear combination of average brightness value of different grid size ranging from 3 x 3 to 21 x 21 pixels infrared images and normalized visible brightness value from visible

images. The probability of rain-on and rain analysis use infrared and visible brightness values $\frac{1}{2}$ and $2\frac{1}{2}$ hours after the satellite passed. The result showed increasing of rainfall probability as the brightness temperature decrease but the visible brightness value increases. The results of studied, high rainfall values were always associated with high infrared brightness but it did not always imply high rainfall values. The estimated rainfall showed overestimation for lower rainfall values and underestimation for higher rainfall values.

Vicente and Scofield (1998) estimated rainfall in real time from GOES8 satellite data in Amazonia region. The method computed rainfall amount on a regression relationship between cloud top temperature from $10.7\ \mu\text{m}$ band and surface rainfall rate from 10 cm. radar data. The power law regression equation is $Rain = 1.1183 * 10^{11} \exp(-3.6382 * 10^{-2} * T^{12})$, where Rain is the rain rate in mm./hr. and T is the cloud top temperature in Kelvin. It was adjusted by moisture correction factor (relative humidity (RH) and precipitable water (PW)) from ETA model and cloud growth rate correction factor or cloud top temperature gradient collocated pixel in two consecutive half hour IR image. The hourly rainfall rate computation for each pixel by pixel of IR image is $Rain = (Rain_{\text{minimum}} + 2Rain_{\text{medium}} + Rain_{\text{maximum}}) / 4$. The technique runs in real time and provides 1, 3 and 6 hour rainfall rate every half-hour and 24 hour totals once a day.

Inoue and Aonashi (2000) compared cloud information from TRMM VIRS with rain measurements from the Precipitation Radar (PR) for rain cases during June 1998 over a frontal zone in East Asia. The authors selected the following four parameters: 1) Radiance ratio of 0.6 and $1.6\ \mu\text{m}$ (Ch1/Ch2), 2) Brightness

Temperature Difference (BTD) between 11 and 12 μm (BTD45), 3) BTD between 3.8 and 11 μm (BTD34), and 4) T_b in channel 4 as the cloud information. The flags of “rain certain” stratiform rain, bright band existence, and convective rain observed by the PR, and integrated rain rate from the rain bottom to the rain top were used as the rainfall information. From the comparison between rain/no rain information by the PR and the four cloud parameters, they found that values of the radiance ratio of Ch1/Ch2 was larger than 25, BTD45 smaller than 1.5K, and BTD34 smaller than 8K are effective in delineating rain area.

Hsu *et al.* (2002) used GOES satellite data estimate rainfall at Las Vegas on July 8, 1990. The method used relationship of cold cloud top temperature and rainfall relationship at a pixel resolution of $0.04^\circ \times 0.04^\circ$ is assigned as power law regression function: $r = C_1 \exp(C_2 T^{C_3})$, where T is pixel cloud top temperature in Kelvin, r is surface rainfall rate and C_1 , C_2 , and C_3 are constants, which are estimated from ground-based radar rainfall distribution of each cloud texture.

Islam *et al.* (2002) estimated rainfall by GMS5 data in Bangladesh over a period of 61 days from June 1, 1996. The rainfall was estimate by the Convective Stratiform Technique (CST) algorithm in order to calculate rainfall from GMS5 data. CST used satellite IR data to distinguish between convective and stratiform components of a meso-scale convective cloud system. They compared CST with the 3 hourly rainfall data from 33 rain gauges. The CST value was 0.7 mm./day larger than rain gauge value.

Billa *et al.* (2004) researched of quantitative precipitation forecasting using cloud-based techniques on AVHRR/NOAA data for flood warning system at Langat river basin, Malaysia. They used channel 1, 2, and 4 of AVHRR data to classify five

classes of features represent the land, sea, low stratus cloud, mid altos cloud, high cirrus cloud and threshold cold cloud temperature below 235K was taken as the indicator of rain.

Preeyaphorn and Kobkiat (2003) researched rainfall estimation used thermal infrared image from GMS4 satellite in 1994 in Thailand. They used relationship between cloud top temperature from thermal infrared image and rainfall from rain gauge in non-linear equation, $P = aT^b$, when T is cloud top temperature in Kelvin (K), P is rainfall in millimeter (mm.) from rain gauge, a and b is coefficients. The non-linear regression equations of rainfall estimation in each part of Thailand are as follow;

$$P = 4.3932 \times 10^{58} T^{-24.80} \text{ in the dry season, Northern} \quad (2.3)$$

$$P = 1.8462 \times 10^{22} T^{-8.9300} \text{ in the rainy season, Northern} \quad (2.4)$$

$$P = 1.1102 \times 10^{13} T^{-4.8288} \text{ in Northern} \quad (2.5)$$

$$P = 4.4905 \times 10^{10} T^{-3.8012} \text{ in Northeastern} \quad (2.6)$$

$$P = 5.2384 \times 10^{12} T^{-4.6683} \text{ in Eastern} \quad (2.7)$$

$$P = 2.4916 \times 10^{11} T^{-4.0840} \text{ in Southern} \quad (2.8)$$

The equations are used to predict rainfall in that area when cloud top temperature is determined from GMS satellite imagery. The results of rainfall estimation using ground based data and satellite remote sensing provided an accurate rainfall map.

Saisunee (2004) studied rainfall estimate for flood management of Pasak river basin in Thailand used satellite imagery. In this study, rainfall estimate was initially accomplished by computing the power-law regression relationship between cloud top

temperature in infrared band of GMS-5 satellite and observed rainfall rate at the synoptic station. This regression was derived from the statistical record of cloud top temperature converted from the consecutive hourly GMS-5 satellite images and the 3 hour rainfall rate measured at 3 synoptic stations (Muang, Lomsak, and Wichianburi). The result of power-law as follow;

$$P = 2.52 \times 10^{28} \cdot T_p^{-11.411} \quad \text{for Muang station} \quad (2.9)$$

$$P = 7.57 \times 10^{24} \cdot T_p^{-9.555} \quad \text{for Lomsak station} \quad (2.10)$$

$$P = 1.796 \times 10^{26} \cdot T_p^{-10.525} \quad \text{for Wichianburi station} \quad (2.11)$$

Where P is the value of convective rainfall rate in mm./ 3 hr. and T_p is the value of the cloud top temperature from hourly GMS satellite image in degree Kelvin.

The result of rainfall estimate expected to challenge the further study to transform the estimated values of rainfall into the flood hydrograph by using appropriate rainfall-runoff model.

Suh *et al.* (2004) estimated rainfall at southern Korea in June to August 2003. The rainfall estimation technique used the infrared data of GOSE 8 and 9 to compute real time rainfall amounts based on a power-law regression algorithm. They used GOES infrared imagery data and 400 points of automatic weather station data for the analysis of relation between observed rainfall rate and cloud top temperature. The power law for the estimation of rainfall rate is $R = 1.1183 \times 10^{11} \exp(-3.6382 \times 10^{-2} \cdot T^{1.2})$. When R means rainfall rate in mm. and T means cloud top temperature in Kelvin. The relation was much higher when the rainfall was strong and the power law

underestimated the rainfall rate. The correlation coefficients are 0.40-0.53, based on the power law between cloud top temperature and hourly rainfall rates.

As the relevant research reviewing, the researcher used the data from the satellite i.e. NOAA, GOES, and GMS together with the other data for estimating the rainfall in several models, real time, near-real time, every hour, daily, monthly and etc. The researcher has an idea to research the near-real time rainfall estimation using APT data from NOAA satellite and meteorological data by constructing APT system for receiving APT data in real time. Also, the APT image can be used with the meteorology data as the near-real time in order to create the rainfall estimation model.

The parameters of rainfall condition consist of 3 parameters namely, vapor water in the atmosphere, particles of dust, and the process of cooling which can cause condensation. The rainfall cannot be formed without any of these 3 parameters. (Royal Irrigation Department, 2008) Many weather and meteorological parameters used for rainfall analysis are shown in Appendix C.

CHAPTER III

RESEARCH METHODOLOGY

Basically, the processes of near-real time rainfall estimation using APT data from NOAA satellites and meteorological data research consist of 4 parts as shown in Figure 3.1. First, hardware were assembled and installed to be the system which can receive APT signal from NOAA satellites- NOAA 12, NOAA 15, NOAA 17, and NOAA 18. Second, time-series NOAA/APT data covering whole Thailand were received and reformatted. Third, a module of near-real time rainfall model was developed using MATLAB. The module is composed of climatic condition analysis which is applying T_b (brightness temperature) from APT images, RH and P from near-real time meteorological data of METAR report, and rain rate estimation analysis for relationship of T_b and rain rate. Fourth, selected NOAA/APT data were input through the module and results were validated by accuracy assessment.

3.1 APT receiving system construction

3.1.1 APT receiving system assembly

The APT receiving system was assembled from hardware as follows:

- 1) Antenna: the crossed-dipole antenna is a right circular polarized one.

This exactly matches the antenna pattern from the satellite and also serves to reject linearly polarized earth based signals.

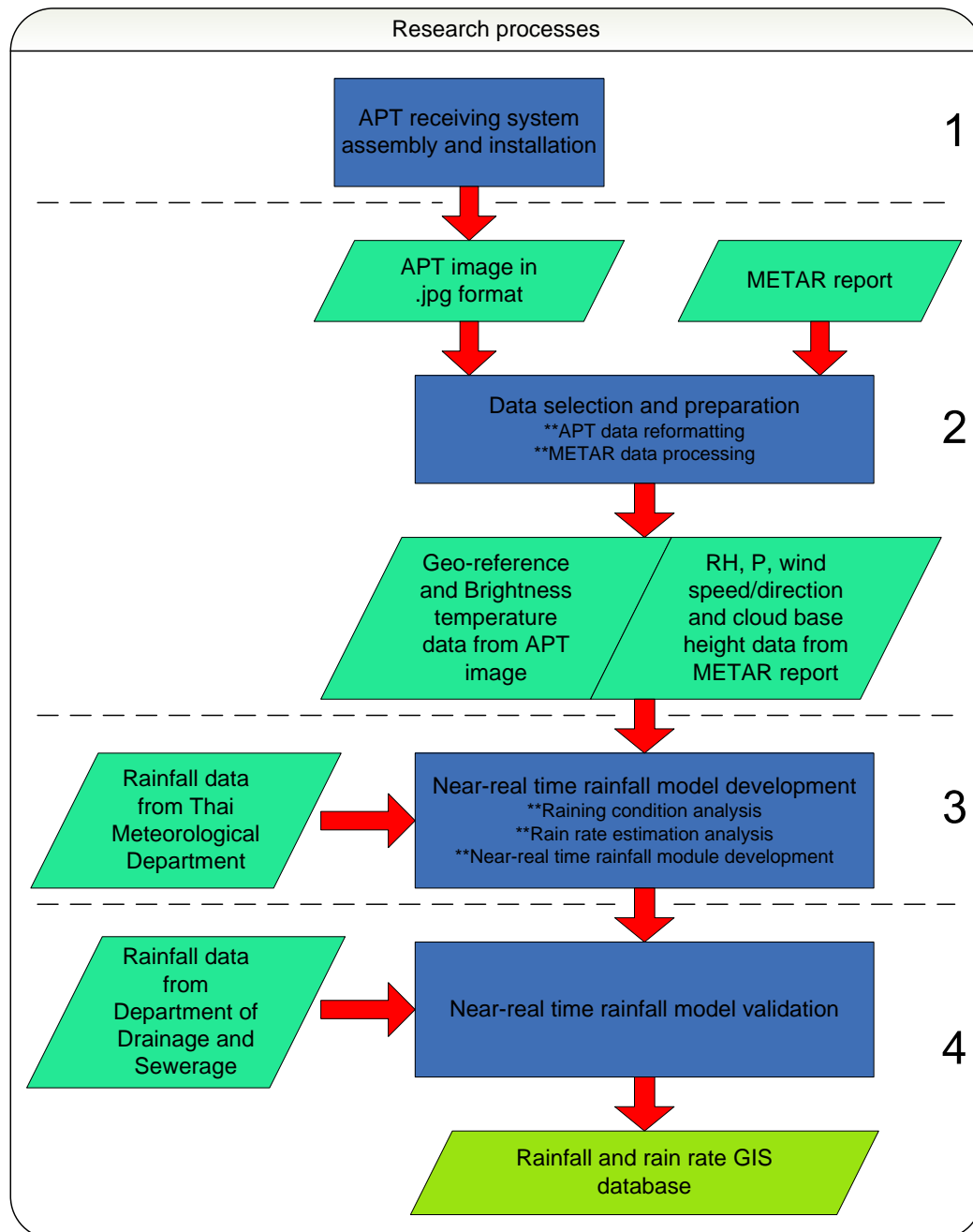


Figure 3.1 Diagram of research processes.

2) RF pre-amplifier: it was assembled from the kits of Hamtronics model LNK-137. This model can operate in 130-160 MHz frequency range, bandwidth 4 MHz, and gain 18 dB.

3) FM receiver: it was assembled from the kits of Emgo model RX137141MHz.

3.1.2 APT receiving system installation

APT receiving system components consisting of hardware (Figure 3.2) i.e. crossed-dipole antenna, RF pre-amplifier, FM receiver, sound card and decoder software in a PC system were installed at $13^{\circ} 51' 14.03''$ N and $100^{\circ} 36' 28.28''$ E in Bangkok (<http://geocities.com/chonmapatt/APTstation.html>).

A preamplifier is necessary because the signal transmitted by the satellites is weak. The receiver then demodulates the radio signals into audio tones and send to microphone or line-in port of the soundcard in a computer which performs the analog-to-digital conversion of signals and recorded them as a wave file (.wav). The wave file is then decoded by WXtoImg software to generate and display APT images. The control port of the receiver is also connected to the RS-232 port of the computer for adjust frequency of APT signal to each NOAA satellite which is controlled by the WXtoImg software.

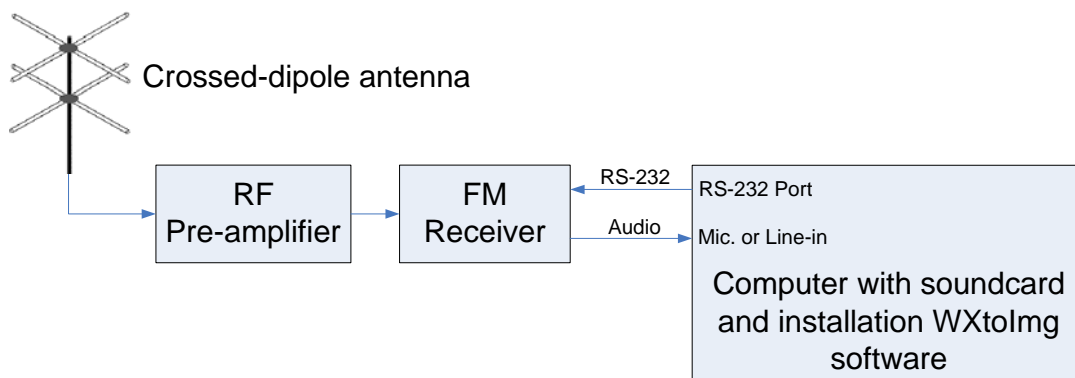


Figure 3.2 APT receiving system components.

WxtoImg software is used to decode APT signals and create APT data in form of images. Various functions for decoding of WxtoImg software can be set as follows:

Enhancement: Contrast enhance (NOAA Ch B only)

Projection: Equidistant Cylindrical

Reference latitude: 13

Reference longitude: 101

North boundary (latitude): 21

South boundary (latitude): 5

West boundary (longitude): 97

East boundary (longitude): 106

Scale output width: 540 (pixels)

Resampling method: Bilinear

The WXtoImg software, developed by Abstract Technologies New Zealand Limited (2008), is a fully automated APT decoder. It supports real-time recording, decoding, viewing APT image, map overlays, advanced color enhancements, multi-pass images, projection transformation, text overlays, temperature display, GPS interfacing, FM receiver controlling, etc.

3.2 Data selection and preparation

3.2.1 APT data selection

1) APT image data received daily from the installed system (see detail of NOAA satellites orbiting schedule in the Appendix D) during 2005-2007 were selected by time matching with rainfall data recorded at the 11 airport stations distributed in the whole country (see Appendix E) by the TMD. The rainfall data have

been recorded every 3 hours of a day which are at 01:00, 04:00, 07:00, 10:00, 13:00, 16:00, 19:00, and 22:00. The images with clearing signals and falling within the range of ± 15 minutes of those exact times of recording were selected from the time-series receiving APT data. APT data selected will be used to establish the relationship between T_b and rain rate recorded by the TMD at the stations. The time range of 15 minutes is also corresponding to the time range of data recording at the stations in the validated area.

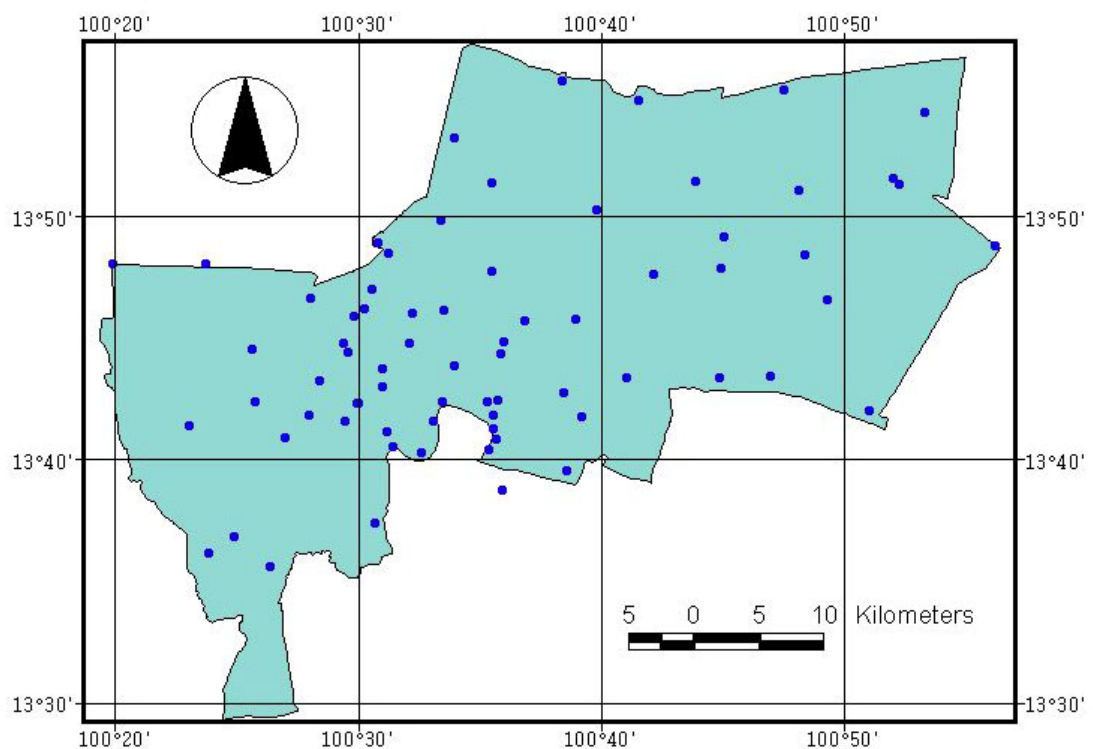


Figure 3.3 Positions of rainfall measurement stations of the Department of Drainage and Sewerage of Bangkok Metropolitan Administration.

2) Another APT image data selection is for model validation. The validated area for the study is Bangkok which has total 71 rainfall measurement stations of the Department of Drainage and Sewerage, Bangkok Metropolitan (Figure

3.3). In year 2006, 21 stations were established and functioned while became 55 stations in year 2007 and 71 stations in year 2008. Rainfall data at these stations will be recorded every 15 minutes. APT images with clear signals, received during 2006-2008, were selected for further reformat and then extracted as point data spatially corresponding to 71 stations in Bangkok. These data will be further matched to rainfall data recorded at the 71 stations by date and the closest time.

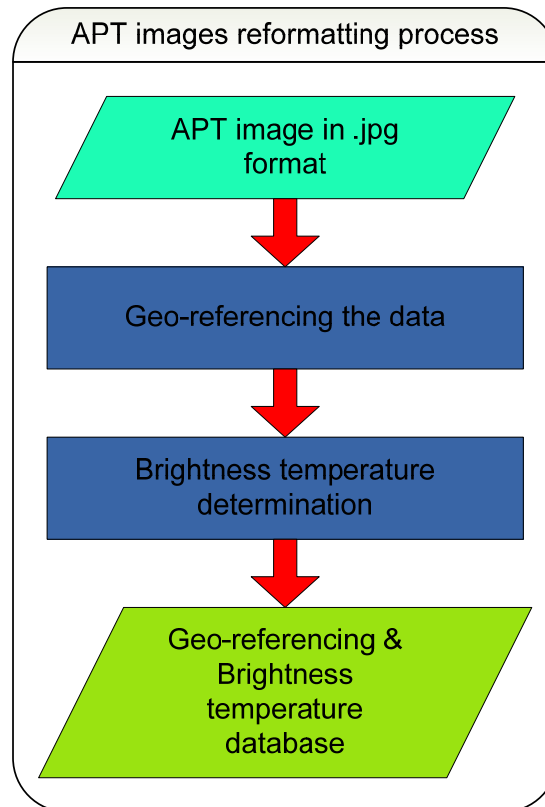


Figure 3.4 APT images reformatting process flow chart.

3.2.2 APT data reformatting process

WXtoImg, APT decoder software, can display data in forms of images with data of pixel position, DN values, and brightness temperature. Unfortunately, it

does not support all functions required for applications. Images can be exported into several formats e.g. joint photographic (.jpg), bit mapped (.bmp), portable network graphics (.png), portable any map (.pnm), portable gray map (.pgm), and portable bit map (.pbm) but without geo-referenced position (latitude/ longitude) and temperature data that are needed to work with general Remote Sensing and GIS software. Therefore, the reformat of exported APT images is required. The reformat process can be mainly separated into geo-referencing the data and brightness temperature determination as shown in Figure 3.4.

3.2.2.1 Data geo-referencing

Due to the curved earth surface, each APT image from each satellite orbit has to be projected to be flat plane. Thus, equidistant cylindrical projection is used for this purpose. The projected image is further processed for geo-referencing in next step.

APT images saved in the file format of .jpg, from the receiving system, can be geo-referenced using Image World File method through ArcView geo-reference extension. The result is image file in the format of .jpgw. The WORLD file is an ASCII text file that contains specially formatted coordinate information about where the image is, in relation to the surface of the earth. Its format is as follows:

0.01663574 (line 1)

0.00000000 (line 2)

0.00000000 (line 3)

-0.01664937 (line 4)

xx.xxxxxxxx (line 5)

xx.xxxxxxxx (line 6)

line 1 = x-dimension of a pixel in map unit estimated from coordinates of the upper-left, upper-right pixel, and the number of pixel in the row.

line 2 = rotation terms.

line 3 = rotation terms.

line 4 = y-dimension of a pixel in map unit estimated from coordinates of the upper-left, lower-left pixel, and the number of pixel in the column. The y-scale is always a negative number.

line 5 = x coordinate at the center of the upper-left pixel of the image.

line 6 = y coordinate at the center of the upper-left pixel.

3.2.2.2 Brightness temperature (T_b) determination

The MATLAB module was developed in this study to determine T_b . The determination processes in the module consists of the following 2 steps.

1) Converting DN of APT images to the radiance (E) using Equation 3.1.

The input C data into the equation requires a 10-bit value (0-1023) but DN of an APT image is an 8-bit gray scale value (0-255). Therefore, a 8-bit value has to be transformed to a 10-bit value.

$$E = C.S + I \quad (3.1)$$

Where $E =$ Radiance in $\text{mW}/\text{m}^2\text{-sr}\text{-cm}^{-1}$

$C =$ Input DN value (0-1023)

$S =$ Slope value ($-0.160156 \text{ mW}/\text{m}^2\text{-sr}\text{-cm}^{-1}$)

$I =$ Intercept value ($159.088867 \text{ mW}/\text{m}^2\text{-sr}\text{-cm}^{-1}$)

(National Aeronautics and Space Administration, 1998)

2) Converting the radiance (E) from Equation 3.1 to be the brightness temperature using Equation 3.2.

$$T_b = \frac{C_2 \cdot V}{\ln\left(1 + \frac{C_1 \cdot V^3}{E}\right)} \quad (3.2)$$

Where T_b = Brightness temperature in Kelvin

$$C_1 = 1.1910659 \cdot 10^{-5} \text{ mW/m}^2\text{-sr-cm}^{-1}$$

$$C_2 = 1.438833 \text{ cm-K}$$

V = Central wave number for CH4 AVHRR in cm^{-1}

$$\text{Central wave number of NOAA12} = 920.7173 \text{ cm}^{-1}$$

$$\text{Central wave number of NOAA15} = 925.4075 \text{ cm}^{-1}$$

$$\text{Central wave number of NOAA17} = 926.2947 \text{ cm}^{-1}$$

$$\text{Central wave number of NOAA18} = 928.1460 \text{ cm}^{-1}$$

(National Aeronautics and Space Administration, 1998.)

3.2.3 METAR data processing

The METAR data are aviation routine weather report observed at airport stations around the world. Reports are generated every 30 minutes. A typical METAR report contains data for the temperature, dew point, wind speed and direction, precipitation, cloud cover and its heights, visibility, RH, P, etc. The data are in codes as shown in Figure 3.5. These codes will be decoded using the Mweather software which is a freeware for decoding weather information from MATAR data to be readable format as an example shown in Figure 3.6. The METAR data were used in this study in 2 ways as follows:

METAR VTBD 111700Z 13003KT 9999 FEW020 SCT120 BKN300 28/23 Q1008 NOSIG
 METAR VTBS 111700Z 14007KT 9999 FEW020 BKN300 29/24 Q1008 NOSIG
 METAR VTCC 111700Z 02003KT 9999 SCT035 BKN300 25/24 Q1006 A2973
 METAR VTSS 111700Z 00000KT 9999 FEW018 SCT120 BKN300 24/23 Q1010 A2984
 METAR VTSP 111700Z VRB03KT 9000 SCT018 BKN110 BKN300 26/24 Q1011 A2985
 METAR VTBU 111700Z 00000KT 9999 FEW020CB SCT040 BKN120 28/27 Q1008 A2977 CB SE LTG
 METAR VTCT 111700Z 00000KT 9999 BKN030 BKN110 25/24 Q1005 A2968 RMK/RWY03 INFO A

Figure 3.5 Code in METAR data.

ICAO	Station Name	Location	Time	Temperature	Dew Point	RH	Wind	Visibility	Pressure	Sky Condition	Weather
VTBD	Bangkok/Don Muan	13-55N 100-35E	28 / 19:00	28.0gC	23.0gC	74%	S (190 degrees) at 1 m/s	8000m	1006.1 mb	Scattered Cumulonimbus ...	Light Rain with ...
VTBS	N/A	N/A	28 / 19:00	28.0gC	23.0gC	74%	WSW (240 degrees) at 7 m/s	7000m	1006.1 mb	Few Cumulonimbus cloud...	Light Rain Shower
VTCT	Chiang Rai Intl	19-57N 99-53E	28 / 19:00	28.0gC	22.0gC	70%	Calm	> 10000m	1005.1 mb	Broken clouds at 670m, B...	
VTPH	N/A	N/A	28 / 19:00	26.0gC	23.0gC	84%	Calm		1006.1 mb	Scattered clouds at 910...	
VTSE	Surat Thani	09-07N 99-20E	28 / 19:00	26.0gC	25.0gC	94%	Calm	8000m	1007.1 mb	Few clouds at 610m, Bro...	
VTSC	Narathiwat	06-31N 101-45E	28 / 15:00	31.0gC	24.0gC	66%	ENE (70 degrees) at 4 m/s	> 10000m	1004.1 mb	Scattered clouds at 670...	
VTSF	Nakhon Si Thammar	08-32N 99-57E	28 / 17:00	25.0gC	24.0gC	94%	Calm	7000m	1006.4 mb	Broken clouds at 490m, F...	Light Rain with ...
VTSG	Krabi	08-06N 98-59E	28 / 19:00	24.0gC	22.0gC	89%	N (10 degrees) at 2 m/s	6000m	1007.1 mb	Scattered clouds at 610...	
VTSK	N/A	N/A	25 / 10:00	28.0gC	25.0gC	84%	Calm	> 10000m	1010.5 mb	Scattered clouds at 610...	
VTSM	Samui	09-33N 100-04E	28 / 19:00	26.0gC	23.0gC	84%	NW (320 degrees) at 5 m/s	9000m	1007.8 mb	Few clouds at 610m, Bro...	Thunderstorm
VTSP	Phuket Intl Airp	08-07N 98-19E	28 / 19:00	27.0gC	23.0gC	79%	NNW (330 degrees) at 2 m/s	> 10000m	1007.1 mb	Few clouds at 610m, Bro...	
VTSR	Ranong	09-58N 98-37E	27 / 18:00	26.0gC	24.0gC	89%	SSE (150 degrees) at 1 m/s	9000m	1004.7 mb	Broken clouds at 760m, ...	
VTSS	Hat Yai	06-55N 100-26E	28 / 19:00	24.0gC	23.0gC	94%	Calm	6000m	1006.1 mb	Scattered clouds at 610...	
VTST	Trang	07-31N 99-37E	28 / 16:00	25.0gC	24.0gC	94%	NNE (20 degrees) at 2 m/s	7000m	1005.1 mb	Few clouds at 610m	
VTUK	Khon Kaen	16-25N 102-49E	28 / 19:00	24.0gC	23.0gC	94%	WNW (300 degrees) at 3 m/s	8000m	1005.8 mb	Broken clouds at 670m, ...	Light Rain
VTUU	Ubon/Ratchathani	15-15N 104-52E	28 / 13:00	32.0gC	23.0gC	59%	N (360 degrees) at 3 m/s	8000m	1006.1 mb	Scattered clouds at 760...	

Figure 3.6 Readable format of METAR data after decoding.

1) RH and P data of 11 airport stations mentioned in 3.2.1 were prepared and used to establish the decision tree for determining raining condition (rain or no rain) as described in 3.3.1.

2) RH, P, wind direction and speed, and cloud base height from 2 airport stations, Suvarnabhumi airport and Donmuang airport, were used for

validation purpose as described in 3.4. RH and P data were interpolated using Inverse distance weighted (IDW) method in order that they can be picked up spatially corresponding to 71 stations in Bangkok area which were used for validating the model. Unfortunately, there are no other sources in the surrounding area. Although it does not good sources to apply IDW from only two source points available, RH and P from these two stations show not much difference. Therefore, the results are not affected significantly by this limitation. Wind direction, wind speed, and cloud base height were further applied to calculation of cloud shift due to the wind as explained in 2) of 3.4.

3.2.4 Input data preparation for near-real time rainfall model

To operate the near-real time rainfall model, input data resulting from 3.2.2 and 3.2.3 are required. The attribute data include positions of point data, T_b , RH, and P within the validated area.

3.3 Near-real time rainfall model development

3.3.1 Climatic data analysis for raining condition

The raining or no raining is the expected result of the raining condition analysis. The data used for analysis include T_b from APT image, raining condition, RH and P from METAR report at 11 airport stations. The TIR band of APT image used in the study shows the relation between brightness and cloud temperature which identifies the cloudy area. The area with low T_b or high reflection (more white) can be higher potential for cloud and rain cluster than the area with high T_b or lower reflection. RH and P are the supporting data for identifying the potential of cloud cluster for rainfall because APT image with the same T_b may provide different cloud

types, which may not be the cloud and rain cluster. The area with high RH provides higher potential for rainfall because of having higher humid/water in the air, proximate to the saturation point. Any area with high values of RH at surface and altitude levels indicates that it is the area of higher potential for rainfall. The P is one of climate change parameter. In low pressure trough areas have probability of rainfall.

Data used for this analysis are T_b from APT data, raining condition, RH, and P from METAR data reports of 11 airport stations.

1) To match T_b of images selected (the result of 3.2) with time-related METAR rainfall data of 11 airport stations. The events having probability of raining and without probability of raining can be separated.

2) To further determine more accurate probability of the events with probability of raining selected from 1) by establishing a relationship of the events and RH and P consequently.

3) The result appeared in forms of decision trees with certain conditions of T_b , RH, and P.

The decision tree established will be further used to determine the raining condition at 71 stations in Bangkok area for validating the model by comparing with the rain rate measured at those stations.

3.3.2 Rain rate estimation models formulation

Only T_b and rain rate data of events having probability of raining, selected from 1) of 3.2.1, were used to formulate 4 regression models expressed their relations based on data of the year 2005, 2006, 2007, and the whole 3 years.

3.3.3 MATLAB module development of near-real time rainfall models

The results of rainfall decision tree and rain rate regression models, from 3.3.1 and 3.3.2, were developed to be the MATLAB module. The module developed will allow input data in forms of table of .xls format containing geographic coordinate, T_b in Kelvin, RH, and P of point data covering the study area. The output data are in the same format showing raining condition (raining or no raining) and rain rate of the point data.

3.4 Near-real time rainfall model validations

The selected APT images as mentioned in 2) of 3.2.1 were processed and employed to validate with results from the models through MATLAB module developed. The rain rate estimated from the module is in the unit of mm/3 hours. Therefore, the estimated rain rate should be adjusted to be the unit of mm/15 minutes in order that it can be validated with the measured data from the 71 stations which rainfall are measured every 15 minutes. The mode, average and ratio of rainfall time period within every 3 hours, from the records of the 28 even number stations, in May-October year 2007 was used to adjust the rain rate estimated from the module. The validations were performed accordingly:

- 1) The input data of T_b of APT images with clear signals of the year 2006-2008 and RH and P interpolated from the METAR reports of Suvarnabhumi and Donmuang Airports were performed through the rainfall estimation module. Then, the output data of raining condition and rain rate were compared to rainfall data of the 71 stations by closest time-related matching for accuracy assessments.

2) By using wind speed, direction, and cloud base height data of the METAR reports from Suvarnabhumi and Donmuang Airports, all point data of each event in 1) were shifted. The raining and rain rate data of points corresponding to the stations were picked up and used to compare with 15-minute-later records of each station for accuracy assessments. The coordinate shifting of point data according to wind were the result of the following Wind Profile Power Law equation.

$$\frac{U}{U_r} = \left(\frac{Z}{Z_r} \right)^\alpha \quad (3.3)$$

Where U = Wind speed at Z height (m/s)

U_r = The known wind speed at a reference height Z_r (m/s)

Z = Roughness height of surface (m)

Z_r = Reference height above ground surface (m)

α = An empirically derived coefficient that varies dependent upon the stability of the atmosphere. For neutral stability conditions, k is approximately 0.143. (Wikipedia, 2008)

3) The accuracy assessments were operated with raining condition and rain rate data in terms of percentage of error and Root Mean Square Error (RMSE), respectively. Due to the limitation of equipment recording ability, only rain rate higher than 0.5 mm can be recorded at the stations. Therefore, the comparisons were performed in two ways: comparison between the measured and the estimated rain rate of each point, and the comparison only points with estimated rain rate higher than 0.5 mm.

3.5 Equipments and data

1. APT receiving system.

2. Software

2.1 Wxtoimg software for APT signal decoding and creating APT image.

2.2 ArcView 3.2 software for GIS analysis.

2.3 Mweather software for METAR data decoding.

2.4 MATLAB R2006a software for establishing near-real time rainfall model.

3. Data

3.1 APT images from self-constructed receiving system

3.2 Rainfall data of the Meteorology Department and the Department of Drainage and Sewerage of Bangkok Metropolitan Administration.

3.3 METAR data from www.wunderground.com.

CHAPTER IV

RESULTS AND DISCUSSION

4.1 Installed APT receiving system

The hardware of the receiving system including antenna, RF pre-amplifier, and FM receiver were assembled and hooked to the PC system and then installed for NOAA-APT data receiving operation in Bangkok. The hardware is strong structure and so lightweight that it can be easily transported and set up anywhere.

4.1.1 Assembled APT receiving system

1) The crossed-dipole antenna consists of two $1/2$ wavelength horizontal dipoles that were oriented 90 degrees from each other. A phasing line was used to connect one dipole 90 degrees out of phase to the second one for circular polarization and crossed reflector. The antenna elements and reflectors were made from aluminum tube. The length of dipole elements is 50 cm. whereas the length of reflector elements is 105 cm. The span between crossed dipole to crossed reflector is about 50 cm. The crossed-dipole antenna is a right circular polarized antenna. This exactly matches the antenna pattern from the satellite and also serves to reject linearly polarized earth based signals (see Figure 4.1).

2) The RF pre-amplifier was assembled from the kits of Hamtronics model LNK-137 as shown in Figure 4.2. This model can operate in 130-160 MHz of frequency range, 4 MHz of bandwidth, and 18 dB of gain. The operating frequency of preamplifier was tuned to be 137.50 MHz to match with APT signals. Through

coaxial cable, DC 12V power from the receiver can be supplied to the preamplifier and the amplified signals can be fed to the receiver.



Figure 4.1 The crossed-dipole antenna of the receiving system.



Figure 4.2 The RF pre-amplifier.

3) The FM receiver was assembled from the kits of Emgo model RX137141MHz as shown in Figure 4.3. This model can operate in 137-141 MHz frequency range which covers APT signal carrier. The APT carrier frequency for each

NOAA satellite can be controlled by WXtoImg software via RS-232 cable. It performs FM signals demodulation to be the 2,400 Hz AM sub-carrier (audio wave) and sends to the sound card in the PC system.



Figure 4.3 The FM receiver.

4.1.2 Installed APT receiving system

The receiving system was installed at $13^{\circ} 51' 14.03''$ N and $100^{\circ} 36' 28.28''$ E near Soi Lat Pla Khao 64 in Bangkok as shown in Figure 4.4. The crossed-dipole antenna was installed on the roof with 15 m above the ground and connected with 25 m RG-58A/U coaxial cable to the preamplifier. A preamplifier is necessary because the signal transmitted by the satellites is weak. The receiver then demodulates the radio signals into audio tones and sends to microphone or line-in port of the soundcard in a computer which performs the analog-to-digital conversion of signals and recorded them as a wave file (.wav). The wave file is then decoded by WXtoImg software to generate and display APT images in near-real time. The control port of the receiver is also connected through the RS-232 port of the computer for adjust

frequency control of APT signal to each NOAA satellite. The adjustment of demodulator of FM receiver allows receiving APT signal at 137.10, 137.50, and 137.62 MHz.

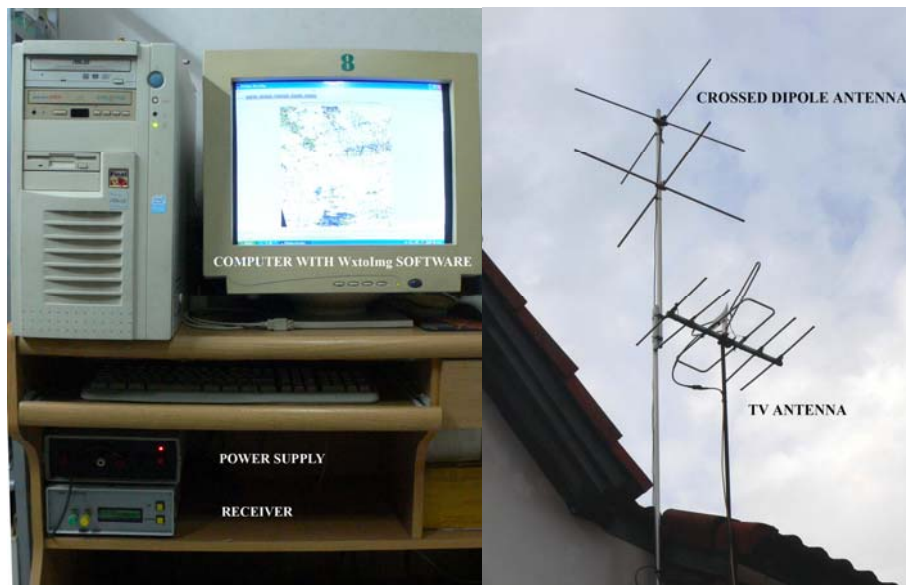


Figure 4.4 The installed APT receiving system at Bangkok.

After verifying the equipment of the APT receiving system, the necessary equipment and software were installed to receive the APT image orbiting pass Thailand. The system installed can receive the APT image signals from the NOAA 12, 15, 17, and 18 satellites only because 4 satellites sent APT data on study time, which are covered Thailand and neighborhood. The quality of the signals received will be better when the satellite orbits passing right on top of receiving station. With this installing position, the signals received covering the southern part of Thailand are somewhat incomplete because the antenna is not high enough and high buildings exist in the south of the station.

The Figure 4.5a shows the APT data when the satellite orbit passing directly on top of the station which look better than data received when the satellite orbit is far off nadir from the station (Figure 4.5b). The APT data have been received and collected since May 2005. Images with less distortion of Thailand will be selected for research. This also can be observed from duration time which satellites use to pass over the station.

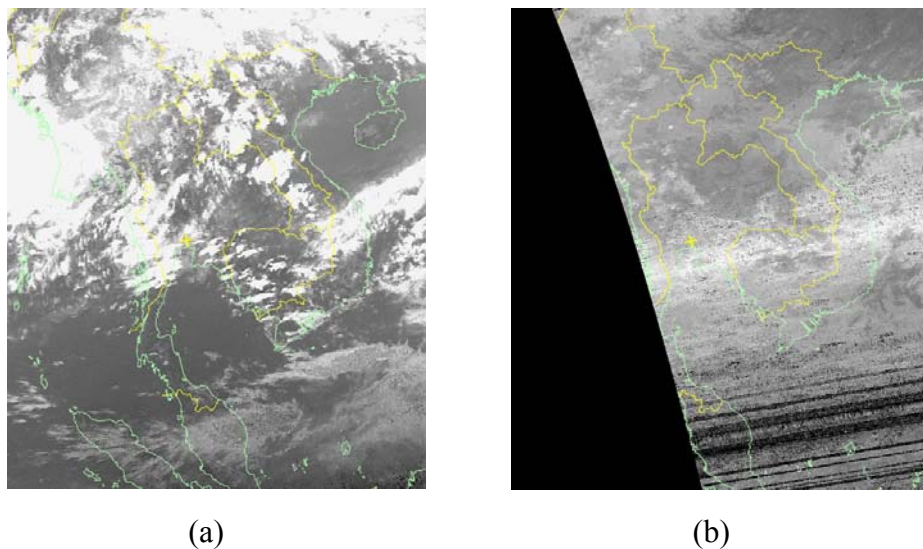


Figure 4.5 APT data from the receiving system constructed.

4.2 Processed APT and METAR data

4.2.1 Selected APT data

According to the selection criteria mentioned in 3.2.1, numbers of APT images were selected for 2 purposes as follows:

1) For raining condition analysis, the 23, 23, and 25 good-quality images were selected from the whole images received in year 2005, 2006, and 2007, respectively. Totally 71 APT images were selected for this purpose.

2) For the model validation, 7, 11, and 15 images covering Bangkok were selected from images received in year 2006, 2007, and 2008, respectively. Totally 33 APT images were selected for this purpose.

4.2.2 Processed APT data

4.2.2.1 Geo-referenced APT images

Selected APT images in the file format of .jpg were geo-referenced using Image World File method through ArcView geo-reference extension, as an example shown in Figure 4.6. The format of geo-referenced images is in form of .jpgw and can be further imported into the module for T_b determination developed by MATLAB.

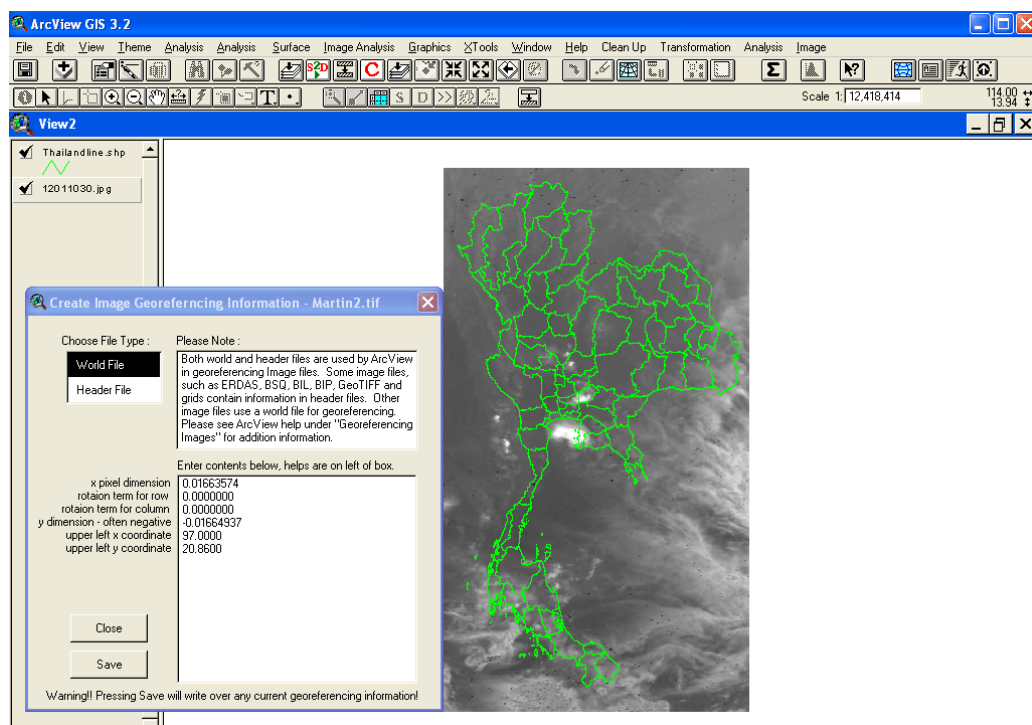


Figure 4.6 An example of geo-referenced APT image with overlay of Thailand administrative boundary.

4.2.2.2 Results of T_b determination

The sets of T_b were determined from processed APT data using the developed MATLAB module as mentioned in 3.2.2.2. The module was designed to work with imported APT data from NOAA 12, NOAA15, NOAA 17, and NOAA 18 only because the determination functions require constant value which is particularly the central wave number of each NOAA satellites as expressed in Equation 3.2. Figure 4.7 shows the interface of the module developed. From the interface, it shows that T_b in Kelvin and Celsius can be determined from APT data from both input data in forms of point by point and the subset of image data which resulted in .xls or .dbf file (Figure 4.8).

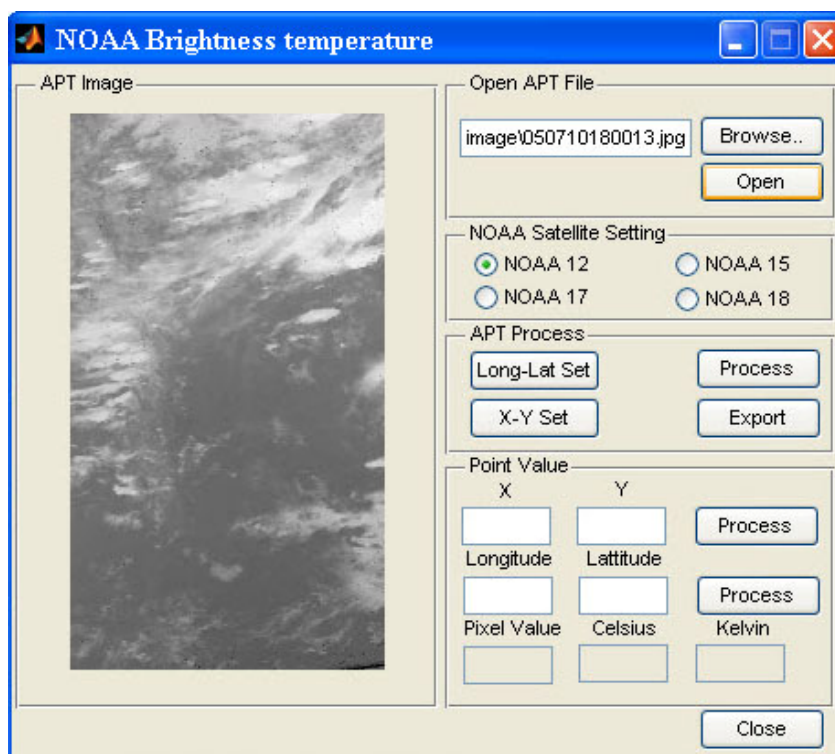


Figure 4.7 T_b determination interface of the module developed using MATLAB.

	A	B	C	D	E	F	G
1	X	Y	LONG	LAT	DN	TB_K	TB_C
2	194	416	100.26039782	13.95051145	161	258.5788	-14.5812
3	195	416	100.27703356	13.95051145	170	253.2095	-19.9505
4	196	416	100.29366930	13.95051145	180	246.7670	-26.3930
5	197	416	100.31030504	13.95051145	196	235.0609	-38.0991
6	198	416	100.32694078	13.95051145	222	209.3502	-63.8098
7	199	416	100.34357652	13.95051145	230	197.8484	-75.3116
8	200	416	100.36021226	13.95051145	241	173.3272	-99.8328
9	201	416	100.37684800	13.95051145	244	161.4197	-111.7403
10	202	416	100.39348374	13.95051145	244	161.4197	-111.7403
11	203	416	100.41011948	13.95051145	244	161.4197	-111.7403
12	204	416	100.42675522	13.95051145	244	161.4197	-111.7403
13	205	416	100.44339096	13.95051145	244	161.4197	-111.7403
14	206	416	100.46002670	13.95051145	244	161.4197	-111.7403
15	207	416	100.47666244	13.95051145	244	161.4197	-111.7403
16	208	416	100.49329818	13.95051145	244	161.4197	-111.7403
17	209	416	100.50993392	13.95051145	244	161.4197	-111.7403
18	210	416	100.52656966	13.95051145	244	161.4197	-111.7403
19	211	416	100.54320540	13.95051145	244	161.4197	-111.7403
20	212	416	100.55984114	13.95051145	244	161.4197	-111.7403
21	213	416	100.57647688	13.95051145	244	161.4197	-111.7403
22	214	416	100.59311262	13.95051145	244	161.4197	-111.7403
23	215	416	100.60974836	13.95051145	244	161.4197	-111.7403
24	216	416	100.62638410	13.95051145	244	161.4197	-111.7403
25	217	416	100.64301984	13.95051145	244	161.4197	-111.7403
26	218	416	100.65965558	13.95051145	244	161.4197	-111.7403
27	219	416	100.67629132	13.95051145	244	161.4197	-111.7403

Figure 4.8 Data table of determined T_b values of the subset of an APT image.

4.2.3 Processed METAR data

From 11 airport stations, their METAR data selected to match to the selected APT image data were prepared and tabulated in terms of date, time, NOAA number, airport ICAO code, T_b , RH, P, raining condition (rain or no rain). A complete data set of one APT image will consist of 11 records as an example shown in Figure 4.9. These data were further used for raining condition analysis described in 4.3.1.

From 2 airport stations, Suvarnabhumi airport and Donmuang airport, as method explained in 2) of 3.2.3, results were in forms of a table of point data within the validated area and their attributes of point positions, RH, and P as an example shown in Figure 4.10.

	Date	Time	NOAA No	ICAO Code	Tb_K	RH	Pressure	Rain_status
1	01.06.05	18:25	15	VTBD	243.1684	94	1001.0	1
2	01.06.05	18:25	15	VTSS	273.4211	59	1006.1	0
3	03.06.05	6:31	15	VTBD	269.7258	89	1003.0	0
4	03.06.05	6:31	15	VTSS	249.9119	94	1007.1	1
5	03.06.05	6:31	15	VTSP	260.4051	84	1006.4	0
6	11.06.05	6:42	15	VTBD	261.4036	79	1005.1	0
7	11.06.05	6:42	15	VTSM	273.4211	89	1007.8	0
8	11.06.05	6:42	15	VTSB	273.8819	94	1007.1	0
9	11.06.05	6:42	15	VTSF	266.8324	94	1007.5	0
10	15.06.05	6:47	15	VTBD	263.6170	84	1005.1	0
11	15.06.05	6:47	15	VTSM	266.3048	79	1008.5	0
12	15.06.05	6:47	15	VTSB	260.8410	94	1007.5	0
13	15.06.05	6:47	15	VTSF	248.6584	89	1007.8	0
14	15.06.05	6:47	15	VTSP	264.2325	79	1006.8	0

Figure 4.9 T_b and METAR data set for raining condition analysis.

	A	B	C	D	E	F
1	X	Y	LONG	LAT	RH	PRESSURE
2	194	416	100.26039782	13.95051145	83.7953	1005.0287
3	195	416	100.27703356	13.95051145	83.8134	1005.0262
4	196	416	100.29366930	13.95051145	83.8309	1005.0239
5	197	416	100.31030504	13.95051145	83.8477	1005.0216
6	198	416	100.32694078	13.95051145	83.8638	1005.0194
7	199	416	100.34357652	13.95051145	83.8791	1005.0173
8	200	416	100.36021226	13.95051145	83.8937	1005.0153
9	201	416	100.37684800	13.95051145	83.9075	1005.0134
10	202	416	100.39348374	13.95051145	83.9206	1005.0116
11	203	416	100.41011948	13.95051145	83.9327	1005.0098
12	204	416	100.42675522	13.95051145	83.9440	1005.0082
13	205	416	100.44339096	13.95051145	83.9544	1005.0068
14	206	416	100.46002670	13.95051145	83.9638	1005.0054
15	207	416	100.47666244	13.95051145	83.9721	1005.0042
16	208	416	100.49329818	13.95051145	83.9794	1005.0031
17	209	416	100.50993392	13.95051145	83.9856	1005.0022
18	210	416	100.52656966	13.95051145	83.9906	1005.0015
19	211	416	100.54320540	13.95051145	83.9944	1005.0009
20	212	416	100.55984114	13.95051145	83.9968	1005.0005
21	213	416	100.57647688	13.95051145	83.9980	1005.0003
22	214	416	100.59311262	13.95051145	83.9978	1005.0004
23	215	416	100.60974836	13.95051145	83.9964	1005.0005
24	216	416	100.62638410	13.95051145	83.9937	1005.0010
25	217	416	100.64301984	13.95051145	83.9901	1005.0016
26	218	416	100.65965558	13.95051145	83.9856	1005.0023
27	219	416	100.67629132	13.95051145	83.9806	1005.0032

Figure 4.10 RH and P data table derived from METAR data of Suvarnabhumi airport and Donmuang airport.

4.2.4 Input data for near-real time rainfall model

The 33 APT images were selected and extracted only point data falling into the validated area. Their attributes, which are positions of point data and T_b , were then combined with RH and P from METAR data as an example shown in Figure 4.11. They were input data for near-real time rainfall model.

	A	B	C	D	E	F	G	H	I
1	X	Y	LONG	LAT	DN	TB_K	TB_C	RH	PRESSURE
2	194	416	100.26039782	13.95051145	161	258.5788	-14.5812	83.7953	1005.0287
3	195	416	100.27703356	13.95051145	170	253.2095	-19.9505	83.8134	1005.0262
4	196	416	100.29366930	13.95051145	180	246.7670	-26.3930	83.8309	1005.0239
5	197	416	100.31030504	13.95051145	196	235.0609	-38.0991	83.8477	1005.0216
6	198	416	100.32694078	13.95051145	222	209.3502	-63.8098	83.8638	1005.0194
7	199	416	100.34357652	13.95051145	230	197.8484	-75.3116	83.8791	1005.0173
8	200	416	100.36021226	13.95051145	241	173.3272	-99.8328	83.8937	1005.0153
9	201	416	100.37684800	13.95051145	244	161.4197	-111.7403	83.9075	1005.0134
10	202	416	100.39348374	13.95051145	244	161.4197	-111.7403	83.9206	1005.0116
11	203	416	100.41011948	13.95051145	244	161.4197	-111.7403	83.9327	1005.0098
12	204	416	100.42675522	13.95051145	244	161.4197	-111.7403	83.9440	1005.0082
13	205	416	100.44339096	13.95051145	244	161.4197	-111.7403	83.9544	1005.0068
14	206	416	100.46002670	13.95051145	244	161.4197	-111.7403	83.9638	1005.0054
15	207	416	100.47666244	13.95051145	244	161.4197	-111.7403	83.9721	1005.0042
16	208	416	100.49329818	13.95051145	244	161.4197	-111.7403	83.9794	1005.0031
17	209	416	100.50993392	13.95051145	244	161.4197	-111.7403	83.9856	1005.0022
18	210	416	100.52656966	13.95051145	244	161.4197	-111.7403	83.9906	1005.0015
19	211	416	100.54320540	13.95051145	244	161.4197	-111.7403	83.9944	1005.0009
20	212	416	100.55984114	13.95051145	244	161.4197	-111.7403	83.9968	1005.0005
21	213	416	100.57647688	13.95051145	244	161.4197	-111.7403	83.9980	1005.0003
22	214	416	100.59311262	13.95051145	244	161.4197	-111.7403	83.9978	1005.0004
23	215	416	100.60974836	13.95051145	244	161.4197	-111.7403	83.9964	1005.0005
24	216	416	100.62638410	13.95051145	244	161.4197	-111.7403	83.9937	1005.0010
25	217	416	100.64301984	13.95051145	244	161.4197	-111.7403	83.9901	1005.0016
26	218	416	100.65965558	13.95051145	244	161.4197	-111.7403	83.9856	1005.0023
27	219	416	100.67629132	13.95051145	244	161.4197	-111.7403	83.9806	1005.0032

Figure 4.11 An example of input data for near-real time rainfall model.

4.3 The developed near-real time rainfall model

4.3.1 Decision tree for raining condition analysis

The climatic analysis for raining condition is the process of analysis for seeking the positions which have the opportunity to rain. The 3 parameters, T_b from selected APT data, RH and P values from METAR data report with temporal corresponding to selected APT images were used in this process. The relationships of T_b , RH, and P to raining condition (raining or no raining) as an example shown in

Figure 4.9 were analyzed orderly. The 755 records of data during May to October in year 2005-2007 were employed for analysis. These three parameters were categorized based on relationship of them to raining condition. In cases of raining, their probabilities were estimated. Finally, the decision tree of raining condition analysis was able to establish.

1) Relationship of T_b and raining condition data

The T_b and the raining condition of 755 data records (see Appendix F) were plotted as shown in Figure 4.12. Then, T_b can be categorized into 3 groups, namely $< 250K$ for high possibility to raining, $250K-270K$ for some possibility to raining, and $> 270K$ for no raining.

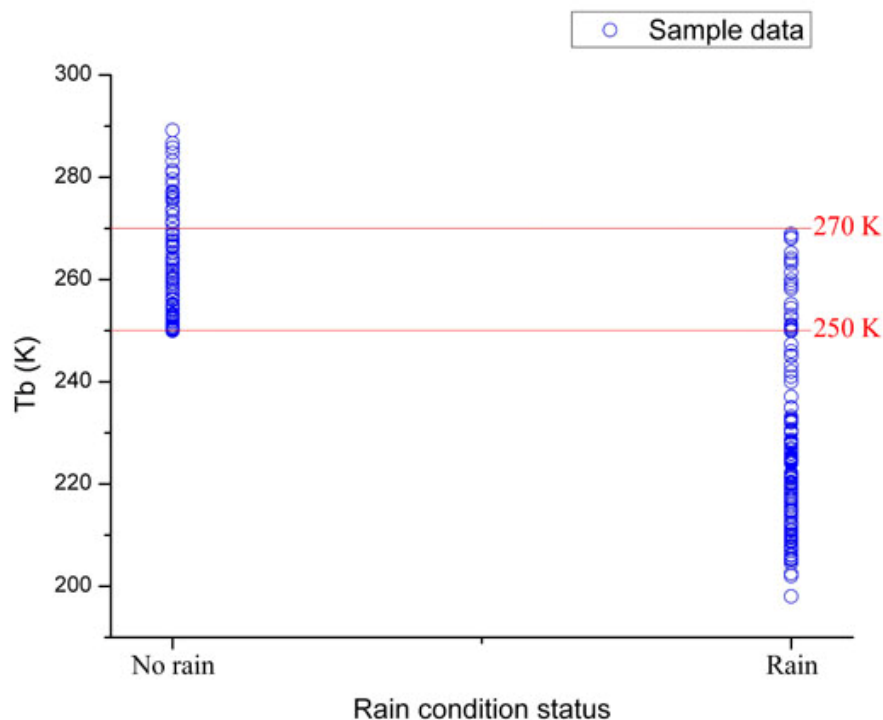


Figure 4.12 Relationship between T_b and raining condition.

2) Relationship of RH and P to raining condition data

The 755 data records of RH and P related to the raining condition were plotted as shown in Figure 4.13 and Figure 4.14 respectively. RH can be categorized into 3 groups, namely $\geq 89\%$ for high possibility to raining, 71-88% for some possibility to raining, and $< 71\%$ for no raining.

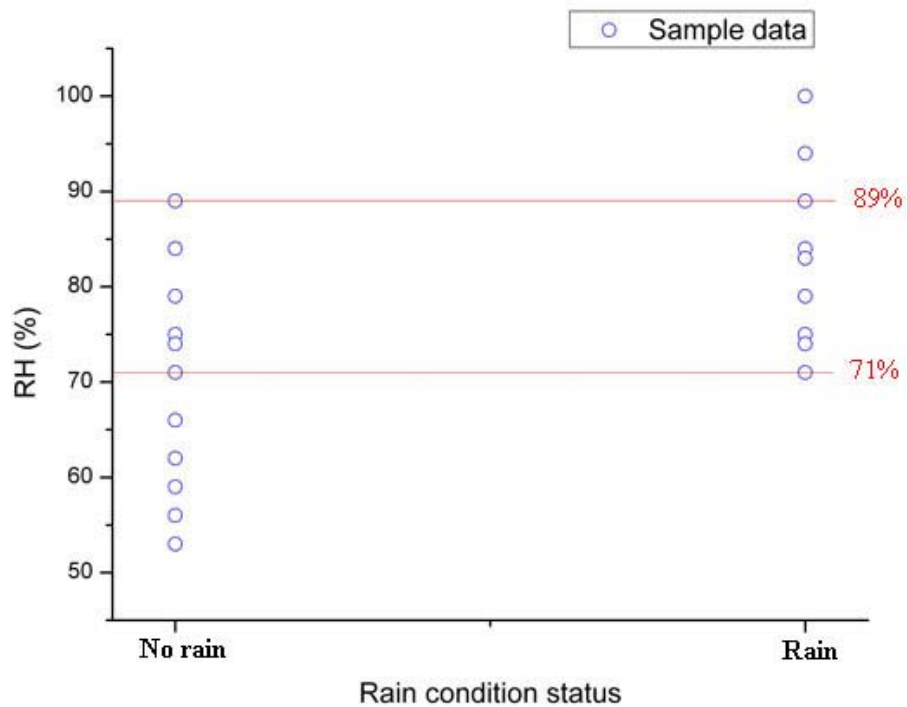


Figure 4.13 Relationship between RH and raining condition.

The P can be categorized into 3 groups which are < 1005 MB, 1005-1010 MB and > 1010 MB. The relationships of these three categories to raining condition were varied according to varying categories of T_b and RH.

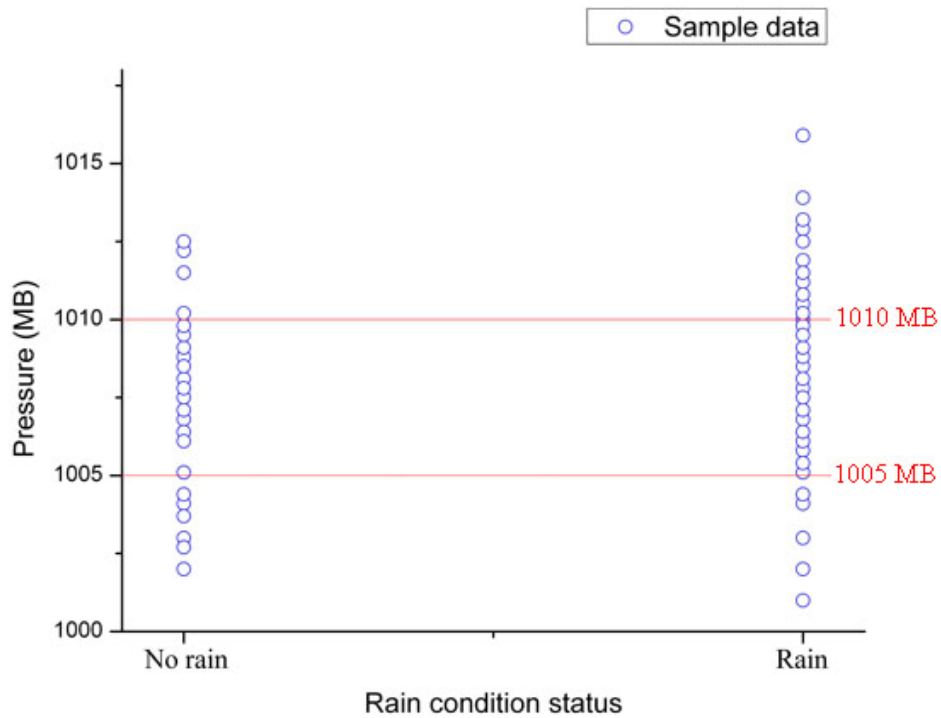


Figure 4.14 Relationship between P and raining condition.

3) Decision tree

Categories of T_b , RH, and P related to raining condition as discussed above were able to express as decision tree for rain conditioning analysis as shown in Figure 4.15 (more detail see Appendix G).

According to data analysis on the raining condition, based on T_b , RH and P values, each value can be divided into 3 groups (Figure 4.12-4.14). T_b and RH can identify the period with certain, possible and impossible raining potential so these two values are the keys for decision tree analysis respectively. T_b is the first value for consideration because it can accurately identify the cloud, forming the rain. The area with high RH is also highly potential for rainfall. P cannot be clearly divided into three groups but it can be used to filter the value forming rain in some case, led to

more accurate decision tree analysis. According to trial to P adjustment used for decision tree, it was found that P, ranging 1005-1010 MB can filter the status of rainfall more accurate.

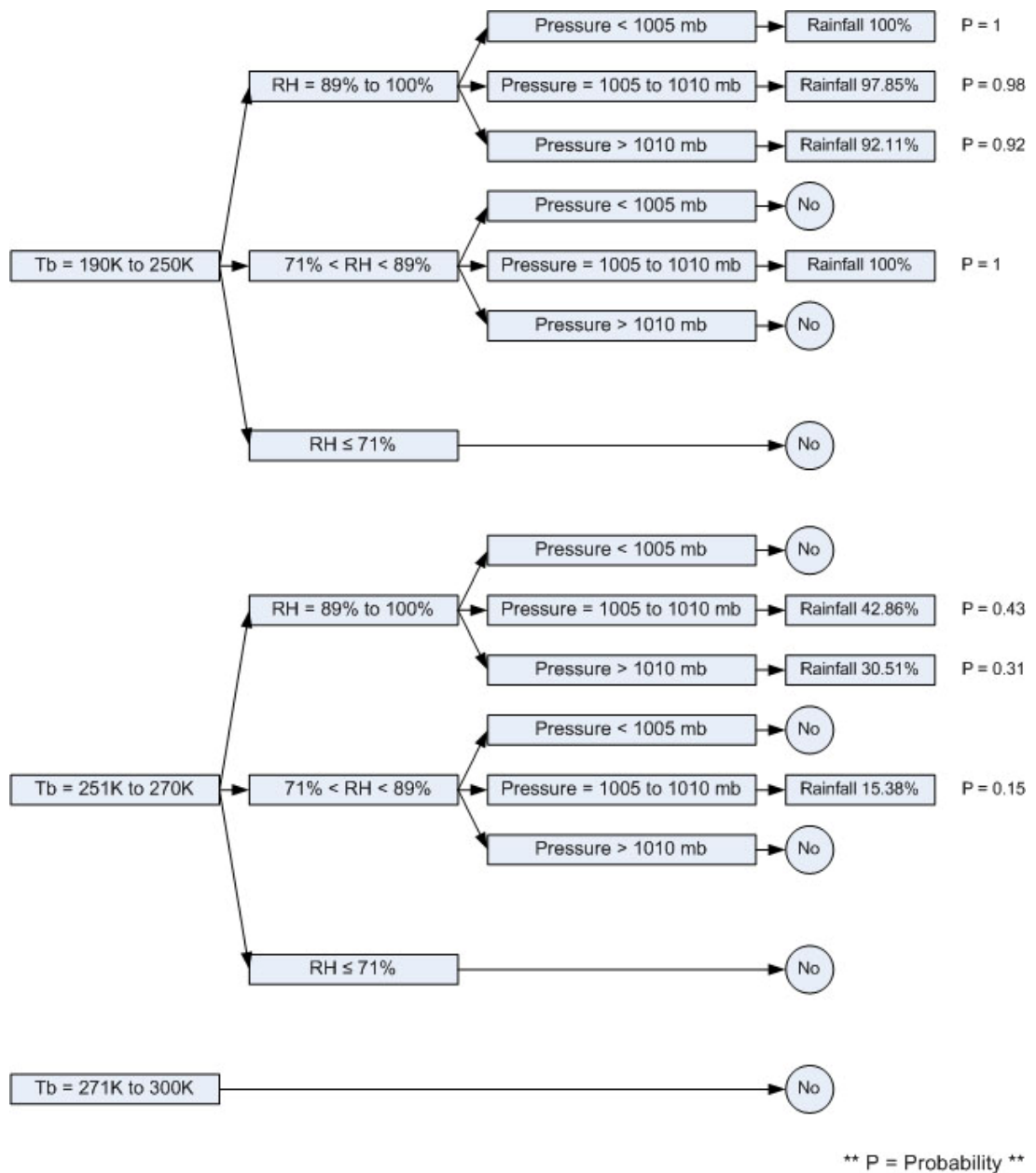


Figure 4.15 Decision tree for rain conditioning analysis.

Theoretically, if $P < 1005$ MB, there is more chance to be rain. Skeptically, in this study only 8 cases that $P < 1005$ MB existed and they all showed entirely no rain.

4.3.2 Regression models for rain rate estimation

Only T_b of events having probability of raining, which were filtered using decision tree (Figure 4.15) as mentioned in 1) of 3.2.1 and rain rate data recorded by the TMD covering data of years 2005, 2006, 2007, and the whole 3 years, were plotted and formulated to be 4 regression models.

1) In year 2005, 152 records of T_b and rain rate values were plotted as shown in Figure 4.16 and regression fit curve can be expressed in Equation 4.1, where x is T_b in Kelvin. Coefficient of determination R^2 is 0.93.

$$\text{Rainrate} = 35345.93348 \exp\left(\frac{-x}{26.84541}\right) - 3.41178 \quad (4.1)$$

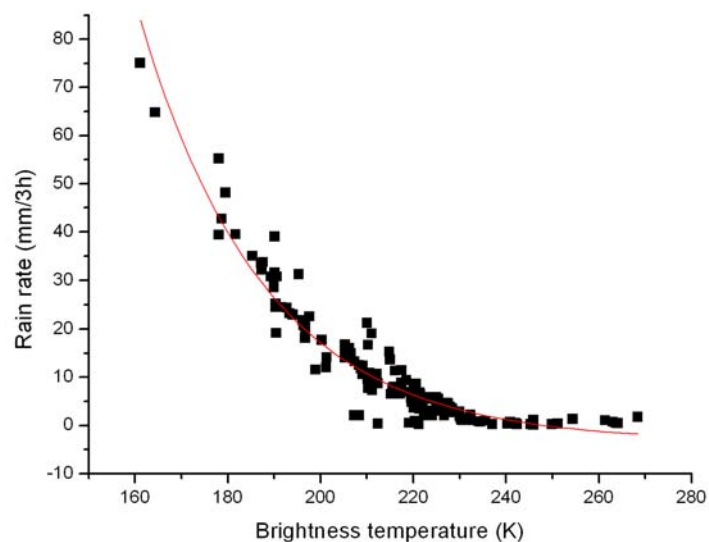


Figure 4.16 Fit curve of T_b and rain rate records in year 2005.

2) In year 2006, 163 records of T_b and rain rate values were plotted as shown in Figure 4.17 and regression fit curve can be expressed in Equation 4.2, with R^2 of 0.90.

$$\text{Rainrate} = 61887.18365 \exp\left(\frac{-x}{19.17829}\right) + 0.9992 \quad (4.2)$$

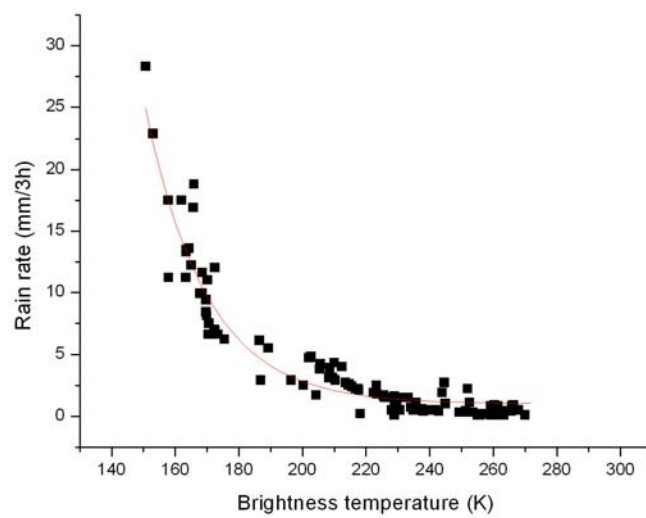


Figure 4.17 Fit curve of T_b and rain rate records in year 2006.

3) In year 2007, 145 records of T_b and rain rate values were plotted as shown in Figure 4.18 and regression fit curve can be expressed in Equation 4.3, with R^2 of 0.92.

$$\text{Rainrate} = 155998.55576 \exp\left(\frac{-x}{18.46962}\right) + 0.88151 \quad (4.3)$$

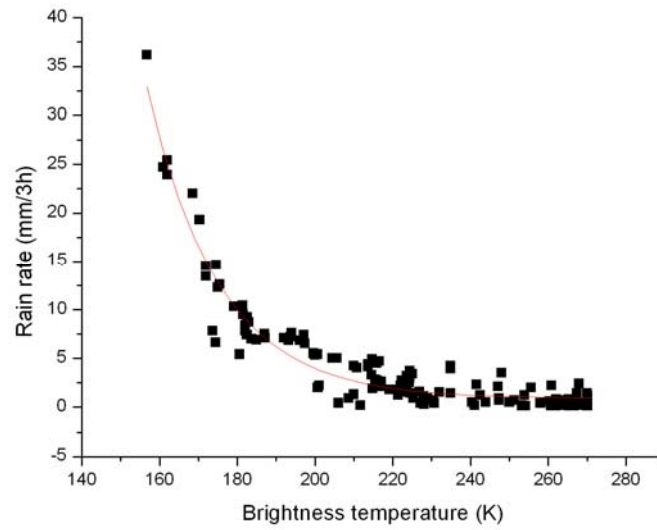


Figure 4.18 Fit curve of T_b and rain rate records in year 2007.

4) In year 2005-2007, 460 records of T_b and rain rate values were plotted as shown in Figure 4.19 and regression fit curve can be expressed in Equation 4.4, with R^2 of 0.41.

$$\text{Rainrate} = 526.3657 \exp\left(\frac{-x}{53.67379}\right) - 3.94351 \quad (4.4)$$

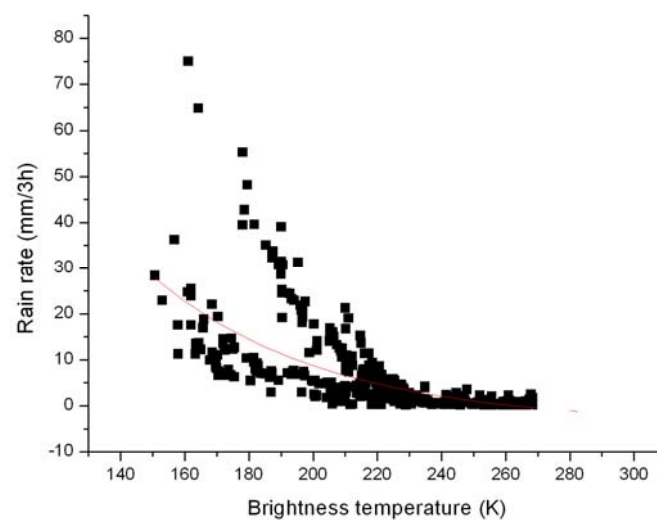


Figure 4.19 Fit curve of T_b and rain rate records in year 2005-2007.

These regression equations are tabulated as shown in Table 4.1.

Table 4.1 Regression equations showing relationships between T_b and rain rates recorded in year 2005, 2006, 2007, and 2005-2007.

Year recorded	Regression equation
2005	$Rainrate = 35345.93348 \exp\left(\frac{-x}{26.84541}\right) - 3.41178$
2006	$Rainrate = 61887.18365 \exp\left(\frac{-x}{19.17829}\right) + 0.9992$
2007	$Rainrate = 155998.55576 \exp\left(\frac{-x}{18.46962}\right) + 0.88151$
2005-2007	$Rainrate = 526.3657 \exp\left(\frac{-x}{53.67379}\right) - 3.94351$

Where x is T_b in Kelvin.

These equations were further operated with T_b from APT images and rain rate data recorded by the 71 stations in Bangkok area for the validation purpose.

4.3.3 The developed MATLAB module for the near-real time rainfall model

The principle of near-real time rainfall estimation model design is to combine decision tree for raining condition analysis and the regression models for rain rate estimation to be together. The operation steps of the model can be displayed as flow diagram in Figure 4.20. This was developed to be the module using MATLAB coding. Examples of MATLAB codes in parts of raining condition analysis and rain rate estimation were shown in Appendix H.

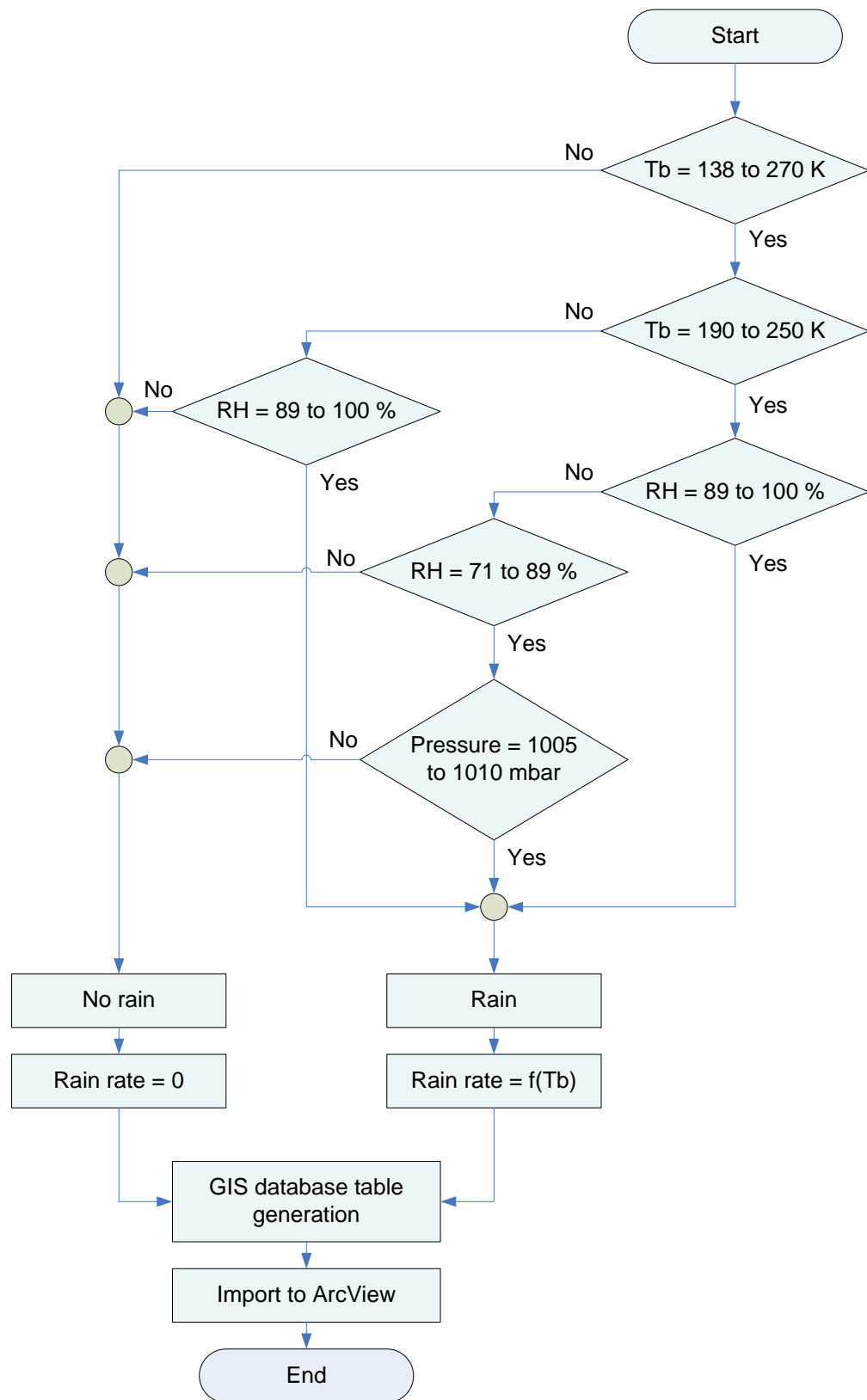


Figure 4.20 Flow diagram of the near-real time rainfall model.

The interface of the module with dialogue boxes of input data, output data, estimation process and buttons of run and view was displayed in Figure 4.21. The output data table from the module consists of point locations in Latitude and Longitude, raining condition (1-raining and 0-no raining), and rain rate as shown in Figure 4.22. The output data can be further generated to be GIS layer of grid point data with attributes of raining condition and rain rate estimated from regression models (Figure 4.23). As same as other GIS data layers, it can be queried for certain answer, for example, showing points with raining and no raining as displayed in Figure 4.24.

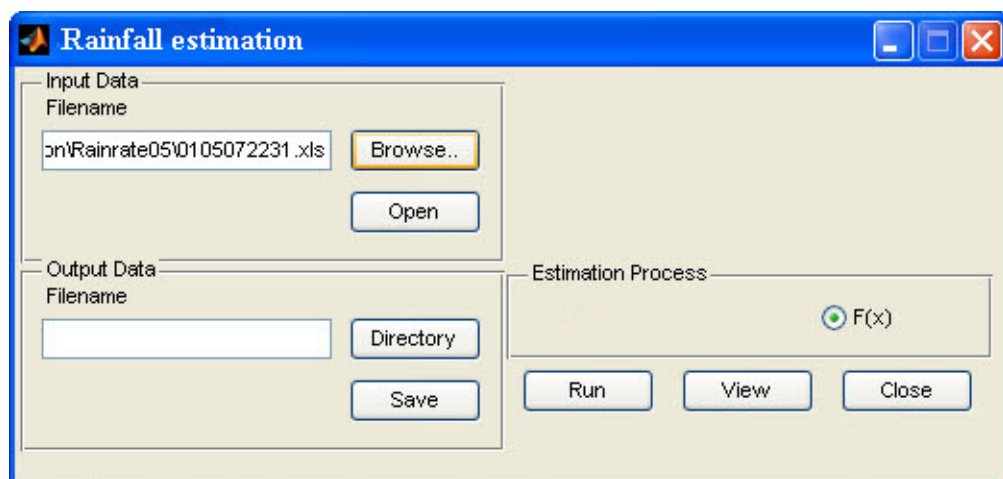


Figure 4.21 Module interface of the near-real time rainfall model, developed using MATLAB.

	A	B	C	D	E	F
1	X	Y	LONG	LAT	RAINFALL	RAINRATE
2	194	416	100.26039782	13.95051145	0	0
3	195	416	100.27703356	13.95051145	0	0
4	196	416	100.29366930	13.95051145	1	0.756614063
5	197	416	100.31030504	13.95051145	1	2.095058434
6	198	416	100.32694078	13.95051145	1	10.82194633
7	199	416	100.34357652	13.95051145	1	19.93328533
8	200	416	100.36021226	13.95051145	0	0
9	201	416	100.37684800	13.95051145	0	0
10	202	416	100.39348374	13.95051145	0	0
11	203	416	100.41011948	13.95051145	0	0
12	204	416	100.42675522	13.95051145	0	0
13	205	416	100.44339096	13.95051145	0	0
14	206	416	100.46002670	13.95051145	0	0
15	207	416	100.47666244	13.95051145	0	0
16	208	416	100.49329818	13.95051145	0	0
17	209	416	100.50993392	13.95051145	0	0
18	210	416	100.52656966	13.95051145	0	0
19	211	416	100.54320540	13.95051145	0	0
20	212	416	100.55984114	13.95051145	0	0
21	213	416	100.57647688	13.95051145	0	0
22	214	416	100.59311262	13.95051145	0	0
23	215	416	100.60974836	13.95051145	0	0
24	216	416	100.62638410	13.95051145	0	0
25	217	416	100.64301984	13.95051145	0	0
26	218	416	100.65965558	13.95051145	0	0
27	219	416	100.67629132	13.95051145	0	0

Figure 4.22 An example of output data table from the module of near-real time rainfall model.

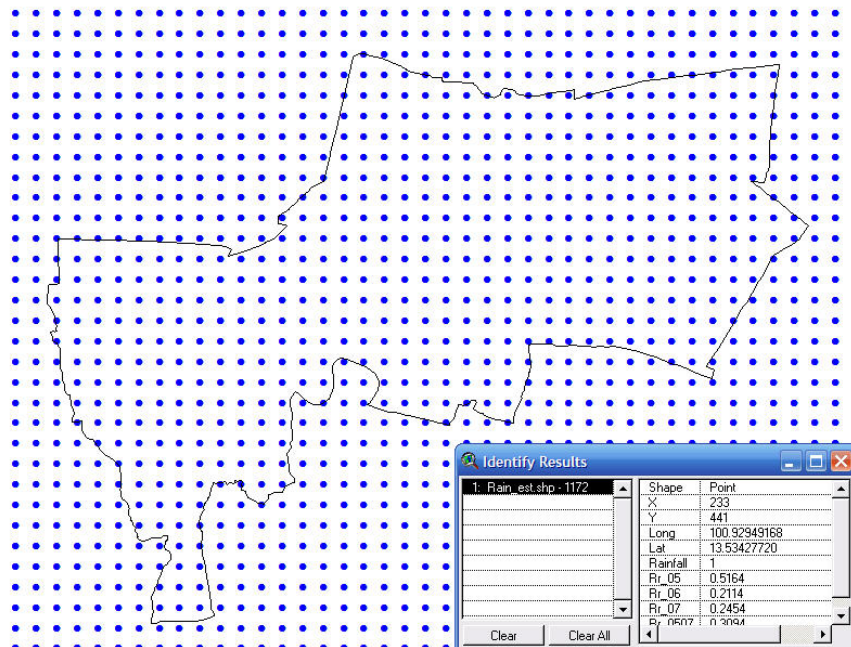


Figure 4.23 GIS grid point data with attributes of raining condition and rain rates.

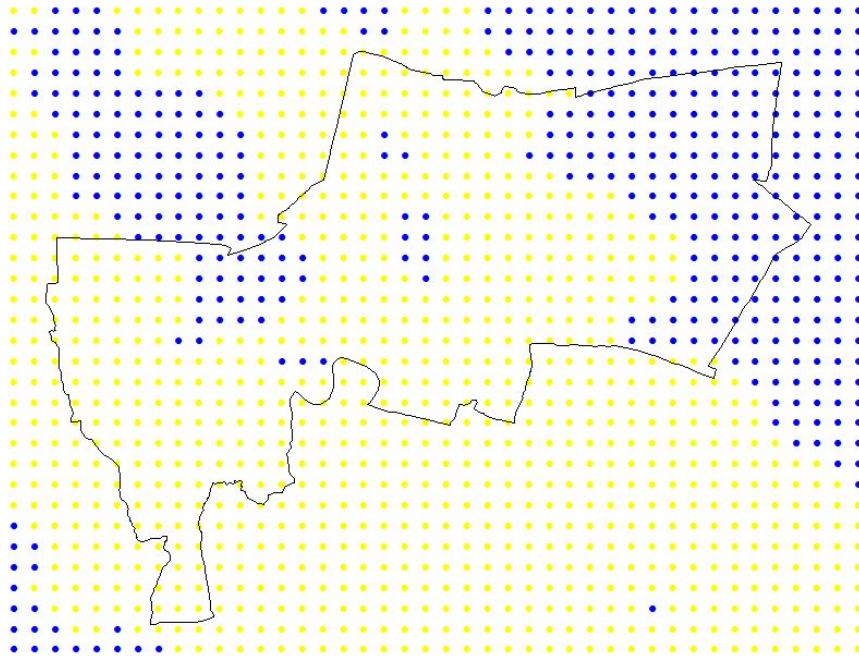


Figure 4.24 Grid point data showing raining (yellow) and no-raining (blue).

4.4 Results of near-real time rainfall model validation

The total 33 APT images in June-October, 2006-2008 were selected for georeferencing and T_b determination and then input into the model. To validate the developed near-real time rainfall model is to take the results from the model to compare with the rainfall values measured from 71 rainfall measurement stations in Bangkok which are scattered around the study area. Due to the fact that the actual time interval of rainfall measurement is in every 15 minutes, therefore, the rain rate estimated from the module which is in the unit of mm/3 hours has to be adjusted to be in the unit rain rate measured in mm/15 minutes too. The mode, average, and ratio of rainfall measurement period within every 3 hours, from the records of the 28 stations (selected from total 71 rainfall measurement stations of the Department of Drainage and Sewerage, Bangkok Metropolitan), in May-October year 2007, were determined

and used as controlling conditions in accuracy assessment. From these data, the results show that the mode, average, and ratio of rainfall periods within every 3 hours is 2, 3.576, and 12 periods, respectively. Therefore, the outputs of rain rate estimated from the model have to be divided by these numbers before using to compare with the actual measurement values.

To firstly validate the near-real time rainfall model is to verify whether it rains or not at the corresponding position between any pixels of image which provides T_b and the station. The second is to assess the accuracy of rain rate received from the model and the actual measurement from the stations. This validation was operated with and without involvement of wind speed and direction at the measurement time and 15 minutes after that.

Also, due to the limitation of the measurement equipment which can detect only rain rate ≥ 0.5 mm, the comparisons were conducted additionally to this limitation of the equipment.

4.4.1 Without wind involvement

4.4.1.1 Comparison of raining condition

a) With rain rate estimation from models(equations) of the years 2005, 2006, 2007, and 2005-2007, the results revealed that the raining condition errors (the raining condition resulted from the models and stations were different) are equal in all types of time interval considered and they are respectively 35.569%, 39.285%, 26.757%, and 35.569% as shown in Table 4.2. The average of errors from those equations is 34.295%.

Table 4.2 Near-real time raining condition errors resulted from the models of the years 2005, 2006, 2007, and 2005-2007.

	Time interval type	Model	Raining condition error (%)	Average raining condition error (%)
Raining condition error in near-real time	Mode	Year 2005	35.569	34.295
		Year 2006	39.285	
		Year 2007	26.757	
		Year 2005-2007	35.569	
	Average	Year 2005	35.569	34.295
		Year 2006	39.285	
		Year 2007	26.757	
		Year 2005-2007	35.569	
	Ratio	Year 2005	35.569	34.295
		Year 2006	39.285	
		Year 2007	26.757	
		Year 2005-2007	35.569	

b) With rain rate estimation ≥ 0.5 mm, from models of the years 2005, 2006, 2007, and 2005-2007, the results revealed that the raining condition errors are different among different types of time interval as shown in Table 4.3. The minimum average raining condition error is 16.502% which falls in to the ratio type of time interval. The errors are 13.945%, 24.625%, 15.135%, and 12.301%, respectively.

4.4.1.2 Comparison of rain rate

a) With rain rate estimation from models of the years 2005, 2006, 2007, and 2005-2007, the results revealed that rain rate RMSEs (the rain rate resulted from the models and stations were different) are different among different types of time interval as shown in Table 4.4. The minimum average rain rate RMSE is 0.602 mm/15minutes. which falls into the ratio type of time interval. The RMSEs are 0.576, 0.535, 0.728, and 0.567 mm/15minutes, respectively.

Table 4.3 Near-real time raining condition error resulted from the models of the years 2005, 2006, 2007, and 2005-2007 which assume that rain rate < 0.5 is equal to 0 mm.

	Time interval type	Model	Raining condition error (%)	Average raining condition error (%)
Raining condition error in near-real time	Mode	Year 2005	31.832	25.435
		Year 2006	12.369	
		Year 2007	24.625	
		Year 2005-2007	32.914	
	Average	Year 2005	29.743	22.580
		Year 2006	11.270	
		Year 2007	18.463	
		Year 2005-2007	30.842	
	Ratio	Year 2005	13.945	16.502
		Year 2006	24.625	
		Year 2007	15.135	
		Year 2005-2007	12.301	

Table 4.4 Near-real time rain rate RMSEs resulted from the models of the years 2005, 2006, 2007, and 2005-2007.

	Time interval type	Model	Rain rate RMSE (mm/15 minutes)	Average rain rate RMSE (mm/15 minutes)
Rain rate RMSE in near-real time	Mode	Year 2005	1.165	0.903
		Year 2006	0.676	
		Year 2007	0.798	
		Year 2005-2007	0.971	
	Average	Year 2005	0.821	0.727
		Year 2006	0.591	
		Year 2007	0.750	
		Year 2005-2007	0.747	
	Ratio	Year 2005	0.576	0.602
		Year 2006	0.535	
		Year 2007	0.728	
		Year 2005-2007	0.567	

b) With rain rate estimation ≥ 0.5 mm, from models of the years 2005, 2006, 2007, and 2005-2007, the results revealed that rain rate RMSEs are different among different types of time interval as shown in Table 4.5. The minimum average rain rate RMSE is 0.583 mm/15 minutes. which falls into the ratio type of time interval. The RMSEs are 0.545, 0.525, 0.728, and 0.532 mm/15 minutes, respectively.

Table 4.5 Near-real time rain rate RMSEs resulted from the models of the year 2005, 2006, 2007, and 2005-2007 which assumes that rain rate < 0.5 is equal to 0 mm.

	Time interval type	Model	Rain rate RMSE (mm/15 minutes)	Average rain rate RMSE (mm/15 minutes)
Rain rate RMSE in near-real time	Mode	Year 2005	1.172	0.907
		Year 2006	0.681	
		Year 2007	0.801	
		Year 2005-2007	0.973	
	Average	Year 2005	0.825	0.711
		Year 2006	0.526	
		Year 2007	0.744	
		Year 2005-2007	0.748	
	Ratio	Year 2005	0.545	0.583
		Year 2006	0.525	
		Year 2007	0.728	
		Year 2005-2007	0.532	

4.4.2 With wind involvement

4.4.2.1 Comparison of raining condition

a) With rain rate estimation from models of the years 2005, 2006, 2007, and 2005-2007, the results revealed that the raining condition errors are equal in all types of time interval considered and they are respectively 35.176%, 38.602%, 26.434%, and 35.176% as shown in Table 4.6. The average of errors from those equations is 33.847%.

Table 4.6 After 15 minutes received APT data raining condition error resulted from the models of the years 2005, 2006, 2007, and 2005-2007.

	Time interval type	Model	Raining condition error (%)	Average raining condition error (%)
Raining condition error after 15 minutes received APT data	Mode	Year 2005	35.176	33.847
		Year 2006	38.602	
		Year 2007	26.434	
		Year 2005-2007	35.176	
	Average	Year 2005	35.176	33.847
		Year 2006	38.602	
		Year 2007	26.434	
		Year 2005-2007	35.176	
	Ratio	Year 2005	35.176	33.847
		Year 2006	38.602	
		Year 2007	26.434	
		Year 2005-2007	35.176	

b) With rain rate estimation ≥ 0.5 mm, from models of the years 2005, 2006, 2007, and 2005-2007, the results revealed that the raining condition errors are different among different types of time interval as shown in Table 4.7. The minimum average raining condition error is 13.497% which falls into the ratio type of time interval. The errors are 14.428%, 11.932%, 15.158%, and 12.471%, respectively.

4.4.2.2 Comparison of rain rate

a) With rain rate estimation from models of the years 2005, 2006, 2007, and 2005-2007, the results revealed that rain rate RMSEs (the rain rate resulted from the models and stations were different) are different among different types of time interval as shown in Table 4.8. The minimum average rain rate RMSE is 0.538 mm/15 minutes. which falls into the ratio type of time interval. The RMSEs are 0.528, 0.458, 0.655, and 0.511 mm/15 minutes, respectively.

Table 4.7 After 15 minutes received APT data, raining condition error resulted from the models of the years 2005, 2006, 2007, and 2005-2007 which assume that rain rate < 0.5 is equal to 0 mm.

	Time interval type	Model	Raining condition error (%)	Average raining condition error (%)
Raining condition error after 15 minutes received APT data	Mode	Year 2005	32.035	30.817
		Year 2006	35.847	
		Year 2007	24.152	
		Year 2005-2007	31.232	
	Average	Year 2005	29.700	22.467
		Year 2006	12.587	
		Year 2007	19.305	
		Year 2005-2007	28.276	
	Ratio	Year 2005	14.428	13.497
		Year 2006	11.932	
		Year 2007	15.158	
		Year 2005-2007	12.471	

Table 4.8 After 15 minutes received APT data, rain rate RMSEs resulted from the models of the years 2005, 2006, 2007, and 2005-2007.

	Time interval type	Model	Rain rate RMSE (mm/15 minutes)	Average rain rate RMSE (mm/15 minutes)
Rain rate error after 15 minutes received APT data	Mode	Year 2005	1.084	0.838
		Year 2006	0.602	
		Year 2007	0.737	
		Year 2005-2007	0.930	
	Average	Year 2005	0.764	0.662
		Year 2006	0.515	
		Year 2007	0.680	
		Year 2005-2007	0.688	
	Ratio	Year 2005	0.528	0.538
		Year 2006	0.458	
		Year 2007	0.655	
		Year 2005-2007	0.511	

b) With rain rate estimation ≥ 0.5 mm, from models of the years 2005, 2006, 2007, and 2005-2007, the results revealed that rain rate RMSEs are different among different types of time interval as shown in Table 4.9. The minimum average rain rate RMSE is 0.521 mm/15minutes. which falls into the ratio type of time interval. The RMSEs are 0.504, 0.499, 0.650, and 0.481 mm/15minutes, respectively.

Table 4.9 After 15 minutes received APT data, rain rate RMSEs resulted from the models of the years 2005, 2006, 2007, and 2005-2007 which assume that rain rate < 0.5 is equal to 0 mm.

	Time interval type	Model	Rain rate RMSE (mm/15 minutes)	Average rain rate RMSE (mm/15minutes)
Rain rate error after 15 minutes received APT data	Mode	Year 2005	1.089	0.838
		Year 2006	0.600	
		Year 2007	0.735	
		Year 2005-2007	0.929	
	Average	Year 2005	0.766	0.645
		Year 2006	0.453	
		Year 2007	0.684	
		Year 2005-2007	0.675	
	Ratio	Year 2005	0.504	0.521
		Year 2006	0.449	
		Year 2007	0.650	
		Year 2005-2007	0.481	

4.5 Discussion on validation results

4.5.1 Raining condition error discussion

When the actual rain rates from the model were considered, raining condition error (rain / no rain error) of each model (2005, 2006, 2007, and 2005-2007) is the same in every time interval type (mode, average, and ratio). With wind

involvement in consideration, it shows that the error is still the same for each time interval but less error.

To make it corresponding to the measurement ability of rain gauges, if the rain rate from each model is < 0.5 it was regarded to be equal to 0 mm. In cases like these, the results show that the raining condition errors of all models are reduced. The ratio time interval shows minimum error while the mode time interval shows the highest as shown in Figure 4.25. This indicates that the model that can provide the best result for raining condition is the model of the year 2006 with ratio time interval. Therefore, if this model is applied for prediction the result can be expected to have an error up to 11.270%.

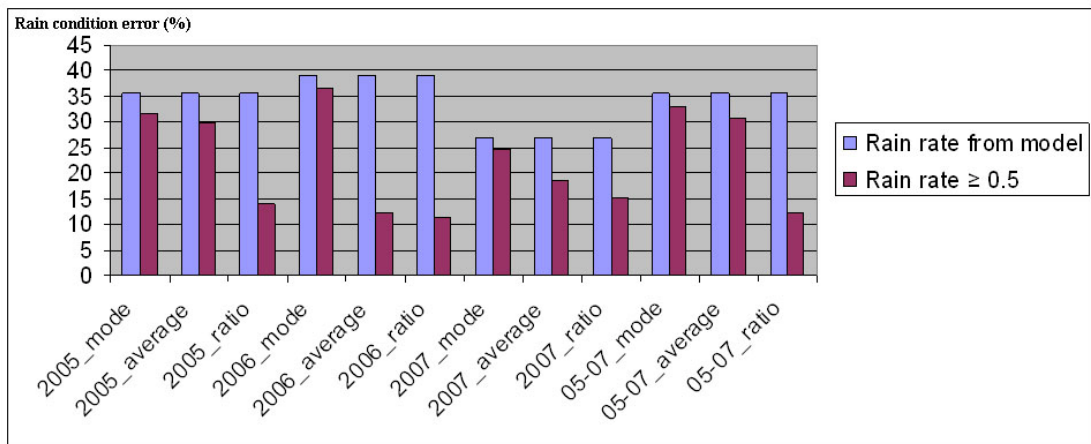


Figure 4.25 Comparison of raining condition errors between the actual rain rates estimated from the models and when measurement ability of rain gauge is involved.

When wind speed and direction were applied for consideration, the raining condition errors of all models are the same for each time interval type and the errors are decreased for all models as shown in Figure 4.26. Therefore, it indicates that the

wind show influence on prediction accuracy. If the more accurate wind behavior can be provided, the better result can be expected.

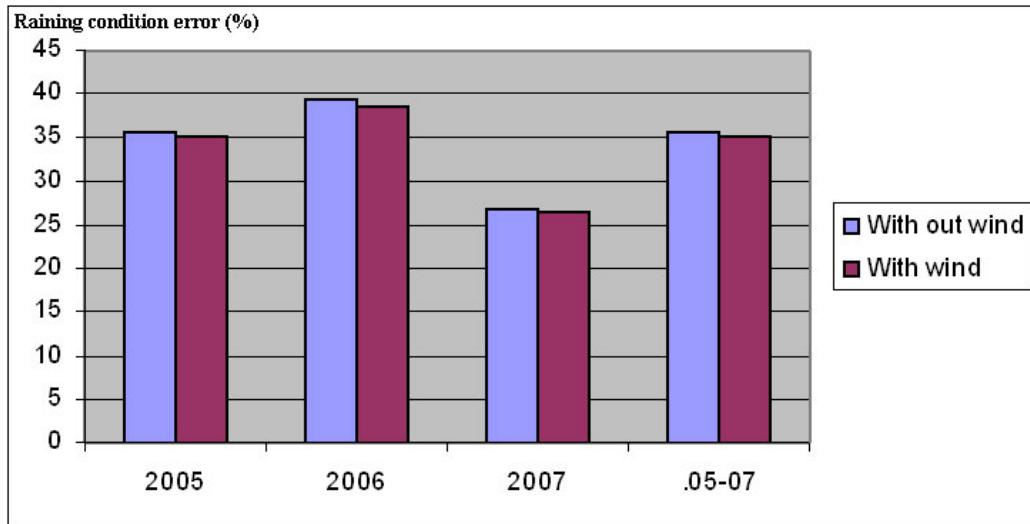


Figure 4.26 Comparison of raining condition errors when wind and without wind are considered.

However, when measurement ability of rain gauge is brought to consider with wind and without wind, the results show not much different as shown in Figure 4.27. Almost all of differences are less than 2%. Again, using the ratio time interval of the 2006 model still shows the best results with least errors which are 11.270% and 11.932% without wind and with wind, respectively.

4.5.2 Rain rate RMSE discussion

When RMSEs of rain rates from the models and measurement ability of rain gauge are considered (rain rate < 0.5 is equal to 0 mm.), the results show that the predicted rain rates using 2006 are the best (Figure 4.28). They show comparative lowest errors in all types of time interval. Within the model 2006, using the ratio and

average time interval are about the same. They show the best results. It means that if the 2006 model is used, the best predicted rain rate could be error ± 0.525 mm/15 minutes and the worst could be ± 1.172 mm/15 minutes when the 2005 model is used.

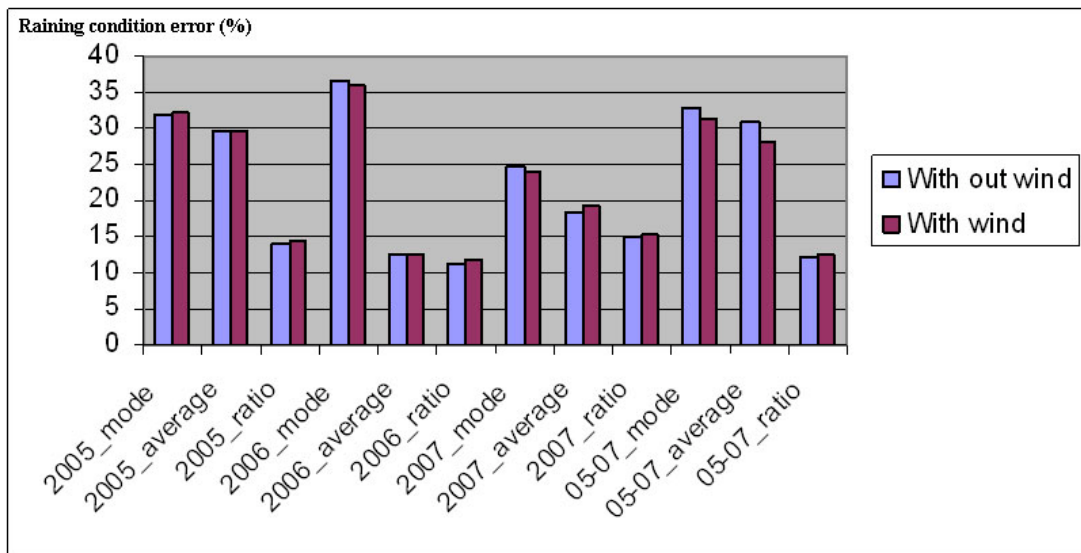


Figure 4.27 Comparison of raining condition errors when wind and measurement ability of rain gauge are considered simultaneously.

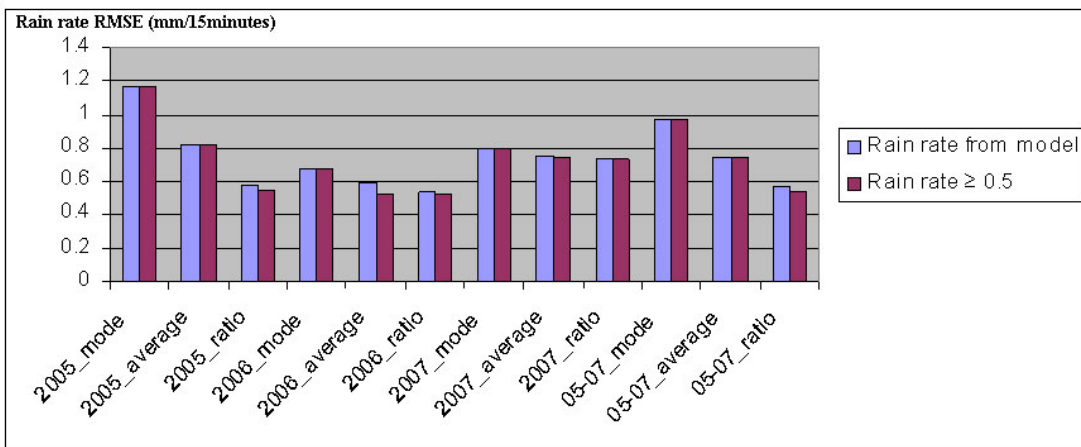


Figure 4.28 Comparison of rain rate RMSEs with and without measurement ability of rain gauge involved.

Figure 4.29 and Figure 4.30 show the comparison of rain rate RMSEs of the models when wind speed and direction are brought to consider without and with measurement ability of rain gauge involved, respectively. It is obvious that, for both Tables, with wind consideration provides better results. However, the differences are not highly significant. It is very interesting to note that the 2006 model of both Tables still provides the best results. Its conditions of ratio time interval and wind show the lowest errors which is 0.458 and 0.449 mm/15 minutes. Therefore, the best predicted rain rate can be achieved using the 2006 model while the worst can be when using the 2005 model.

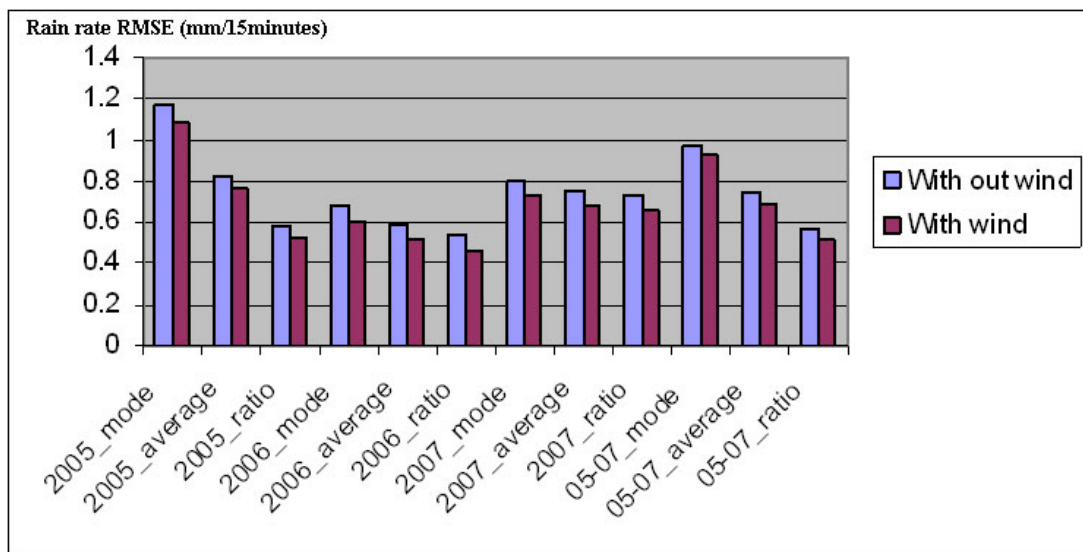


Figure 4.29 Comparison of rain rate RMSEs when wind and without wind are considered.

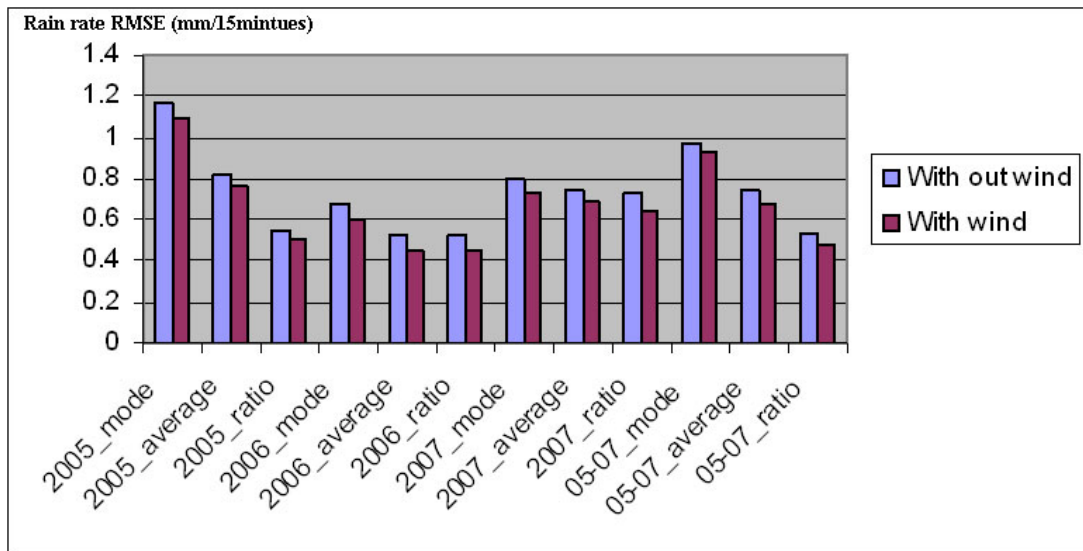


Figure 4.30 Comparison of rain rate RMSEs when wind, and measurement ability of rain gauge are considered simultaneously.

CHAPTER V

CONCLUSION AND RECOMMENDATION

5.1 Conclusions

1) The main objective of this study is to construct low cost and easy installation NOAA-APT receiving system and to develop near-real time rainfall estimation model. The selected APT data received were reformatted in terms of conversion to be GIS point data, geo-referencing and T_b determination. These data together with ground meteorological data including RH and P were input into the rainfall models which can return the spatial rain condition and rain rate. The rainfall models were developed as the module using MATLAB.

2) The APT signals receiving system was constructed at the location, Soi Lat Pla Khao 64 in Bangkok. The system operation and data acquired have been constantly examined for longer than six years. It is proved that the APT receiving system is low cost, easy self-construction and installation, providing free and reliable data anytime when required, and creating no interference to any radio communication system. The signals received are available for real-time processing.

3) Two modules developed under the MATLAB environment have been working properly. These include the modules for converting DN of APT images to be T_b and for determining spatially rain condition and rain rate. The time spends from the beginning of acquiring data through the modules operation will be within half an hour.

4) The decision tree applied to rainfall model in part of rain condition determination was tested using data in years 2006-2008 from totally 71 stations in Bangkok area. It is able to conclude that the testing shows good results with the error between 16.502-25.435% when the measurement ability of rain gauge is taken in to consideration.

5) Four models, 2005, 2006, 2007, and 2005-2007 (Table 4.1), of rain rate estimation were developed in this study based on data in years 2005-2007 from totally 11 TMD stations distributed all over Thailand. The models were tested using data in years 2006-2008 from totally 71 stations in Bangkok area. The results show that the 2006 model, $Rainrate = 61887.18365 \exp\left(\frac{-x}{19.17829}\right) + 0.9992$ with ratio time interval provides the best result whether wind is taken to consider or not. The RMSEs of the best results of wind and without wind considerations are 0.449 and 0.525 mm/15 minutes. The 2005 model with mode time interval provides the worst testing results with error 1.084 and 1.172 mm/15 minutes when wind and without are taken to consider.

6) The APT image has spatial resolution of 4x4 km while rain measuring stations are regarded as point data. Data from a point were then used to represent a whole pixel. This more or less can lead to cause errors of the models.

7) The relationship between T_b and rain rate values of 2005 different show less accuracy compared to ones of 2006 and 2007. This could be because the APT receiving system was in the beginning period which was being adjusted. If the 2005 data were not used in rain rate analysis, the better results could be expected.

8) The validation results could be more accurate, if the rain gauge measurements in SCADA system of the Department of Drainage and Sewerage of

Bangkok Metropolitan Administration rainfall in Bangkok have been calibrated every year. In general, the rainfall data recorded can be the most accurate in the first installed year only and recalibration is required constantly.

9) RH and P used in decision tree analysis were selected at the minimum period far from APT images captured time, no matter they were before or after raining. If they could have been selected when raining, the result should have been better. Anyway, to do so, the data used for analysis will be reduced obviously because of the limited number of APT images during rain.

10) In this study, all raining values were used for analysis. Data with very low rainfall rate can cause low accurate result. Therefore, using the high rainfall rate can cause better result. Again, samples used for analysis could be reduced significantly because of the limited number of APT images recorded at the same time of rainfall recorded by the TMD.

From the above conclusion, it can be confirmed that all study objectives are achieved as required.

5.2 Recommendation and further improvement

With experience gained from this study, the recommendation for further study that expect the better result is related to improvement of receiving system, input data, and module development as the followings.

1) Related to the receiving system, noises from other frequency radio signals and from electrical equipment in the same AC line should be filtered out. This will increase the efficiency of the receiving system. The data will be cleaner and better for further usage.

2) In this study, only thermal IR band was used. If NIR (band 2) of APT data are additionally applied as a variable together with TIR (band 4) in the rainfall model, it could be expected that the rain condition determination and rain rate estimation will provide more accurate result. However, bi-spectral technique cannot be applied to rainfall estimation during the night because no NIR channel of APT data.

3) The results of this study show that the model with ratio time interval always provide better results compared to other time intervals. It can probably explain that the T_b of cloud related to rain requires certain time which is longer than 15 minutes to develop. Therefore, it is recommended that usage of the series of T_b in the model should be worth trying.

4) This study used all records of rain that were matched to APT images without seasonal separation as before, within, and after rainy season. For further study, it is recommended to select the data used for rain condition and rain rate regression analyses individually by the period before rainy season (before 16 May), in rainy season (15 May-15 October), and after rainy season (after 16 October) based on the classification by the Bureau of Royal Rainmaking and Agricultural Aviation. This can lead to higher accuracy of analytical results.

5) Instead of developing to be separate modules, it will be more convenient and time effective if all processes can be developed as one module working under the environment of GIS software.

REFERENCES

- กระทรวงเกษตรและสหกรณ์. (2006). เกณฑ์ช่วยการตัดสินใจในการปฏิบัติการฝนหลวง.
[ออนไลน์]. ได้จาก: <http://www.moac.go.th/builder/brradkm/images/5001Decision%20making.doc>.
- กระทรวงเกษตรและสหกรณ์. (2008). การตัดสินใจวางแผนปฏิบัติการฝนหลวง. [ออนไลน์]. ได้จาก: <http://www.moac.go.th/builder/brradkm/images/5205decision.pdf>.
- Abstract Technologies New Zealand Limited. (2008). WXtoImg Ver. 2.8.11 software.
[On-line]. Available : [http:// www.wxtoimg.com](http://www.wxtoimg.com).
- Arkin, P. A. and Meisner, B. N. (1987). The Relationship between Large-Scale Convective Rainfall and Cold Cloud over the Western Hemisphere during 1982 -84, American Meteorological Society, Monthly Weather Review Vol. 115, No. 1, pp. 51-74.
- Barrett, E. C. (1970). The estimation of monthly rainfall from satellite data. Monthly weather review, 98, pp. 322-327.
- Bayasgalan, M. and Erdenetuya, M. (1992). Estimation of cloud type, its amount and precipitation area using NOAA – AVHRR data, [On-line]. Available : <http://www.aars-acrs.org/acrs/proceeding/ACRS1992/Papers/PS392-12.htm>.
- Benabadji, N., Hassini, A., and Belbachir, A. H. (2004). Hardware and Software Considerations to Use NOAA Images. [On-line]. Available : http://www.cder.dz/download/Art7-1_1.pdf.
- Billa, L., Mansor, S., and Mahmud, R. A. (2004). Spatial information technology in flood early warning systems: an overview of theory, application and latest

developments in Malaysia, Disaster Prevention and Management, Volume 13, No.5, pp. 356-363.

Csiszar, I. and Kerenyi, J. (1996). Combined use of radar and satellite information for precipitation estimation in Hungary, Geoscience and Remote Sensing Symposium, International Volume 2, pp. 1114-1116.

Department of Drainage and Sewerage. (2009). SCADA System, [On-line]. Available: <http://203.155.220.231:8080/scada>.

Eric, K. S. *et al.* (2006). Weather satellite imaging system. [On-line]. Available : <http://www.markroland.com/engineering/APT>.

Gjertsen, U. (1997). The seasonal variation of cloud parameters over Central Europe: a fuzzy approach for the analysis of NOAA-APT data, Atmospheric Research Volume 45, Issue 2, October 1997, pp. 123-152.

Gola, M. (2008). Simple system for reception NOAA-METEOR-GOSE-METEOSAT. [On-line]. Available : <http://www.emgola.cz>.

Gower, J. F. R. *et al.* (1989). A precise APT receiver for cloud and sea surface temperature imaging, Geoscience and Remote Sensing Symposium, International Volume 4, pp. 2463-2465.

Hayes, P. (2000). The Zebedy Collapsible QHF antenna. Remote Image Group Journal, Issue No 62, September 2000, pp. 18-22.

Heinzmann, U. (1993). Analysis of Cloud Type and Distribution Using NOAA-AVHRR-APT Data and Ground Observations in the Upper Rhine Valley, [On-line]. Available : <http://pages.unibas.ch/geo/mcr/Publications>.

- Hilario, D. F. (1998). Short Duration Rainfall Estimation Using GMS IR and VIS Images, [On-line]. Available : <http://www.gisdevelopment.net/aars/acrs/1998/ts2/ts2005.asp>.
- Hollander, R. and Jansen, R. (1999). The resonant Quadrifilar Helix antenna. Remote Image Group Journal, Issue No 58, September 1999, pp. 14-29.
- Howard, S. (2008). The Lindenblad: The Ultimate Satellite Omni Antenna, [On-line]. Available : <http://www.amsat.org/amsat/articles/w6shp/lindy.html>.
- Hsu, K., Gao, X., and Sorooshian, S. (2002). Rainfall estimation using cloud texture classification mapping, [On-line]. Available : <http://www.isac.cnr.it/~ipwg/meetings/madrid/pdf/hsu.pdf>.
- Inoue, T. (1993). Rainfall estimation from split window data, Geoscience and Remote Sensing Symposium, International Volume 2 , pp. 611-613.
- Inoue, T. and Aonashi, K. (2000). A comparison of cloud and rainfall information from instantaneous visible and infrared scanner and precipitation radar observations over a frontal zone in east Asia during June 1998, Journal of Applied Meteorology, 39, pp. 2292-2301.
- Islam, M. R. and Exell, R. H. B. (1996). Solar Radiation Mapping from Satellite Image Using a Low Cost System. Solar Energy, Volume 56, Number 3, March 1996 , pp. 225-237.
- Islam, N. M. *et al.* (2002). Application of a Method to Estimate Rainfall in Bangladesh Using GMS-5 Data, Journal of Natural Disaster Science, Volume 24, No.2, pp. 83-89 [On-line]. Available : http://www.drs.dpri.kyoto-u.ac.jp/jsnds/download.cgi?jsdn_24_2-5.pdf.

- Jansen, R. (1995). De Quadrifilar 137 antenna. De Kunstmaan, December 1995, pp. 181-186.
- Jansen, R. (2000). The PITA 137 Folding RQH antenna. Remote Image Group Journal, Issue No 61, June 2000, pp. 24-35.
- John, N. (1992). Hardware and software considerations for use of NOAA polar orbiter datasets. [On-line]. Available : <http://blizzard.rwic.und.edu/~nordlie/papers/997a.html>.
- Kidder, S. Q. and Vonder Haar, T. H. (1995). Satellite meteorology: an introduction. Academic Press, San Diego, USA.
- Learning Center for Earth Science and Astronomy of Thailand. (2008). APT image. [On-line]. Available : <http://www.chanwittaya-cgeo.net>.
- Loh, S. C. (2001). Image from South-East Asia. Remote Image Group Journal, Issue No 66, September 2001, pp. 47.
- National Aeronautics and Space Administration. (1998). Calibration of AVHRR Data, NOAA Polar Orbiter Data (POD) User's Guide Section 3.3, [On-line]. Available : <http://www2.ncdc.noaa.gov/docs/podug/html/c3/sec3-3.htm>.
- National Aeronautics and Space Administration. (2000). APT System, The NOAA KLM User's Guide Section 4.2, [On-line]. Available : <http://www2.ncdc.noaa.gov/docs/klm/html/c4/sec4-2.htm>.
- National Aeronautics and Space Administration. (2007). NOAA Satellite Operation Status and Information, NOAA Satellite Status Information, [On-line]. Available : <http://www.oso.noaa.gov/poesstatus>.
- Ouma, G. O., Chane, A., and Muthama, N. J. (2005). Validation of satellite-derived rainfall estimates: The Ethiopian case study, 7th Kenya Meteorological

Society Workshop on Meteorological Research, Applications and Services,
Nairobi.

Pepper, M. (1994). A compact, cheap, volute antenna for polar orbiters. Remote
Image Group Journal, Issue No 37, June 1994, pp. 37-40.

Pestemalci, V., Kandirmaz, H. M., Yegingil, I., and Yildiz, B. Y. (2004).
Determination of the Land Surface Temperature of the Cukurova Region
Using NOAA APT Data, Chinese Journal of Physics, Vol. 42, No. 6, pp. 776-
785.

Preeyaphorn, K. and Kobkiat, P. (2003). The rainfall estimation using remote sensing
in Thailand. [On-line]. Available : https://pindex.ku.ac.th/file_research/WE60.doc.

Ralph, E. T. (2008). Analog APT station, [On-line]. Available : http://taggart.glg.msu.edu/wsh/analog_APT.htm.

Resonance Publications Inc. (2007). Weather satellite, [On-line]. Available : <http://www.resonancepub.com/weather.htm>.

Royal Irrigation Department. (2008). Precipitation, [On-line]. Available : http://irrigation.rid.go.th/rid1/Onfarm1/interesting/interestiog_01250651.php.

Saisunee, B. (2004). Rainfall estimate for flood management using meteorological
data from satellite imagery. [On-line]. Available : <http://www.wrrc.dpri.kyoto-u.ac.jp/~aphw/APHW2004/proceedings/JSD/56-JSD-A554/56-JSD-A554.pdf>.

Steven, M. G. (1995). The Florida State University College of Education integrating
weather satellite ground station technology into the K-12 classroom [On-line].
Available : <http://www.met.fsu.edu/explores/Steve/thesis.html>.

- Suh, M. S. *et al.* (2004). Estimation of rainfall over Korean peninsula using GOES-9 satellite imagery data. [On-line]. Available : [http://www.wrrc.dpri.kyoto-u.ac.jp/~aphw/APHW2004/proceedings/APHW-Others/56-OTH-A1722/56-OTH-A1722\(manuscript\).pdf](http://www.wrrc.dpri.kyoto-u.ac.jp/~aphw/APHW2004/proceedings/APHW-Others/56-OTH-A1722/56-OTH-A1722(manuscript).pdf).
- Sykes, B. and Cobey, B. (1997). Taming The QFH. Remote Image Group Journal, Issue No 48, March 1997, pp. 17-21.
- Taylor, A. M. (1997). A home-built Lindenblad antenna for 137 MHz band. Remote Image Group Journal, Issue No 48, March 1997, pp. 12-16.
- Thorp, B. (1998). The copper pipe QFH. Remote Image Group Journal, Issue No 53, June 1998, pp. 68-72.
- Tsanders Space Research Lab. (2008). The face of Europe from Space. University of Latvia. [On-line]. Available : <http://home.lanet.lv/~satim>.
- Vanlint, C. (1996). A portable/Collapsible Quadrifilar Helix Antenna for the 137 MHz APT band. Remote Image Group Journal, Issue No 44, March 1996, pp. 8-13.
- Vicente, A. G. and Scofield A. R. (1998). Satellite rainfall estimates in real time for applications to flash flood watches and warnings, heavy precipitation forecasting and assimilation on numerical weather prediction models, [On-line]. Available : <http://www.srh.noaa.gov/topics/attach/html/ssd98-18.htm>.
- Wikipedia. (2008). The wind profile power law, [On-line]. Available : http://en.wikipedia.org/wiki/Wind_profile_power_law.

APPENDIX A

APT SYSTEM

The Automatic Picture Transmission System

The Automatic Picture Transmission (APT) system is an analog image transmission system developed for use on weather satellites. It was introduced in the 1960s. APT provides a reduced resolution data stream from the AVHRR instrument. Any two of the AVHRR channels can be chosen by ground command for processing and ultimate output to the APT transmitter. A visible channel is used to provide visible APT imagery during daylight, and one IR channel is used constantly (day and night). A second IR channel can be scheduled to replace the visible channel during the nighttime portion of the orbit. The analog APT signal is transmitted continuously and can be received in real time by relatively unsophisticated, relatively low-cost user stations at locations in most countries of the world. A user station anywhere in the world can receive local data at least twice a day from each satellite as it passes nearly overhead.

The APT characteristics processed AVHRR instrument data AM modulates a 2400 Hz sub carrier. The maximum sub carrier modulation is defined as the amplitude of the gray scale. The AM modulated sub carrier is subsequently used to FM modulate the transmitter operating in the 137-138 MHz band. Table A.1 summarizes the pertinent APT transmission characteristics.

Table A.1 Carrier frequency of APT signal form NOAA satellite.

NOAA satellite	Carrier frequency (MHz)
NOAA 12	137.50 (Decommissioned-23/05/2007)
NOAA 15	137.50
NOAA 17	137.62
NOAA18	137.9125

(National Aeronautics and Space Administration, 2007)

Table A.2 APT Characteristics.

Line Rate	120 line/min
Data Channels	2 transmitted from 6 Channels
Data Resolution	4.0 km
Carrier Modulation	2.4 KHz AM sub carrier on FM carrier
Transmitter Frequency (MHz)	137.50 or 137.62 or 137.9125
Transmitter Power (EOL)	5 W (37dBm)
Radiated Power (dBm @ 63 degrees)	36.7

(National Aeronautics and Space Administration, 2000)

The APT broadcast transmission is composed of two image channels, telemetry information, and synchronization data, with the image channels typically referred to as Video A and Video B. All this data is transmitted as a horizontal scan line. A complete line is 2080 pixels long, with each image using 909 pixels and the remainder going to the telemetry and synchronization. Lines are transmitted at 2 per second, which equates to a 4160 words per second, or 4160 baud. The images are corrected for nearly constant geometric resolution prior to being broadcast, as such the images are free of distortion caused by the curve of the Earth.

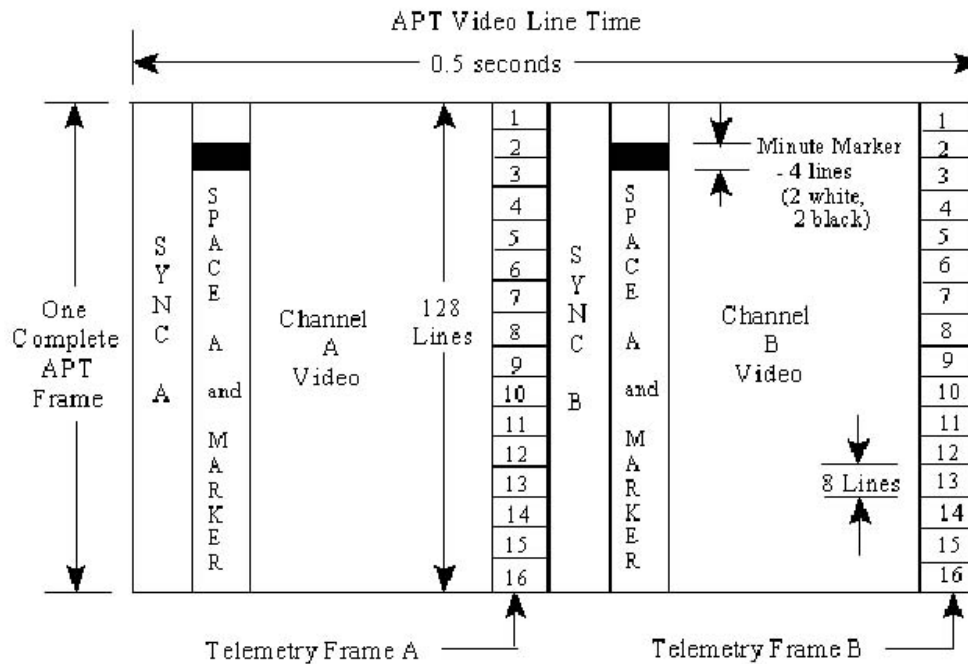


Figure A.1 APT frame format. (National Aeronautics and Space Administration, 2000)

The APT ground station receiving system. A block diagram of a minimum ground station components is presented in Figure A.2. The antenna for the APT system consists of an omnidirectional and circularly polarized beam. A preamplifier is necessary because the signal transmitted by the satellites is weak. The receiver then converts the radio signals into audio tones, and the decoder converts the audio tones, which represent analogue voltage levels generated by the sensors into digital data. The computer receives these data through an analogue to digital converter. It is necessary to have an orbital prediction program and current orbital elements for the satellites to determine when they will be visible from the ground station. In the APT system, the predictions tell the operator when to have the system active, and any slight error is generally not important.

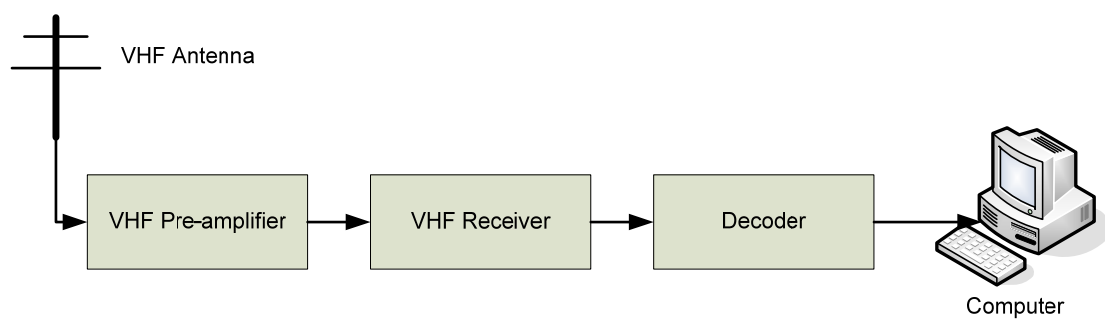


Figure A.2 APT ground station receiving system.

APPENDIX B

TYPES OF ANTENNA

a) Turnstile antenna

A turnstile antenna with a reflector is one of the many types that has been developed primarily for omnidirectional VHF communications. The basic turnstile consists of two horizontal half-wave antenna elements mounted at right angles to each other in the same horizontal plane. When these two antennas are excited with equal currents 90 degrees out of phase, the typical figure-eight patterns of the two antennas merge to produce the nearly circular pattern. The reflector consists of two horizontal cross reflector elements fixed under the half-wave antenna elements. Turnstile antenna underneath it makes a good antenna for space communications because it produces a circularly polarized signal pattern and also has a broad, high angle pattern. Due to these characteristics, there is no need to rotate the antenna.

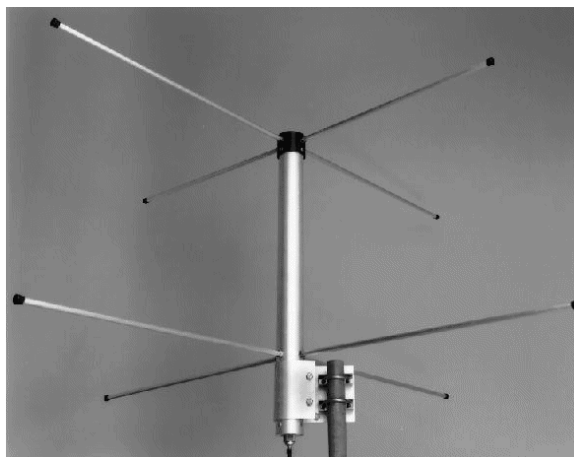


Figure B.1 Turnstile antenna. (Resonance Publications Inc., 2007)

b) Quadrifilar Helix Antenna

The Quadrifilar helix is one of the most popular designs because of its relatively compact size. It provides an optimum antenna for narrow bandwidth application requiring a broad beamwidth, cardioid shaped radiation pattern and excellent circular polarization. The Quadrifilar helix antenna generically they employ two bifilar helix antennas with orthogonal radiuss (Quadrafilar helix) fed inphase quadrature with a folded balun to feed the antenna, with the two ports connected to a hybrid coupler to produce circular polarization. The 90-degree phase relationship between bifilars needed to feed two identical orthogonal bifilars with a quadrature hybrid using a balun. The 90-degree phase difference is realized at the expense of losing power to the hybrid, adding the hybrid weight to the system and requiring two cables to feed the two bifilars.



Figure B.2 QFH Antenna. (Ralph, E. T., 2008)

c) Lindenblad antenna

The Lindenblad antenna consists of four half wave folded dipoles slanted 30 degrees to the horizon, oriented 90 degrees to each other in azimuth, spaced 0.3 wavelength apart. They are tied together by four half wave 300 ohms twinlead lines that divide the folded dipole's impedance by four where they connect to the coax feedline.

Lindenblad antennas have a deaf spot located directly above the antenna, and when a satellite passes directly overhead, the signal may be lost in the Lindenblad's cone of silence for a few seconds. All antennas have directions in which they are more sensitive or less sensitive, and designing an omnidirectional antenna involves compromises, as one cannot truly make it equally sensitive in all directions. A Lindenblad maximizes its sensitivity towards the horizon, where a rising/setting satellite is relatively far away and its signal correspondingly weak. Lower elevations are also where LEO satellites spend most of their time during a typical satellite pass, so it makes sense to have this as the region where the antenna is most sensitive.



Figure B.3 Lindenblad antenna. (Howard, S., 2008)

APPENDIX C

PARAMETERS OF RAINFALL CONDITION

Parameters of rainfall condition

Parameters of rainfall condition consist of 3 parameters;

1) Vapor water in the atmosphere: The rain rate depends on the vapor water quantity in the atmosphere. The high vapor water quantity brings to the high rain rate.

2) Particle of dust: The particle of dust is like the core absorbing the vapor water in the atmosphere to form the rain.

3) Cooling process brings to the condensation to rainfall.

The rainfall cannot be formed without any of these 3 parameters. Many meteorological parameters are also the factors for cloud and rain formation, varied on day and season. The variation is so high to understand their behavior and relation to cloud and rain formation, which is the main obstacle for effective rainfall estimation. Therefore, understanding the relations of meteorological variations is necessary. It is inevitable for us to use the data with least error but great sample size as most as possible. Following weather and meteorological data are analyzed for rainfall possibility.

1) Surface atmosphere data: This data includes air pressure, the extreme temperature in last day, RH at the surface, cloud type and quantity, etc. The air pressure is the main factor because it brings to other weather conditions, for example,

the increased pressure brings to the high pressure expansion, make to colder weather. The weather change depends on the force of high pressure. In summer, the high pressure brings to severe thunderstorm. The lower pressure implies the weaker force of high pressure, make to higher temperature and lower rain. In case of the greater lowering air temperature brings to the expansion of low pressure, make to rainfall.

2) Wind at ground and upper data: This data concerns about westerly trough, easterly wave, convergence, wind direction, and wind speed. Wind brings to the humidity so the humidity rate depends on wind direction and speed. Changing wind direction in short period (within 1-3 hours) can be the cause of the increasing or decreasing cloud quantity. Wind speed and direction can be measured at many altitude levels, ranging from 5,000 and 10,000-18,000 feet.

3) RH data: This data shows the potential area for rainfall formation. The high RH area is the potential area for rainfall probability. The RH can be measured at 700 and 850 MB altitude levels.

4) Satellite images data: This data indicates cloud formation and type in many areas, related to high pressure, low pressure area, and storm, for example, VIS image shows the white area for cloudy area, and grey or black area for clear sky. The thicker cloud it is, the higher reflection value it is bringing to brighten image than the area with light cloud but the satellite image cannot identify the cloud levels; low, middle, high or vertical levels. The cloud type and altitude level is shown in Table C.1. The IR image shows the relation of brightness and cloud temperature. The warmer temperature cloud cluster is darker than the cooler one. Therefore, for low level cloud, the image is reflected with grey or black color. The higher level cloud

which is cooler will be reflected with brighten image to white color. The black area is the earth surface.

Table C.1 Cloud classification, base on altitude level.

Cloud type	Name of cloud	Altitude (km)
High cloud	Cirrus (Ci)	6-18
	Cirrostratus (Cs)	
	Cirrocumulus (Cc)	
Middle cloud	Altostratus (As)	2-8
	Alto cumulus (Ac)	
Low cloud	Stratocumulus (Sc)	Surface-2
	Nimbostratus (Ns)	
Cumuliform cloud	Cumulus (Cu)	Surface-18
	Cumulonimbus (Cb)	

5) Upper level atmosphere data : This data includes the humidity, temperature and air pressure indicating the structure of atmosphere layer in various altitudes and cloud formation process, for example, time for cloud formation, altitude of cloud base, weather stability. The suitability of these values depends on rainfall probability in each area. (กระทรวงเกษตรและสหกรณ์, 2008)

The rainy season can be divided into 3 periods, based on following criteria;

1) Dry season (November-February) : In this season, rarely it rains in upper area of Thailand, except the following conditions;

- High pressure (cold weather) attacking with the low pressure (warm weather).

- The convergence of southern and southeast winds.

- Western air wave flow.

- Southerly or Southeast wind

2) Season change (March-May) : It rains more in March and April, based on the similar weather condition to dry season in 1). In early May, the cyclone will be formed in Andaman Sea and ocean track so the rainfall is more.

3) Rainy season (June-October) : In this period, the rain is influenced by low pressure arisen from thermal desorption, tropical cyclone in Andaman sea and monsoon trough which these 3 conditions are related. In October, the high pressure gives influence to rainfall during the initial high pressured days.

These weather conditions can be varied each year. The weather conditions of each day can be divided into 2 periods because of different seasons as follows;

1) The period before 16 May and after 16 October are the periods before and after rainy season.

2) The period from 15 May-15 October are the rainy season or monsoon period, based on humidity, wind speed and weather stability indicator, more details shown in the Table C.2. (กระทรวงเกษตรและสหกรณ์, 2006)

Table C.2 Criteria appropriate climate for a day.

Item	Parameters	Appropriate of weather conditions		
		Best	Moderate	Not appropriate
1	RH average (%) at 0-10,000 feet.			
	1. before 16 May & after 15 October	> 75	74-65	< 65
	2. 16 May-15 October	> 85	84-75	< 75
2	RH average (%) at 10,000-18,000 feet.			
	1. before 16 May & after 15 October	> 70	69-60	< 60
	2. 16 May-15 October	> 80	79-70	< 70
3	Wind speed average (knot) at 10,000-15,000 feet.	< 15	15-25	> 25

Table C.2 (Continued).

Item	Parameters	Appropriate of weather conditions		
		Best	Moderate	Not appropriate
4	Cloud base of Cumulus (feet)			
	1. before 16 May & after 15 October	< 4,500	4,500-5,000	> 5,000
	2. 16 May-15 October	< 4,000	4,000-4,500	> 4,500
5	RH at cloud base (%)			
	1. before 16 May & after 15 October	> 80	80-70	< 70
	2. 16 May-15 October	> 90	90-80	< 80
6	Air Stability Index			
	1. Showalter Index ^{1/}	< -0.5 to 2	-0.5 to 2	> 2
	2. Lifted Index ^{2/}	< -0.5	-0.5 to 1	> 1
7	The possibility of surface temperature to convective temperature ^{3/}	Yes	Yes	No

Remarks : ^{1/} is the estimation value for difference of the temperature of air cluster at lowest level , closed to the surface atmosphere at 50 MB and 500 MB levels.

^{2/} is the estimation value for difference of the highest temperature of air cluster at lowest level , closed to the surface atmosphere at 50 MB or lofted to 500 MB levels.

^{3/} is the temperature of lofting surface air cluster because of heat.

APPENDIX D

NOAA SATELLITE ORBITING TIME SCHEDULE

Satellite passes for Bangkok, Thailand (13°51'N 100°36'E)
 while above 8.0 degrees with maximum elevation (MEL) over 20.0 degrees
 from 01/08/2009 12:14:05 SE Asia Standard Time (01/08/2009 05:14:05 UTC).

01/08/2009 SE Asia Standard Time

Satellite	Dir	MEL	Long	Local Time	UTC Time	Duration	Freq
NOAA 19	N	44E	107E	13:26:50	01/08 06:26:50	11:16	137.9125
NOAA 18	N	77E	102E	13:40:57	01/08 06:40:57	11:52	137.1000
NOAA 15	N	65W	98E	17:01:54	01/08 10:01:54	11:14	137.5000
NOAA 17	N	81E	102E	21:22:13	01/08 14:22:13	11:18	137.6200

02/08/2009 SE Asia Standard Time

Satellite	Dir	MEL	Long	Local Time	UTC Time	Duration	Freq
NOAA 19	S	75E	102E	02:04:05	01/08 19:04:05	11:45	137.9125
NOAA 18	S	64W	97E	02:18:30	01/08 19:18:30	11:40	137.1000
NOAA 15	S	45W	94E	05:32:26	01/08 22:32:26	10:52	137.5000
NOAA 17	S	70W	98E	09:52:53	02/08 02:52:53	11:23	137.6200
NOAA 19	N	34E	110E	13:16:53	02/08 06:16:53	10:43	137.9125
NOAA 18	N	59E	105E	13:30:30	02/08 06:30:30	11:42	137.1000
NOAA 15	N	67E	103E	16:38:01	02/08 09:38:01	11:16	137.5000
NOAA 17	N	43E	107E	20:59:20	02/08 13:59:20	10:43	137.6200

03/08/2009 SE Asia Standard Time

Satellite	Dir	MEL	Long	Local Time	UTC Time	Duration	Freq
NOAA 19	S	57E	105E	01:53:56	02/08 18:53:56	11:33	137.9125
NOAA 18	S	84W	100E	02:07:54	02/08 19:07:54	11:48	137.1000
NOAA 15	S	86W	100E	05:08:19	02/08 22:08:19	11:24	137.5000
NOAA 17	S	63E	104E	09:29:41	03/08 02:29:41	11:22	137.6200
NOAA 19	N	26E	112E	13:07:03	03/08 06:07:03	9:59	137.9125
NOAA 18	N	44E	107E	13:20:10	03/08 06:20:10	11:19	137.1000
NOAA 19	N	23W	88E	14:47:48	03/08 07:47:48	9:38	137.9125
NOAA 15	N	35E	109E	16:14:36	03/08 09:14:36	10:22	137.5000
NOAA 17	N	23E	113E	20:36:59	03/08 13:36:59	9:09	137.6200
NOAA 17	N	24W	89E	22:16:35	03/08 15:16:35	9:18	137.6200

04/08/2009 SE Asia Standard Time

Satellite	Dir	MEL	Long	Local Time	UTC Time	Duration	Freq
NOAA 19	S	43E	107E	01:43:49	03/08 18:43:49	11:14	137.9125
NOAA 18	S	74E	102E	01:57:22	03/08 18:57:22	11:45	137.1000
NOAA 15	S	50E	106E	04:44:35	03/08 21:44:35	11:04	137.5000
NOAA 17	S	34E	110E	09:06:55	04/08 02:06:55	10:27	137.6200

Figure D.1 Sample of NOAA satellite pass list over receiving station.

APPENDIX E

LIST OF 12 AIRPORT STATIONS

Table E.1 The position of 12 airport stations.

ICAO code	Station name	Latitude	Longitude
VTBD	Don Muang	13° 54' 45.00" N	100° 36' 24.00" E
VTBS	Suvarnabhumi	13° 40' 52.00" N	100° 44' 50.00" E
VTCC	Chiang Mai	18° 46' 01.00" N	098° 57' 46.00" E
VTCT	Chiang Rai	19° 57' 08.00" N	099° 52' 59.00" E
VTSB	Surat Thani	09° 07' 57.00" N	099° 08' 08.00" E
VTSF	Nakhon Si Thammarat	08° 32' 23.00" N	099° 56' 41.00" E
VTSM	Koh Samui	09° 32' 52.00" N	100° 03' 44.00" E
VTSP	Phuket	08° 06' 48.00" N	098° 19' 01.00" E
VTSS	Hat Yai	06° 56' 00.00" N	100° 23' 35.00" E
VTUD	Udon Thani	17° 23' 11.00" N	102° 47' 18.00" E
VTUK	Khon Kaen	16° 28' 00.00" N	102° 47' 01.00" E
VTUU	Ubon Ratchathani	15° 15' 05.00" N	104° 52' 13.00" E

Source : <http://gc.kls2.com/airport/>

APPENDIX F

RAINING CONDITION DATA FOR CLIMATIC ANALYSIS

Table F.1 Raining condition data for climatic analysis.

Tb_K	RH	Pressure	Rain status	Tb_K	RH	Pressure	Rain status
243.1684	94	1001.0	1	220.0000	89	1010.2	1
273.4211	59	1006.1	0	251.1947	94	1012.5	1
269.7258	89	1003.0	0	263.0691	100	1011.5	1
249.9119	94	1007.1	1	265.2397	89	1010.2	1
260.4051	84	1006.4	0	250.6141	89	1011.5	1
261.4036	79	1005.1	0	250.2521	89	1010.2	1
273.4211	89	1007.8	0	254.9884	75	1003.0	0
273.8819	89	1007.1	0	251.7258	75	1007.8	0
266.8324	89	1007.5	0	261.4036	83	1005.4	1
263.6170	84	1005.1	0	264.1613	94	1006.4	1
266.3048	79	1008.5	0	267.3569	79	1006.4	0
260.8410	89	1007.5	0	263.6170	94	1007.5	1
258.6584	89	1007.8	1	284.8160	75	1002.7	0
264.2325	79	1006.8	0	261.4036	89	1006.1	0
264.0035	89	1008.1	0	259.9679	74	1010.2	0
264.1613	84	1006.1	0	266.3048	79	1008.5	0
280.9383	84	1009.8	0	260.8410	89	1007.5	0
286.6517	89	1009.5	0	259.9584	89	1007.8	0
285.7931	89	1009.1	0	264.2325	79	1006.8	0
279.5726	79	1008.5	0	264.0035	89	1008.1	0
277.0614	89	1009.8	0	264.1613	84	1006.1	0
267.4598	59	1008.8	0	280.9383	84	1009.8	0
259.2338	79	1009.1	1	286.6517	89	1009.5	0
275.9357	53	1007.8	0	285.7931	89	1009.1	0
262.6214	75	1007.8	0	279.5726	79	1008.5	0
262.6214	66	1008.5	0	277.0614	89	1009.8	0
261.4036	79	1005.1	0	267.4598	59	1008.8	0
259.1295	79	1006.1	0	259.2338	79	1009.1	1
273.4211	89	1007.8	0	275.9357	53	1007.8	0
272.5402	89	1007.1	0	262.6214	75	1007.8	0
266.8324	89	1007.5	0	262.6214	66	1008.5	0
259.9161	89	1007.8	1	261.4036	79	1005.1	0
258.1617	100	1006.1	1	259.1295	79	1006.1	0
250.9410	89	1003.0	1	273.4211	89	1007.8	0

Table F.1 (Continued).

Tb_K	RH	Pressure	Rain status	Tb_K	RH	Pressure	Rain status
270.9436	89	1009.8	0	261.4036	89	1006.1	0
285.7931	89	1007.5	0	259.9679	74	1010.2	0
252.3407	79	1009.5	0	255.1911	89	1009.1	0
259.5029	89	1011.5	0	267.8782	89	1009.1	0
253.0733	89	1009.1	1	254.3786	94	1009.1	1
221.2544	100	1009.8	1	270.9436	89	1009.8	0
283.1738	89	1009.5	0	285.7931	89	1007.5	0
261.9625	89	1008.8	0	252.3407	79	1009.5	0
278.6514	89	1008.1	0	259.5029	89	1011.5	0
268.0000	89	1009.5	1	253.0733	89	1009.1	0
268.9117	89	1009.1	0	221.2544	100	1009.8	1
275.3566	75	1009.5	0	283.1738	89	1009.5	0
271.4445	89	1009.8	0	261.9625	89	1008.8	0
250.6584	89	1010.2	0	278.6514	89	1008.1	0
219.1752	94	1010.2	1	268.0000	89	1009.5	1
254.9884	89	1012.2	0	268.9117	89	1009.1	0
271.4445	89	1012.5	0	275.3566	75	1009.5	0
220.0000	89	1010.2	1	271.4445	89	1009.8	0
251.1947	94	1012.5	1	250.5840	89	1010.2	0
263.0691	100	1011.5	1	219.1752	94	1010.2	1
265.2397	89	1010.2	0	254.9884	89	1012.2	0
250.6141	89	1011.5	0	271.4445	89	1012.5	0
250.2521	89	1010.2	0	220.0000	89	1010.2	1
254.9884	75	1003.0	0	251.1947	94	1012.5	1
251.7258	75	1007.8	0	263.0691	100	1011.5	1
261.4036	83	1005.4	1	265.2397	89	1010.2	0
264.1613	94	1006.4	1	250.6141	89	1011.5	0
267.3569	79	1006.4	0	250.9521	89	1010.2	0
263.6170	94	1007.5	1	254.9884	75	1003.0	0
260.2745	56	1002.0	0	251.7258	75	1007.8	0
256.1938	84	1003.7	0	261.4036	83	1005.4	1
257.9786	71	1003.0	0	264.1613	94	1006.4	1
276.7825	84	1006.1	0	267.3569	79	1006.4	0
250.6141	79	1009.8	0	263.6170	94	1007.5	1
253.2574	89	1009.1	0	260.2745	56	1002.0	0
260.0181	89	1009.5	0	256.1938	84	1003.7	0
273.4211	79	1005.1	0	257.9786	71	1003.0	0
257.3811	89	1006.4	0	276.7825	84	1006.1	0
275.3566	89	1007.1	0	250.6141	79	1009.8	0
212.3925	89	1006.1	1	253.2574	89	1009.1	0
263.1777	89	1009.1	0	260.0181	89	1009.5	0
289.2149	79	1007.8	0	273.4211	79	1005.1	0
275.8343	89	1008.5	0	257.3811	89	1006.4	0
257.9948	74	1009.5	0	275.3566	89	1007.1	0
271.4445	89	1004.1	0	212.3925	89	1006.1	1
263.6170	89	1004.4	0	263.1777	89	1009.1	0

Table F.1 (Continued).

Tb_K	RH	Pressure	Rain status	Tb_K	RH	Pressure	Rain status
256.6489	79	1008.1	0	289.2149	79	1007.8	0
245.9664	100	1005.1	1	275.8343	89	1008.5	0
277.2532	84	1004.1	0	257.9948	74	1009.5	0
233.1777	94	1006.1	1	271.4445	89	1004.1	0
281.3894	89	1007.8	0	263.6170	89	1004.4	0
233.1777	84	1007.1	1	256.6489	79	1008.1	0
266.4180	89	1008.1	0	245.9664	100	1005.1	1
268.3965	89	1009.1	1	277.2532	84	1004.1	0
276.3096	89	1007.1	0	233.1777	94	1006.1	1
254.3786	89	1006.1	0	281.3894	89	1007.8	0
266.5000	89	1007.5	0	233.1777	84	1007.1	1
268.9117	100	1007.1	1	266.4180	89	1008.1	0
230.6319	94	1005.8	1	268.3965	89	1009.1	1
237.0817	94	1008.1	1	276.3096	89	1007.1	0
254.7546	89	1007.8	0	254.3786	89	1006.1	0
266.5000	89	1009.1	0	266.5000	89	1007.5	0
266.5000	89	1009.8	0	268.9117	100	1007.1	1
247.3250	100	1008.8	1	230.6319	94	1005.8	1
247.3250	94	1009.1	1	237.0817	94	1008.1	1
260.8410	89	1009.1	0	254.7546	89	1007.8	0
255.9664	89	1009.1	0	266.5000	89	1009.1	0
252.4509	89	1009.1	1	266.5000	89	1009.8	0
215.0000	89	1010.0	1	247.3250	100	1008.8	1
212.0000	94	1010.8	1	247.3250	94	1009.1	1
210.0000	94	1009.1	1	260.8410	89	1009.1	0
220.0000	94	1009.1	1	255.9664	89	1009.1	0
205.0000	94	1008.1	1	252.4509	89	1009.1	0
210.0000	100	1015.9	1	215.0000	89	1010.0	1
207.0000	94	1009.1	1	212.3782	94	1010.8	1
209.0000	89	1010.8	1	210.2839	94	1009.1	1
215.0000	94	1009.1	1	220.0000	94	1009.1	1
206.0000	100	1008.1	1	205.3220	94	1008.1	1
214.0000	94	1009.1	1	210.0000	100	1015.9	1
220.0000	94	1009.1	1	207.0000	94	1009.1	1
207.5000	94	1004.1	1	209.3943	89	1010.8	1
208.0000	94	1009.1	1	215.0000	94	1009.1	1
214.0000	94	1008.1	1	206.1522	100	1008.1	1
214.5000	94	1005.1	1	214.0000	94	1009.1	1
198.0000	100	1006.1	1	220.2278	94	1009.1	1
208.0000	100	1004.1	1	281.3894	89	1007.8	0
207.5000	100	1005.1	1	233.1777	84	1007.1	1
217.5000	94	1004.1	1	266.4180	89	1008.1	0
211.0000	94	1005.1	1	268.3965	89	1009.1	1
230.0000	94	1004.1	1	276.3096	89	1007.1	0
210.0000	94	1006.1	1	254.3786	89	1006.1	0
202.5000	94	1007.1	1	266.5000	89	1007.5	0

Table F.1 (Continued).

Tb_K	RH	Pressure	Rain status	Tb_K	RH	Pressure	Rain status
214.0000	94	1007.1	1	268.9117	100	1007.1	1
217.5000	94	1010.2	1	230.6319	94	1005.8	1
209.0000	94	1010.2	1	237.0817	94	1008.1	1
232.0000	94	1008.1	1	254.7546	89	1007.8	0
218.5000	94	1005.1	1	266.5000	89	1009.1	0
217.0000	94	1005.1	1	266.5000	89	1009.8	0
220.0000	94	1007.1	1	247.3250	100	1008.8	1
211.5000	94	1003.0	1	247.3250	94	1009.1	1
221.0000	94	1006.1	1	260.8410	89	1009.1	0
222.0000	100	1007.1	1	255.9664	89	1009.1	0
218.0000	94	1005.1	1	252.4509	89	1009.1	0
216.5000	94	1009.1	1	215.0000	89	1010.0	1
204.5000	94	1003.0	1	212.3520	94	1010.8	1
210.0000	94	1004.1	1	210.0000	94	1009.1	1
216.0000	94	1003.0	1	220.3682	94	1009.1	1
213.5000	94	1002.0	1	205.0000	94	1008.1	1
211.5000	94	1004.1	1	251.6584	89	1010.2	0
214.0000	94	1010.8	1	219.1752	94	1010.2	1
219.0000	89	1010.2	1	254.9884	89	1012.2	0
214.0000	89	1008.1	1	271.4445	89	1012.5	0
215.0000	89	1012.9	1	220.0000	89	1010.2	1
210.8000	89	1007.1	1	251.1947	94	1012.5	1
210.0000	94	1010.0	1	263.0691	100	1011.5	1
205.5000	94	1006.1	1	265.2397	89	1010.2	0
227.0000	89	1008.1	1	250.6141	89	1011.5	0
212.5000	89	1007.1	1	250.2541	89	1010.2	0
222.0000	75	1009.5	1	254.9884	75	1003.0	0
218.0000	75	1009.5	1	251.7258	75	1007.8	0
221.5000	89	1010.5	1	261.4036	83	1005.4	1
214.0000	94	1009.5	1	264.1613	94	1006.4	1
221.0000	79	1005.4	1	267.3569	79	1006.4	0
216.0000	94	1008.1	1	263.6170	94	1007.5	1
219.7000	89	1008.1	1	260.2745	56	1002.0	0
222.2000	89	1011.2	1	256.1938	84	1003.7	0
230.0000	84	1007.8	1	257.9786	71	1003.0	0
222.0000	94	1008.1	1	276.7825	84	1006.1	0
224.0000	89	1009.1	1	250.6141	79	1009.8	0
225.0000	94	1007.1	1	253.2574	89	1009.1	0
209.7000	89	1006.4	1	260.0181	89	1009.5	0
230.3000	94	1006.1	1	206.0000	100	1008.1	1
230.5000	94	1006.1	1	214.8360	94	1009.1	1
210.0000	94	1007.5	1	220.0000	94	1009.1	1
240.0000	94	1008.5	1	281.3894	89	1007.8	0
216.0000	89	1007.1	1	233.1777	84	1007.1	1
225.1000	74	1008.8	1	266.4180	89	1008.1	0
211.0000	89	1007.1	1	268.3965	89	1009.1	1

Table F.1 (Continued).

Tb_K	RH	Pressure	Rain status	Tb_K	RH	Pressure	Rain status
221.0000	89	1010.2	1	276.3096	89	1007.1	0
225.2000	89	1008.8	1	254.3786	89	1006.1	0
207.6000	89	1010.5	1	266.5000	89	1007.5	0
221.0000	94	1010.5	1	268.9117	100	1007.1	1
214.9000	89	1008.1	1	230.6319	94	1005.8	1
242.0000	94	1008.5	1	237.0817	94	1008.1	1
202.0000	94	1008.5	1	254.7546	89	1007.8	0
224.0000	94	1008.1	1	266.5000	89	1009.1	0
224.3000	89	1007.1	1	266.5000	89	1009.8	0
228.0000	94	1006.8	1	247.3250	100	1008.8	1
241.0000	79	1008.1	1	247.3250	94	1009.1	1
230.0000	84	1008.1	1	260.8410	89	1009.1	0
214.8000	89	1009.1	1	255.9664	89	1009.1	0
215.5000	89	1007.1	1	252.4509	89	1009.1	0
241.0000	89	1007.1	1	215.0000	89	1010.0	1
220.0000	89	1008.8	1	212.0000	94	1010.8	1
228.4000	89	1006.1	1	278.6514	89	1008.1	0
228.0000	84	1005.1	1	268.0000	89	1009.5	1
227.7000	84	1006.8	1	268.9117	89	1009.1	0
226.0000	71	1004.4	1	275.3566	75	1009.5	0
212.0000	94	1006.8	1	271.4445	89	1009.8	0
224.2000	94	1007.8	1	252.6840	89	1010.2	0
228.4000	94	1007.5	1	219.1752	94	1010.2	1
221.8000	94	1011.2	1	254.9884	89	1012.2	0
226.7000	89	1010.5	1	271.4445	89	1012.5	0
216.5000	89	1010.5	1	220.0000	89	1010.2	1
214.7000	89	1008.8	1	251.1947	94	1012.5	1
228.1000	94	1008.8	1	263.0691	100	1011.5	1
235.0000	84	1008.1	1	265.2397	89	1010.2	0
225.4000	94	1009.8	1	250.6141	89	1011.5	0
210.0000	94	1008.8	1	250.5210	89	1010.2	0
228.0000	94	1007.8	1	254.9884	75	1003.0	0
227.8230	89	1006.1	1	251.7258	75	1007.8	0
228.4000	94	1008.5	1	261.4036	83	1005.4	1
220.1000	94	1010.5	1	264.1613	94	1006.4	1
224.7000	100	1009.5	1	267.3569	79	1006.4	0
252.2626	66	1006.4	0	263.6170	94	1007.5	1
206.0000	94	1008.1	1	260.2745	56	1002.0	0
234.9000	89	1007.1	1	256.1938	84	1003.7	0
208.6000	94	1007.5	1	257.9786	71	1003.0	0
228.3000	94	1009.5	1	276.7825	84	1006.1	0
240.0000	94	1011.9	1	250.6141	79	1009.8	0
217.0000	89	1010.5	1	253.2574	89	1009.1	0
217.2000	94	1008.5	1	260.0181	89	1009.5	0
224.5000	94	1009.5	1	273.4211	79	1005.1	0
234.9000	100	1010.8	1	257.3811	89	1006.4	0

Table F.1 (Continued).

Tb_K	RH	Pressure	Rain status	Tb_K	RH	Pressure	Rain status
225.9000	100	1009.1	1	275.3566	89	1007.1	0
245.0000	100	1011.2	1	212.3925	89	1006.1	1
232.2450	89	1012.5	1	243.1684	94	1001.0	1
232.0000	89	1010.5	1	273.4211	59	1006.1	0
224.8000	94	1009.5	1	269.7258	89	1003.0	0
228.7000	94	1011.2	1	249.9119	94	1007.1	1
215.0000	94	1013.2	1	260.4051	84	1006.4	0
232.7540	89	1011.5	1	261.4036	79	1005.1	0
232.5000	89	1009.5	1	273.4211	89	1007.8	0
245.1000	94	1011.2	1	273.8819	89	1007.1	0
208.8000	94	1013.9	1	266.8324	89	1007.5	0
216.0000	94	1011.9	1	263.6170	84	1005.1	0
252.3407	79	1009.5	0	275.3566	89	1007.1	0
259.5029	89	1011.5	0	212.3925	89	1006.1	1
253.0733	89	1009.1	0	263.1777	89	1009.1	0
221.2544	100	1009.8	1	289.2149	79	1007.8	0
283.1738	89	1009.5	0	275.8343	89	1008.5	0
261.9625	89	1008.8	0	257.9948	74	1009.5	0
278.6514	89	1008.1	0	271.4445	89	1004.1	0
268.0000	89	1009.5	1	263.6170	89	1004.4	0
268.9117	89	1009.1	0	256.6489	79	1008.1	0
275.3566	75	1009.5	0	245.9664	100	1005.1	1
271.4445	89	1009.8	0	277.2532	84	1004.1	0
250.6584	89	1010.2	0	233.1777	94	1006.1	1
219.1752	94	1010.2	1	281.3894	89	1007.8	0
254.9884	89	1012.2	0	233.1777	84	1007.1	1
271.4445	89	1012.5	0	266.4180	89	1008.1	0
220.0000	89	1010.2	1	268.3965	89	1009.1	1
251.1947	94	1012.5	1	276.3096	89	1007.1	0
263.0691	100	1011.5	1	254.3786	89	1006.1	0
265.2397	89	1010.2	0	266.5000	89	1007.5	0
250.6141	89	1011.5	0	268.9117	100	1007.1	1
250.2567	89	1010.2	0	230.6319	94	1005.8	1
254.9884	75	1003.0	0	237.0817	94	1008.1	1
251.7258	75	1007.8	0	254.7546	89	1007.8	0
261.4036	83	1005.4	1	266.5000	89	1009.1	0
264.1613	94	1006.4	1	266.5000	89	1009.8	0
267.3569	79	1006.4	0	247.3250	100	1008.8	1
263.6170	94	1007.5	1	247.3250	94	1009.1	1
284.8160	75	1002.7	0	260.8410	89	1009.1	0
261.4036	89	1006.1	0	255.9664	89	1009.1	0
259.9679	74	1010.2	0	252.4509	89	1009.1	0
255.1911	89	1009.1	0	215.0000	89	1010.0	1
267.8782	89	1009.1	0	212.3637	94	1010.8	1
254.3786	94	1009.1	1	210.0000	94	1009.1	1
270.9436	89	1009.8	0	220.4630	94	1009.1	1

Table F.1 (Continued).

Tb_K	RH	Pressure	Rain status	Tb_K	RH	Pressure	Rain status
285.7931	89	1007.5	0	205.0000	94	1008.1	1
252.3407	79	1009.5	0	275.9357	53	1007.8	0
259.5029	89	1011.5	0	262.6214	75	1007.8	0
253.0733	89	1009.1	0	262.6214	66	1008.5	0
221.2544	100	1009.8	1	261.4036	79	1005.1	0
283.1738	89	1009.5	0	259.1295	79	1006.1	0
261.9625	89	1008.8	0	273.4211	89	1007.8	0
278.6514	89	1008.1	0	272.5402	89	1007.1	0
268.0000	89	1009.5	1	266.8324	89	1007.5	0
268.9117	89	1009.1	0	249.9961	89	1007.8	0
275.3566	75	1009.5	0	250.1617	100	1006.1	1
271.4445	89	1009.8	0	250.9410	89	1003.0	1
258.6584	89	1010.2	0	253.1777	62	1007.8	0
219.1752	94	1010.2	1	250.9410	84	1004.4	0
254.9884	89	1012.2	0	284.8160	75	1002.7	0
271.4445	89	1012.5	0	261.4036	89	1006.1	0
220.0000	89	1010.2	1	259.9679	74	1010.2	0
251.1947	94	1012.5	1	255.1911	89	1009.1	0
263.0691	100	1011.5	1	267.8782	89	1009.1	0
265.2397	89	1010.2	0	254.3786	94	1009.1	1
250.6141	89	1011.5	0	270.9436	89	1009.8	0
251.2529	89	1010.2	0	285.7931	89	1007.5	0
254.9884	75	1003.0	0	252.3407	79	1009.5	0
251.7258	75	1007.8	0	259.5029	89	1011.5	0
261.4036	83	1005.4	1	253.0733	89	1009.1	0
264.1613	94	1006.4	1	221.2544	100	1009.8	1
267.3569	79	1006.4	0	283.1738	89	1009.5	0
263.6170	94	1007.5	1	261.9625	89	1008.8	0
260.2745	56	1002.0	0	278.6514	89	1008.1	0
256.1938	84	1003.7	0	268.0000	89	1009.5	1
257.9786	71	1003.0	0	268.9117	89	1009.1	0
276.7825	84	1006.1	0	275.3566	75	1009.5	0
250.6141	79	1009.8	0	271.4445	89	1009.8	0
253.2574	89	1009.1	0	251.6584	89	1010.2	0
260.0181	89	1009.5	0	219.1752	94	1010.2	1
273.4211	79	1005.1	0	254.9884	89	1012.2	0
257.3811	89	1006.4	0	271.4445	89	1012.5	0
275.3566	89	1007.1	0	220.0000	89	1010.2	1
212.3925	89	1006.1	1	251.1947	94	1012.5	1
263.1777	89	1009.1	0	263.0691	100	1011.5	1
289.2149	79	1007.8	0	265.2397	89	1010.2	0
275.8343	89	1008.5	0	250.6141	89	1011.5	0
257.9948	74	1009.5	0	250.3452	89	1010.2	0
271.4445	89	1004.1	0	254.9884	75	1003.0	0
263.6170	89	1004.4	0	251.7258	75	1007.8	0
256.6489	79	1008.1	0	261.4036	83	1005.4	1

Table F.1 (Continued).

Tb_K	RH	Pressure	Rain status	Tb_K	RH	Pressure	Rain status
245.9664	100	1005.1	1	264.1613	94	1006.4	1
277.2532	84	1004.1	0	267.3569	79	1006.4	0
233.1777	94	1006.1	1	263.6170	94	1007.5	1
281.3894	89	1007.8	0	260.2745	56	1002.0	0
233.1777	84	1007.1	1	256.1938	84	1003.7	0
266.4180	89	1008.1	0	257.9786	71	1003.0	0
268.3965	89	1009.1	1	276.7825	84	1006.1	0
285.7931	89	1007.5	0	250.6141	79	1009.8	0
252.3407	79	1009.5	0	253.2574	89	1009.1	0
259.5029	89	1011.5	0	260.0181	89	1009.5	0
253.0733	89	1009.1	0	273.4211	79	1005.1	0
221.2544	100	1009.8	1	257.3811	89	1006.4	0
283.1738	89	1009.5	0	275.3566	89	1007.1	0
261.9625	89	1008.8	0	212.3925	89	1006.1	1
278.6514	89	1008.1	0	263.1777	89	1009.1	0
268.0000	89	1009.5	1	289.2149	79	1007.8	0
268.9117	89	1009.1	0	275.8343	89	1008.5	0
275.3566	75	1009.5	0	263.0691	100	1011.5	1
271.4445	89	1009.8	0	265.2397	89	1010.2	0
268.6584	89	1010.2	0	250.6141	89	1011.5	0
219.1752	94	1010.2	1	250.4529	89	1010.2	0
254.9884	89	1012.2	0	254.9884	75	1003.0	0
271.4445	89	1012.5	0	251.7258	75	1007.8	0
220.0000	89	1010.2	1	261.4036	83	1005.4	1
251.1947	94	1012.5	1	264.1613	94	1006.4	1
263.0691	100	1011.5	1	216.0000	94	1011.9	1
265.2397	89	1010.2	0	252.3407	79	1009.5	0
250.6141	89	1011.5	0	259.5029	89	1011.5	0
253.2522	89	1010.2	0	253.0733	89	1009.1	0
254.9884	75	1003.0	0	221.2544	100	1009.8	1
251.7258	75	1007.8	0	283.1738	89	1009.5	0
261.4036	83	1005.4	1	261.9625	89	1008.8	0
264.1613	94	1006.4	1	278.6514	89	1008.1	0
216.0000	94	1011.9	1	268.0000	89	1009.5	1
252.3407	79	1009.5	0	268.9117	89	1009.1	0
259.5029	89	1011.5	0	275.3566	75	1009.5	0
253.0733	89	1009.1	0	271.4445	89	1009.8	0
221.2544	100	1009.8	1	252.6584	89	1010.2	0
283.1738	89	1009.5	0	219.1752	94	1010.2	1
261.9625	89	1008.8	0	254.9884	89	1012.2	0
278.6514	89	1008.1	0	271.4445	89	1012.5	0
268.0000	89	1009.5	1	220.0000	89	1010.2	1
268.9117	89	1009.1	0	251.1947	89	1012.5	1
275.3566	75	1009.5	0	263.0691	100	1011.5	1
271.4445	89	1009.8	0	265.2397	89	1010.2	0
255.9984	89	1010.2	0	250.6141	89	1011.5	0

Table F.1 (Continued).

Tb_K	RH	Pressure	Rain status	Tb_K	RH	Pressure	Rain status
219.1752	94	1010.2	1	251.2521	89	1010.2	0
254.9884	89	1012.2	0	254.9884	75	1003.0	0
271.4445	89	1012.5	0	251.7258	75	1007.8	0
251.1947	94	1012.5	1	261.4036	83	1005.4	1
263.0691	100	1011.5	1	264.1613	94	1006.4	1
265.2397	89	1010.2	0	267.3569	79	1006.4	0
250.6141	89	1011.5	0	263.6170	94	1007.5	1
250.2214	89	1010.2	0	284.8160	75	1002.7	0
254.9884	75	1003.0	0	261.4036	89	1006.1	0
251.7258	75	1007.8	0	259.9679	74	1010.2	0
261.4036	83	1005.4	1	266.3048	79	1008.5	0
264.1613	94	1006.4	1	260.8410	89	1007.5	0
267.3569	79	1006.4	0	251.8421	89	1007.8	0
220.0000	89	1010.2	1	252.9410	84	1004.4	0
267.8782	89	1009.1	0	284.8160	75	1002.7	0
254.3786	89	1009.1	1	250.9410	89	1003.0	1
259.9679	74	1010.2	0	253.1777	62	1007.8	0
255.1911	89	1009.1	1	253.9161	89	1007.8	0
284.8160	75	1002.7	0	250.1617	100	1006.1	1
261.4036	89	1006.1	0	272.5402	89	1007.1	0
253.1777	62	1007.8	0	266.8324	89	1007.5	0
249.9410	84	1004.4	0				

APPENDIX G

DATA OF DECISION TREE ANALYSIS

Tb	RH	Pressure	Rain	Norain	Probability
190-250	89%-100%	<1005mb	11	0	1.00
190-250	89%-100%	1005mb-1010mb	91	2	.98
190-250	89%-100%	>1010mb	35	3	.92
190-250	71%<RH<89%	<1005mb	0	0	.00
190-250	71%<RH<89%	1005mb-1010mb	10	0	1.00
190-250	71%<RH<89%	>1010mb	0	0	.00
190-250	<71%	<1005mb	0	0	.00
190-250	<71%	1005mb-1010mb	3	0	.00
190-250	<71%	>1010mb	0	0	.00
251-270	89%-100%	<1005mb	0	3	.00
251-270	89%-100%	1005mb-1010mb	9	12	.43
251-270	89%-100%	>1010mb	18	41	.31
251-270	71%<RH<89%	<1005mb	0	5	.00
251-270	71%<RH<89%	1005mb-1010mb	4	22	.15
251-270	71%<RH<89%	>1010mb	0	2	.00
251-270	<71%	<1005mb	0	4	.00
251-270	<71%	1005mb-1010mb	0	3	.00
251-270	<71%	>1010mb	0	0	.00
271-300	89%-100%	<1005mb	0	2	.00
271-300	89%-100%	1005mb-1010mb	0	25	.00
271-300	89%-100%	>1010mb	0	3	.00
271-300	71%<RH<89%	<1005mb	0	4	.00
271-300	71%<RH<89%	1005mb-1010mb	0	11	.00
271-300	71%<RH<89%	>1010mb	0	0	.00
271-300	<71%	<1005mb	0	0	.00
271-300	<71%	1005mb-1010mb	0	2	.00
271-300	<71%	>1010mb	0	0	.00

Figure G.1 Data of decision tree analysis.

APPENDIX H

EXAMPLES OF MATLAB SOURCE CODE

a) Brightness temperature determinate function

```
function temp = Pix2Temp(pix_value,noaa_type)
%% Pixel to temperature
%% Init output
temp = 0;
dn = 0;
%% Check NOAA
switch (noaa_type)
    case 12
        noaa_value = 920.7173;
    case 15
        noaa_value = 925.4075;
    case 17
        noaa_value = 926.2947;
    case 18
        noaa_value = 928.1460;
    otherwise
        noaa_value = 0;
end
%%
if (noaa_value == 0)
else
    if (pix_value>247)
        temp = 0;
    else
        dn = double(((pix_value*4)+((pix_value*4)+3))/2);
        temp = ((1.438833)*(noaa_value))/(reallog(1+(((1.1910659e-
005)*(noaa_value^3))/((-0.160156)*dn)+159.088867) ));
    end
end
end
```

b) Rain condition estimate function

```

function rrate = RainFall(cloud_ktemp,rh,pres)
%% Compute rain rate
%% Defind variable
%cloud_ktemp = cloud temperature(Kelvin)
%rh = RH (%)
%pres = Pressure
%% Init output
rrate = false;
%% Check rain fall
if ((cloud_ktemp >= 138) && (cloud_ktemp <= 270) && (cloud_ktemp == 0)) %
first chk temperature
    if ((cloud_ktemp >= 190) && (cloud_ktemp <= 250) && (cloud_ktemp == 0)) %
second chk temperature
        if (rh > 71) % Chk RH percent
            if (rh > 89) % Second1 Chk RH percent
                rrate = true;
            else
                if ((pres >= 1005) && (pres <= 1010))% Chk RH Pressure
                    rrate = true;
                else
                    rrate = false;
                end
            end
        else
            rrate = false;
        end
    else
        if (rh >= 89) % Chk RH percent
            rrate = true;
        else
            rrate = false;
        end
    end
end
end

```

c) Rain rate estimate function

```
function rain_mm = RainRate(tb)
%% Computr rain rate
% tb = could temperature
%% Init output
rain_mm = 0;
%% RainRate
if (tb == 0)
    rain_mm = 5.40;
else
    temp1 = (-tb)/18.46962;
    tempexp = exp(temp1);
    temp = ((155998.55576*(tempexp))+0.88151);
    if temp < -0
        rain_mm = 0;
    else
        rain_mm = temp;
    end
end
end
```


Table I.1 (Continued).

Date	No. of station	Raining condition error (%)											
		Year 05 equation			Year 06 equation			Year 07 equation			Year 05-07 equation		
		Mode	Average	Ratio	Mode	Average	Ratio	Mode	Average	Ratio	Mode	Average	Ratio
19/08/08	67	52.239	52.239	52.239	52.239	52.239	52.239	52.239	52.239	52.239	52.239	52.239	52.239
22/08/08	67	0.000	0.000	0.000	0.000	0.000	0.000	0.000	0.000	0.000	0.000	0.000	0.000
06/09/08	67	49.254	49.254	49.254	49.254	49.254	49.254	49.254	49.254	49.254	49.254	49.254	49.254
29/09/08	67	2.985	2.985	2.985	2.985	2.985	2.985	2.985	2.985	2.985	2.985	2.985	2.985
03/10/08	66	0.000	0.000	0.000	0.000	0.000	0.000	0.000	0.000	0.000	0.000	0.000	0.000
11/10/08	68	82.353	82.353	82.353	82.353	82.353	82.353	82.353	82.353	82.353	82.353	82.353	82.353
19/10/08	67	86.567	86.567	86.567	86.567	86.567	86.567	86.567	86.567	86.567	86.567	86.567	86.567
26/10/08	61	16.393	16.393	16.393	16.393	16.393	16.393	16.393	16.393	16.393	16.393	16.393	16.393
Average error		35.569	35.569	35.569	39.285	39.285	39.285	26.757	26.757	26.757	35.569	35.569	35.569

Table I.2 (Continued).

Date	No. of station	Raining condition error (%)											
		Year 05 equation			Year 06 equation			Year 07 equation			Year 05-07 equation		
		Mode	Average	Ratio	Mode	Average	Ratio	Mode	Average	Ratio	Mode	Average	Ratio
19/08/08	67	55.224	55.224	55.224	55.224	55.224	55.224	55.224	55.224	55.224	55.224	55.224	55.224
22/08/08	67	0.000	0.000	0.000	0.000	0.000	0.000	0.000	0.000	0.000	0.000	0.000	0.000
06/09/08	67	50.746	50.746	50.746	50.746	50.746	50.746	50.746	50.746	50.746	50.746	50.746	50.746
29/09/08	67	2.985	2.985	2.985	2.985	2.985	2.985	2.985	2.985	2.985	2.985	2.985	2.985
03/10/08	66	1.515	1.515	1.515	1.515	1.515	1.515	1.515	1.515	1.515	1.515	1.515	1.515
11/10/08	68	82.353	82.353	82.353	82.353	82.353	82.353	82.353	82.353	82.353	82.353	82.353	82.353
19/10/08	67	79.105	79.105	79.105	79.105	79.105	79.105	79.105	79.105	79.105	79.105	79.105	79.105
26/10/08	61	14.754	14.754	14.754	14.754	14.754	14.754	14.754	14.754	14.754	14.754	14.754	14.754
Average error		35.176	35.176	35.176	38.602	38.602	38.602	26.434	26.434	26.434	35.176	35.176	35.176

Table I.3 Near-real time raining condition error data from the models of the years 2005, 2006, 2007, and 2005-2007 which assumes that rain rate < 0.5 is equal to 0 mm.

Date	No. of station	Raining condition error (%)											
		Year 05 equation			Year 06 equation			Year 07 equation			Year 05-07 equation		
		Mode	Average	Ratio	Mode	Average	Ratio	Mode	Average	Ratio	Mode	Average	Ratio
15/05/06	21	0.000	0.000	0.000				0.000	0.000	0.000	0.000	0.000	0.000
23/05/06	21	0.000	0.000	0.000				0.000	0.000	0.000	0.000	0.000	0.000
30/05/06	21	0.000	0.000	0.000				0.000	0.000	0.000	0.000	0.000	0.000
01/06/06	21	71.429	66.667	47.619				57.143	47.619	4.762	66.667	57.143	19.048
06/06/06	21	38.095	38.095	38.095				38.095	38.095	38.095	38.095	38.095	38.095
09/06/06	21	0.000	0.000	0.000				0.000	0.000	0.000	0.000	0.000	0.000
18/06/06	21	33.333	42.857	42.857				23.810	38.095	38.095	23.810	19.048	42.857
01/05/07	55	69.091	49.091	0.000	100.000	100.000	100.000				92.727	72.727	0.000
03/06/07	54	1.852	1.852	1.852	1.852	1.852	1.852				1.852	1.852	1.852
05/06/07	55	1.818	1.818	0.000	3.636	0.000	0.000				3.636	1.818	0.000
09/06/07	55	0.000	0.000	0.000	0.000	0.000	0.000				0.000	0.000	0.000
15/07/07	54	72.222	64.815	5.556	72.222	1.852	1.852				77.778	66.667	1.852
19/07/07	55	80.000	74.546	14.546	78.182	14.546	14.456				76.367	72.727	14.546
23/07/07	55	100.000	100.000	3.636	100.000	1.818	0.000				100.000	100.000	0.000
31/07/07	55	83.636	74.546	18.182	83.636	14.546	14.456				83.636	83.636	16.364
18/08/07	53	54.717	37.736	9.434	86.793	9.434	9.434				88.679	71.698	9.434
01/09/07	55	9.091	7.273	1.818	1.818	1.818	1.818				9.091	7.273	1.818
14/10/07	55	0.000	0.000	0.000	0.000	0.000	0.000				0.000	0.000	0.000
03/06/08	65	1.539	1.539	3.077	4.615	4.615	4.615	3.077	3.077	4.615	1.539	1.539	4.615
04/06/08	65	98.462	93.846	6.154	100.000	3.077	0.000	100.000	12.308	0.000	100.000	100.000	0.000
13/06/08	66	12.121	12.121	12.121	12.121	12.121	12.121	12.121	12.121	12.121	12.121	12.121	12.121
02/07/08	67	0.000	0.000	1.493	1.493	1.493	13.433	1.493	1.493	13.433	0.000	0.000	0.000
05/07/08	65	1.539	1.539	1.539	1.539	1.539	1.539	1.539	1.539	1.539	1.539	1.539	1.539
22/07/08	67	25.373	25.373	32.836	20.896	31.343	31.343	22.388	32.836	31.343	23.881	25.373	29.851
06/08/08	67	4.478	4.478	0.000	7.463	0.000	0.000	7.463	0.000	0.000	8.955	4.478	0.000

Table I.3 (Continued).

Date	No. of station	Raining condition error (%)											
		Year 05 equation			Year 06 equation			Year 07 equation			Year 05-07 equation		
		Mode	Average	Ratio	Mode	Average	Ratio	Mode	Average	Ratio	Mode	Average	Ratio
19/08/08	67	44.776	41.791	0.000	38.806	0.000	0.000	40.299	2.985	0.000	44.776	40.299	0.000
22/08/08	67	0.000	0.000	0.000	0.000	0.000	0.000	0.000	0.000	0.000	0.000	0.000	0.000
06/09/08	67	50.000	50.000	26.471	55.224	25.000	25.000	54.412	29.412	26.471	52.941	50.000	26.471
29/09/08	67	2.985	2.985	2.985	2.985	2.985	2.985	2.985	2.985	2.985	2.985	2.985	2.985
03/10/08	66	0.000	0.000	0.000	0.000	0.000	0.000	0.000	0.000	0.000	0.000	0.000	0.000
11/10/08	68	88.235	89.706	77.941	82.353	75.000	61.765	83.824	80.882	61.765	85.294	85.294	72.059
19/10/08	67	79.105	58.209	44.776	80.597	37.313	14.925	80.597	41.791	14.925	85.075	77.612	29.851
26/10/08	61	26.563	40.625	67.188	81.250	81.250	12.500	12.500	60.938	82.813	6.250	23.881	79.105
Average error		31.832	29.743	13.945	12.369	11.270	24.625	24.625	18.463	15.135	32.914	30.842	12.301

Table I.4 After 15 minutes received APT data, raining condition error data from the models of the years 2005, 2006, 2007, and 2005-2007 which assumes that rain rate < 0.5 is equal to 0 mm.

Date	No. of station	Raining condition error (%)											
		Year 05 equation			Year 06 equation			Year 07 equation			Year 05-07 equation		
		Mode	Average	Ratio	Mode	Average	Ratio	Mode	Average	Ratio	Mode	Average	Ratio
15/05/06	21	0.000	0.000	0.000				0.000	0.000	0.000	0.000	0.000	0.000
23/05/06	21	0.000	0.000	0.000				0.000	0.000	0.000	0.000	0.000	0.000
30/05/06	21	0.000	0.000	0.000				0.000	0.000	0.000	0.000	0.000	0.000
01/06/06	21	80.952	76.191	57.143				61.905	52.381	0.000	76.191	23.810	23.810
06/06/06	21	38.095	38.095	38.095				38.095	38.095	38.095	38.095	38.095	38.095
09/06/06	21	0.000	0.000	0.000				0.000	0.000	0.000	0.000	0.000	0.000
18/06/06	21	33.333	38.095	38.095				33.333	38.095	38.095	33.333	19.048	38.095
01/05/07	55	70.910	61.818	3.636	87.273	0.000	0.000				87.273	67.273	0.000
03/06/07	54	1.852	1.852	1.852	1.852	1.852	1.852				1.818	1.818	1.818
05/06/07	55	3.636	1.818	0.000	1.818	0.000	0.000				3.636	1.818	0.000
09/06/07	55	0.000	0.000	0.000	0.000	0.000	0.000				0.000	0.000	0.000
15/07/07	54	57.407	55.556	1.852	61.111	1.852	1.852				68.519	57.407	1.852
19/07/07	55	69.091	65.455	16.364	76.364	18.182	18.182				56.364	47.273	18.182
23/07/07	55	100.000	100.00	3.636	100.000	1.818	0.000				100.000	100.000	0.000
31/07/07	55	87.273	74.546	10.910	89.091	10.909	10.909				63.636	63.636	9.091
18/08/07	53	71.698	35.849	13.208	86.793	13.208	13.208				88.679	79.245	13.208
01/09/07	55	21.818	16.364	7.273	23.636	7.273	5.455				27.273	21.818	5.455
14/10/07	55	0.000	0.000	0.000	0.000	0.000	0.000				0.000	0.000	0.000
03/06/08	65	6.154	6.154	6.154	6.154	6.154	6.154	6.154	6.154	6.154	6.154	6.154	6.154
04/06/08	65	100.000	96.923	13.846	100.000	7.692	0.000	100.000	24.615	0.000	100.000	100.000	1.539
13/06/08	66	12.121	12.121	12.121	12.121	12.121	12.121	12.121	12.121	12.121	12.121	12.121	12.121
02/07/08	67	10.448	10.448	10.448	10.448	11.940	16.418	10.448	10.448	14.925	10.448	10.448	11.940
05/07/08	65	5.970	5.970	5.970	5.970	5.970	5.970	5.970	5.970	5.970	5.970	5.970	5.970
22/07/08	67	4.478	5.970	29.851	1.493	32.836	35.821	1.493	28.358	35.821	0.000	1.493	34.328
06/08/08	67	2.941	1.471	0.000	5.882	0.000	0.000	5.882	0.000	0.000	7.353	1.471	0.000

Table I.4 (Continued).

Date	No. of station	Raining condition error (%)											
		Year 05 equation			Year 06 equation			Year 07 equation			Year 05-07 equation		
		Mode	Average	Ratio	Mode	Average	Ratio	Mode	Average	Ratio	Mode	Average	Ratio
19/08/08	67	52.239	50.746	0.000	50.746	0.000	0.000	50.746	2.985	0.000	52.239	52.239	0.000
22/08/08	67	0.000	0.000	0.000	0.000	0.000	0.000	0.000	0.000	0.000	0.000	0.000	0.000
06/09/08	67	41.791	34.328	32.836	44.776	32.836	32.836	44.776	32.836	32.836	22.388	38.806	32.836
29/09/08	67	2.941	2.941	2.941	2.941	2.941	2.941	2.941	2.941	2.941	2.941	2.941	2.941
03/10/08	66	1.515	1.515	1.515	1.515	1.515	1.515	1.515	1.515	1.515	1.515	1.515	1.515
11/10/08	68	72.059	70.588	61.765	72.059	55.882	47.059	69.118	63.235	47.059	73.529	72.059	48.529
19/10/08	67	64.179	61,194	32.836	68.657	26.866	20.896	67.164	32.836	20.896	73.134	65.672	25.373
26/10/08	61	44.262	54.098	73.771	21.312	75.410	77.049	19.672	72.131	77.049	18.033	40.984	78.689
Average error		32.035	29.700	14.428	35.847	12.587	11.932	24.152	19.305	15.158	31.232	28.276	12.471

Table I.5 Near-real time rain rate RMSE data from the models of the years 2005, 2006, 2007, and 2005-2007.

Date	No. of station	Rain rate RMSE (mm/15 minutes)											
		Year 05 equation			Year 06 equation			Year 07 equation			Year 05-07 equation		
		Mode	Average	Ratio	Mode	Average	Ratio	Mode	Average	Ratio	Mode	Average	Ratio
15/05/06	21	0.000	0.000	0.000				0.000	0.000	0.000	0.000	0.000	0.000
23/05/06	21	0.004	0.002	0.001				0.052	0.029	0.009	0.058	0.032	0.010
30/05/06	21	0.000	0.000	0.000				0.000	0.000	0.000	0.000	0.000	0.000
01/06/06	21	3.657	2.038	0.601				0.934	0.519	0.171	2.194	1.218	0.359
06/06/06	21	1.041	1.041	1.041				1.041	1.041	1.041	1.041	1.041	1.041
09/06/06	21	0.000	0.000	0.000				0.000	0.000	0.000	0.000	0.000	0.000
18/06/06	21	2.429	2.521	2.606				2.398	2.498	2.598	2.269	2.417	2.572
01/05/07	55	1.188	0.664	0.198	0.625	0.350	0.104				1.285	0.718	0.214
03/06/07	54	0.068	0.068	0.068	0.068	0.068	0.068				0.068	0.068	0.068
05/06/07	55	0.162	0.090	0.027	0.128	0.072	0.021				0.215	0.120	0.036
09/06/07	55	0.000	0.000	0.000	0.000	0.000	0.000				0.000	0.000	0.000
15/07/07	54	1.556	0.870	0.264	0.592	0.332	0.113				1.437	0.802	0.243
19/07/07	55	1.627	0.896	0.285	0.613	0.344	0.180				1.524	0.836	0.265
23/07/07	55	2.184	1.221	0.364	0.732	0.409	0.122				1.898	1.061	0.316
31/07/07	55	1.762	0.971	0.307	0.647	0.363	0.190				1.626	0.891	0.281
18/08/07	53	0.787	0.439	0.175	0.586	0.330	0.156				1.069	0.590	0.201
01/09/07	55	0.799	0.748	0.736	0.701	0.713	0.732				0.756	0.722	0.729
14/10/07	55	0.000	0.000	0.000	0.000	0.000	0.000				0.000	0.000	0.000
03/06/08	65	0.397	0.127	0.162	0.163	0.206	0.246	0.125	0.184	0.239	0.105	0.100	0.211
04/06/08	65	2.081	1.164	0.347	0.721	0.403	0.120	0.798	0.446	0.133	1.817	1.016	0.303
13/06/08	66	1.258	1.260	1.262	1.215	1.236	1.255	1.216	1.237	1.255	1.209	1.233	1.254
02/07/08	67	2.223	1.117	0.368	0.369	0.393	0.482	0.428	0.369	0.464	0.694	0.881	0.482
05/07/08	65	0.062	0.062	0.062	0.062	0.062	0.062	0.062	0.062	0.062	0.062	0.062	0.062
22/07/08	67	1.235	0.659	0.253	0.333	0.223	0.240	0.380	0.238	0.238	0.960	0.502	0.225
06/08/08	67	0.271	0.151	0.045	0.180	0.101	0.030	0.185	0.103	0.031	0.336	0.188	0.056

Table I.5 (Continued).

Date	No. of station	Rain rate RMSE (mm/15 minutes)											
		Year 05 equation			Year 06 equation			Year 07 equation			Year 05-07 equation		
		Mode	Average	Ratio	Mode	Average	Ratio	Mode	Average	Ratio	Mode	Average	Ratio
19/08/08	67	1.310	0.732	0.218	0.453	0.253	0.076	0.501	0.280	0.084	1.160	0.649	0.193
22/08/08	67	0.000	0.000	0.000	0.000	0.000	0.000	0.000	0.000	0.000	0.000	0.000	0.000
06/09/08	67	2.631	2.534	2.506	2.455	2.471	2.497	2.461	2.473	2.497	2.559	2.493	2.494
29/09/08	67	0.086	0.086	0.086	0.086	0.086	0.086	0.086	0.086	0.086	0.086	0.086	0.086
03/10/08	66	0.000	0.000	0.000	0.000	0.000	0.000	0.000	0.000	0.000	0.000	0.000	0.000
11/10/08	68	4.549	3.911	3.621	3.598	3.587	3.591	3.628	3.596	3.592	3.864	3.666	3.595
19/10/08	67	3.648	2.332	1.652	1.685	1.636	1.651	1.742	1.642	1.646	2.404	1.829	1.633
26/10/08	61	1.437	1.396	1.746	1.566	1.720	1.887	1.523	1.692	1.878	1.346	1.436	1.775
Average error		1.165	0.821	0.576	0.676	0.591	0.535	0.798	0.750	0.728	0.971	0.747	0.567

Table I.6 After 15 minutes received APT data, rain rate RMSE data from the models of the years 2005, 2006, 2007, and 2005-2007.

Date	No. of station	Rain rate RMSE (mm/15 minutes)											
		Year 05 equation			Year 06 equation			Year 07 equation			Year 05-07 equation		
		Mode	Average	Ratio	Mode	Average	Ratio	Mode	Average	Ratio	Mode	Average	Ratio
15/05/06	21	0.000	0.000	0.000				0.000	0.000	0.000	0.000	0.000	0.000
23/05/06	21	0.001	0.001	0.000				0.038	0.022	0.006	0.040	0.022	0.007
30/05/06	21	0.000	0.000	0.000				0.000	0.000	0.000	0.000	0.000	0.000
01/06/06	21	4.161	2.327	0.693				1.044	0.584	0.174	2.410	1.348	0.402
06/06/06	21	1.041	1.041	1.041				1.041	1.041	1.041	1.041	1.041	1.041
09/06/06	21	0.000	0.000	0.000				0.000	0.000	0.000	0.000	0.000	0.000
18/06/06	21	2.745	2.810	2.873				2.687	2.772	2.861	2.599	2.713	2.840
01/05/07	55	1.341	0.750	0.224	0.599	0.335	0.100				1.176	0.658	0.196
03/06/07	54	0.068	0.068	0.068	0.068	0.068	0.068				0.068	0.068	0.068
05/06/07	55	0.184	0.103	0.031	0.137	0.077	0.023				0.241	0.135	0.040
09/06/07	55	0.000	0.000	0.000	0.000	0.000	0.000				0.000	0.000	0.000
15/07/07	54	1.358	0.759	0.232	0.553	0.310	0.107				1.290	0.720	0.219
19/07/07	55	1.541	0.853	0.290	0.595	0.340	0.198				1.453	0.799	0.269
23/07/07	55	2.112	1.181	0.352	0.726	0.406	0.121				1.865	1.043	0.311
31/07/07	55	1.504	0.829	0.259	0.642	0.360	0.166				1.506	0.829	0.257
18/08/07	53	0.824	0.458	0.192	0.584	0.330	0.173				1.101	0.604	0.212
01/09/07	55	1.001	0.739	0.599	0.641	0.598	0.583				0.891	0.690	0.591
14/10/07	55	0.000	0.000	0.000	0.000	0.000	0.000				0.000	0.000	0.000
03/06/08	65	0.197	0.215	0.233	0.232	0.236	0.239	0.229	0.234	0.238	0.217	0.227	0.236
04/06/08	65	2.346	1.312	0.391	0.741	0.415	0.124	0.834	0.466	0.139	1.935	1.082	0.322
13/06/08	66	1.121	1.121	1.121	1.118	1.120	1.121	1.118	1.120	1.121	1.117	1.119	1.121
02/07/08	67	2.298	1.233	0.318	0.338	0.310	0.222	0.475	0.253	0.176	1.219	0.637	0.190
05/07/08	65	0.381	0.381	0.381	0.381	0.381	0.381	0.381	0.381	0.381	0.381	0.381	0.381
22/07/08	67	1.122	0.531	0.157	0.145	0.073	0.229	0.205	0.070	0.221	0.828	0.350	0.140
06/08/08	67	0.189	0.105	0.031	0.154	0.086	0.026	0.155	0.087	0.026	0.265	0.148	0.044

Table I.6 (Continued).

Date	No. of station	Rain rate RMSE (mm/15 minutes)											
		Year 05 equation			Year 06 equation			Year 07 equation			Year 05-07 equation		
		Mode	Average	Ratio	Mode	Average	Ratio	Mode	Average	Ratio	Mode	Average	Ratio
19/08/08	67	1.405	0.786	0.234	0.503	0.281	0.084	0.553	0.309	0.092	1.267	0.709	0.211
22/08/08	67	0.000	0.000	0.000	0.000	0.000	0.000	0.000	0.000	0.000	0.000	0.000	0.000
06/09/08	67	1.613	1.734	1.909	1.799	1.874	1.957	1.784	1.865	1.954	1.651	1.743	1.908
29/09/08	67	0.086	0.086	0.086	0.086	0.086	0.086	0.086	0.086	0.086	0.086	0.086	0.086
03/10/08	66	0.062	0.062	0.062	0.062	0.062	0.062	0.062	0.062	0.062	0.062	0.062	0.062
11/10/08	68	3.215	2.588	2.278	2.292	2.260	2.247	2.323	2.270	2.248	2.599	2.362	2.256
19/10/08	67	2.759	1.177	2.232	2.205	2.278	2.375	2.171	2.248	2.364	2.269	2.136	2.291
26/10/08	61	1.089	0.972	1.148	1.046	1.114	1.224	1.026	1.098	1.218	1.108	0.995	1.156
Average error		1.084	0.764	0.528	0.602	0.515	0.458	0.737	0.680	0.655	0.930	0.688	0.511

Table I.7 Near-real time rain rate RMSE data from the models of the years 2005, 2006, 2007, and 2005-2007 which assumes that rain rate < 0.5 is equal to 0 mm.

Date	No. of station	Rain rate RMSE (mm/15 minutes)											
		Year 05 equation			Year 06 equation			Year 07 equation			Year 05-07 equation		
		Mode	Average	Ratio	Mode	Average	Ratio	Mode	Average	Ratio	Mode	Average	Ratio
15/05/06	21	0.000	0.000	0.000				0.000	0.000	0.000	0.000	0.000	0.000
23/05/06	21	0.000	0.000	0.000				0.000	0.000	0.000	0.000	0.000	0.000
30/05/06	21	0.000	0.000	0.000				0.000	0.000	0.000	0.000	0.000	0.000
01/06/06	21	3.657	2.035	0.574				0.925	0.494	0.109	2.191	1.209	0.265
06/06/06	21	1.041	1.041	1.041				1.041	1.041	1.041	1.041	1.041	1.041
09/06/06	21	0.000	0.000	0.000				0.000	0.000	0.000	0.000	0.000	0.000
18/06/06	21	2.591	2.644	2.644				2.398	2.644	2.644	2.268	2.418	2.644
01/05/07	55	1.179	0.634	0.000	0.623	0.000	0.000				1.283	0.691	0.000
03/06/07	54	0.068	0.068	0.068	0.068	0.068	0.068				0.068	0.068	0.068
05/06/07	55	0.160	0.090	0.000	0.116	0.000	0.000				0.205	0.105	0.000
09/06/07	55	0.000	0.000	0.000	0.000	0.000	0.000				0.000	0.000	0.000
15/07/07	54	1.555	0.864	0.122	0.585	0.068	0.068				1.436	0.789	0.068
19/07/07	55	1.628	0.894	0.191	0.612	0.191	0.191				1.523	0.834	0.191
23/07/07	55	2.184	1.221	0.123	0.732	0.707	0.000				1.897	1.061	0.000
31/07/07	55	1.762	0.964	0.231	0.647	0.202	0.202				1.626	0.891	0.202
18/08/07	53	0.757	0.401	0.154	0.581	0.154	0.154				1.069	0.556	0.154
01/09/07	55	0.841	0.773	0.742	0.742	0.742	0.742				0.756	0.771	0.742
14/10/07	55	0.000	0.000	0.000	0.000	0.000	0.000				0.000	0.000	0.000
03/06/08	65	0.397	0.127	0.127	0.173	0.263	0.263	0.139	0.191	0.263	0.105	0.100	0.263
04/06/08	65	2.080	1.160	0.165	0.721	0.094	0.000	0.798	0.199	0.000	1.817	1.016	0.000
13/06/08	66	1.263	1.263	1.263	1.263	1.263	1.263	1.263	1.263	1.263	1.263	1.263	1.263
02/07/08	67	2.223	1.117	0.384	0.385	0.402	0.533	0.447	0.382	0.533	0.694	0.891	0.499
05/07/08	65	0.062	0.062	0.062	0.062	0.062	0.062	0.062	0.062	0.062	0.062	0.062	0.062
22/07/08	67	1.238	0.663	0.300	0.333	0.281	0.280	0.380	0.295	0.280	0.960	0.509	0.273
06/08/08	67	0.267	0.149	0.000	0.169	0.000	0.000	0.174	0.000	0.000	0.334	0.169	0.000

Table I.7 (Continued).

Date	No. of station	Rain rate RMSE (mm/15 minutes)											
		Year 05 equation			Year 06 equation			Year 07 equation			Year 05-07 equation		
		Mode	Average	Ratio	Mode	Average	Ratio	Mode	Average	Ratio	Mode	Average	Ratio
19/08/08	67	1.309	0.730	0.000	0.444	0.000	0.000	0.496	0.087	0.000	1.159	0.642	0.000
22/08/08	67	0.000	0.000	0.000	0.000	0.000	0.000	0.000	0.000	0.000	0.000	0.000	0.000
06/09/08	67	2.644	2.542	2.511	2.502	2.511	2.511	2.506	2.513	2.511	2.609	2.533	2.511
29/09/08	67	0.086	0.086	0.086	0.086	0.086	0.086	0.086	0.086	0.086	0.086	0.086	0.086
03/10/08	66	0.000	0.000	0.000	0.000	0.000	0.000	0.000	0.000	0.000	0.000	0.000	0.000
11/10/08	68	4.567	3.929	3.625	3.615	3.605	3.596	3.645	3.616	3.596	3.888	3.690	3.603
19/10/08	67	3.649	2.327	1.669	1.684	1.684	1.674	1.741	1.659	1.674	2.405	1.827	1.644
26/10/08	61	1.468	1.442	1.857	1.570	1.957	1.965	1.527	1.832	1.965	1.351	1.475	1.965
Average error		1.172	0.825	0.545	0.681	0.526	0.525	0.801	0.744	0.728	0.973	0.748	0.532

Table I.8 After 15 minutes received APT data, rain rate RMSE data from the models of the years 2005, 2006, 2007, and 2005-2007

which assumes that rain rate < 0.5 is equal to 0 mm.

Date	No. of station	Rain rate RMSE (mm/15 minutes)											
		Year 05 equation			Year 06 equation			Year 07 equation			Year 05-07 equation		
		Mode	Average	Ratio	Mode	Average	Ratio	Mode	Average	Ratio	Mode	Average	Ratio
15/05/06	21	0.000	0.000	0.000				0.000	0.000	0.000	0.000	0.000	0.000
23/05/06	21	0.000	0.000	0.000				0.000	0.000	0.000	0.000	0.000	0.000
30/05/06	21	0.000	0.000	0.000				0.000	0.000	0.000	0.000	0.000	0.000
01/06/06	21	4.158	2.324	0.681				1.030	0.569	0.000	2.408	0.857	0.302
06/06/06	21	1.041	1.041	1.041				1.041	1.041	1.041	1.041	1.041	1.041
09/06/06	21	0.000	0.000	0.000				0.000	0.000	0.000	0.000	0.000	0.000
18/06/06	21	2.880	2.901	2.901				2.685	2.901	2.901	2.597	2.853	2.901
01/05/07	55	1.330	0.734	0.106	0.593	0.000	0.000				1.173	0.629	0.000
03/06/07	54	0.068	0.068	0.068	0.068	0.068	0.068				0.068	0.068	0.068
05/06/07	55	0.182	0.091	0.000	0.089	0.000	0.000				0.232	0.105	0.000
09/06/07	55	0.000	0.000	0.000	0.000	0.000	0.000				0.000	0.000	0.000
15/07/07	54	1.354	0.751	0.068	0.540	0.068	0.068				1.287	0.707	0.068
19/07/07	55	1.541	0.853	0.213	0.595	0.213	0.213				1.453	0.795	0.213
23/07/07	55	2.112	1.181	0.118	0.726	0.068	0.000				1.865	1.043	0.000
31/07/07	55	1.503	0.817	0.165	0.642	0.165	0.165				1.506	0.826	0.165
18/08/07	53	0.817	0.393	0.182	0.583	0.182	0.182				1.101	0.597	0.182
01/09/07	55	1.001	0.734	0.591	0.650	0.588	0.584				0.904	0.693	0.584
14/10/07	55	0.000	0.000	0.000	0.000	0.000	0.000				0.000	0.000	0.000
03/06/08	65	0.240	0.240	0.240	0.240	0.240	0.240	0.240	0.240	0.240	0.240	0.240	0.240
04/06/08	65	2.346	1.310	0.250	0.741	0.148	0.000	0.834	0.284	0.000	1.935	1.082	0.067
13/06/08	66	1.121	1.121	1.121	1.121	1.121	1.121	1.121	1.121	1.121	1.121	1.121	1.121
02/07/08	67	2.298	1.233	0.318	0.338	0.316	0.247	0.475	0.253	0.220	1.219	0.637	0.200
05/07/08	65	0.381	0.381	0.381	0.381	0.381	0.381	0.381	0.381	0.381	0.381	0.381	0.381
22/07/08	67	1.126	0.547	0.277	0.157	0.287	0.299	0.213	0.268	0.299	0.828	0.360	0.293
06/08/08	67	0.176	0.083	0.000	0.145	0.000	0.000	0.146	0.000	0.000	0.264	0.096	0.000

Table I.8 (Continued).

Date	No. of station	Rain rate RMSE (mm/15 minutes)											
		Year 05 equation			Year 06 equation			Year 07 equation			Year 05-07 equation		
		Mode	Average	Ratio	Mode	Average	Ratio	Mode	Average	Ratio	Mode	Average	Ratio
19/08/08	67	1.405	0.784	0.000	0.501	0.000	0.000	0.551	0.088	0.000	1.267	0.709	0.000
22/08/08	67	0.000	0.000	0.000	0.000	0.000	0.000	0.000	0.000	0.000	0.000	0.000	0.000
06/09/08	67	1.620	1.736	1.997	1.799	1.997	1.997	1.785	1.997	1.997	1.655	1.753	1.997
29/09/08	67	0.086	0.086	0.086	0.086	0.086	0.086	0.086	0.086	0.086	0.086	0.086	0.086
03/10/08	66	0.062	0.062	0.062	0.062	0.062	0.062	0.062	0.062	0.062	0.062	0.062	0.062
11/10/08	68	3.214	2.588	2.276	2.291	2.255	2.246	2.321	2.267	2.246	2.599	2.361	2.251
19/10/08	67	2.757	2.173	2.270	2.211	2.314	2.425	2.179	2.289	2.425	2.269	2.145	2.356
26/10/08	61	1.128	1.038	1.206	1.048	1.231	1.282	1.028	1.209	1.282	1.110	1.042	1.282
Average error		1.089	0.766	0.504	0.600	0.453	0.449	0.735	0.684	0.650	0.929	0.675	0.481

APPENDIX J

VALIDATION RESULTS

Table J.1 Comparison of raining condition errors between the actual rain rates estimated from the models and when measurement ability of rain gauge is involved.

Model	Time interval type	Raining condition error (%)	
		With rain rate estimation from models	With rain rate estimation ≥ 0.5 mm, from models
2005	Mode	35.569	31.832
	Average	35.569	29.743
	Ratio	35.569	13.945
2006	Mode	39.285	36.490
	Average	39.285	12.369
	Ratio	39.285	11.270
2007	Mode	26.757	24.625
	Average	26.757	18.462
	Ratio	26.757	15.135
2005-2007	Mode	35.569	32.914
	Average	35.569	30.842
	Ratio	35.569	12.301

Table J.2 Comparison of raining condition errors when wind and without wind are considered.

Model	Raining condition error (%)	
	With out wind	With wind
2005	35.569	35.176
2006	39.285	38.602
2007	26.757	26.434
2005-2007	35.569	35.176

Table J.3 Comparison of raining condition errors when wind and measurement ability of rain gauge are considered simultaneously.

Model	Time interval type	Raining condition error (%)	
		With out wind	With wind
2005	Mode	31.832	32.035
	Average	29.743	29.700
	Ratio	13.945	14.428
2006	Mode	36.490	35.847
	Average	12.369	12.587
	Ratio	11.270	11.932
2007	Mode	24.625	24.152
	Average	18.462	19.305
	Ratio	15.135	15.158
2005-2007	Mode	32.914	31.232
	Average	30.842	28.276
	Ratio	12.301	12.471

Table J.4 Comparison of rain rate RMSEs with and without measurement ability of rain gauge involved.

Model	Time interval type	Rain rate RMSE (mm/15 minutes)	
		With rain rate estimation from models	With rain rate estimation ≥ 0.5 mm, from models
2005	Mode	1.165	1.172
	Average	0.821	0.825
	Ratio	0.576	0.545
2006	Mode	0.676	0.681
	Average	0.591	0.526
	Ratio	0.535	0.525
2007	Mode	0.798	0.801
	Average	0.750	0.744
	Ratio	0.728	0.728
2005-2007	Mode	0.971	0.973
	Average	0.747	0.748
	Ratio	0.567	0.532

Table J.5 Comparison of rain rate RMSEs when wind and without wind are considered.

Model	Time interval type	Rain rate RMSE (mm/15 minutes)	
		With out wind	With wind
2005	Mode	1.165	1.084
	Average	0.821	0.764
	Ratio	0.576	0.528
2006	Mode	0.676	0.602
	Average	0.591	0.515
	Ratio	0.535	0.458
2007	Mode	0.798	0.737
	Average	0.750	0.680
	Ratio	0.728	0.655
2005-2007	Mode	0.971	0.930
	Average	0.747	0.688
	Ratio	0.567	0.511

Table J.6 Comparison of rain rate RMSEs when wind, and measurement ability of rain gauge are considered simultaneously.

Model	Time interval type	Rain rate RMSE (mm/15 minutes)	
		With out wind	With wind
2005	Mode	1.172	1.089
	Average	0.825	0.766
	Ratio	0.545	0.504
2006	Mode	0.681	0.600
	Average	0.526	0.453
	Ratio	0.525	0.449
2007	Mode	0.801	0.735
	Average	0.744	0.684
	Ratio	0.728	0.650
2005-2007	Mode	0.973	0.929
	Average	0.748	0.675
	Ratio	0.532	0.481

APPENDIX K

EXAMPLES OF APT IMAGE AND THEIR

ANALYTICAL RESULTS

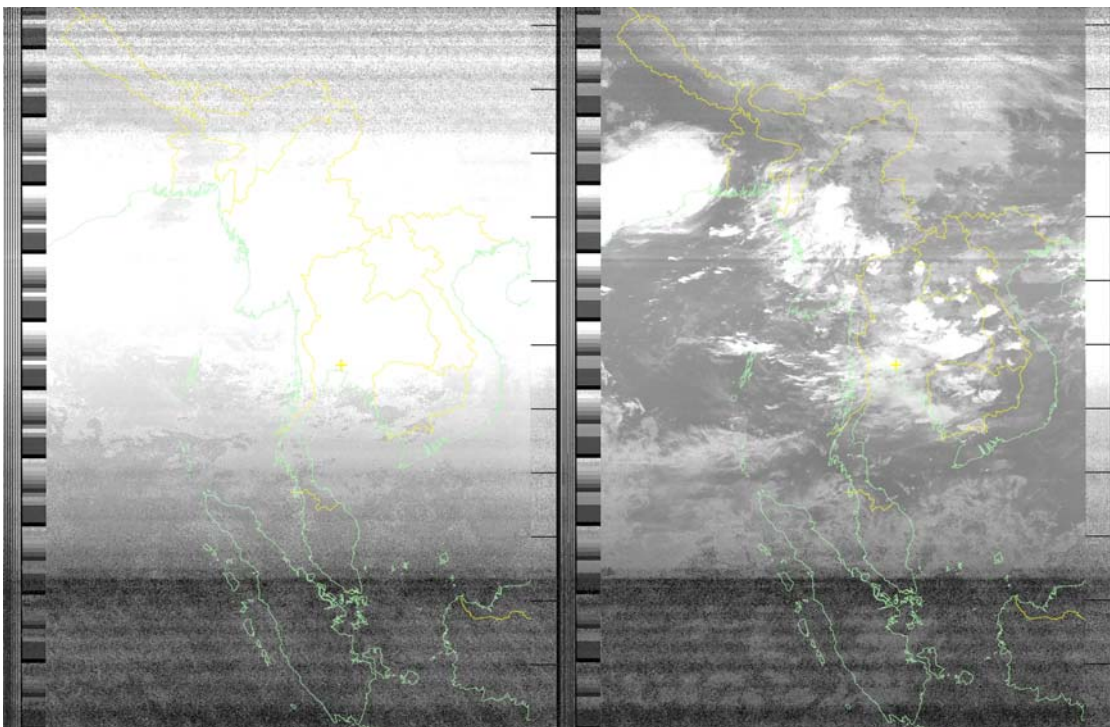


Figure K.1 APT image of NOAA 17, date 03/06/2008, 22:07 form APT receiving system.

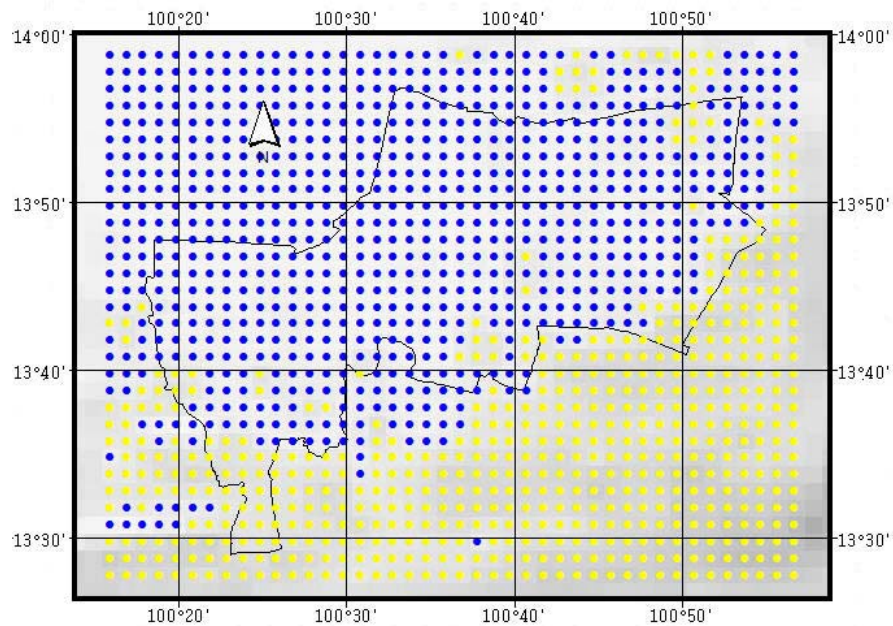


Figure K.2 Grid point data result from APT image, date 03/06/2008 showing raining (yellow) and no-raining (blue).

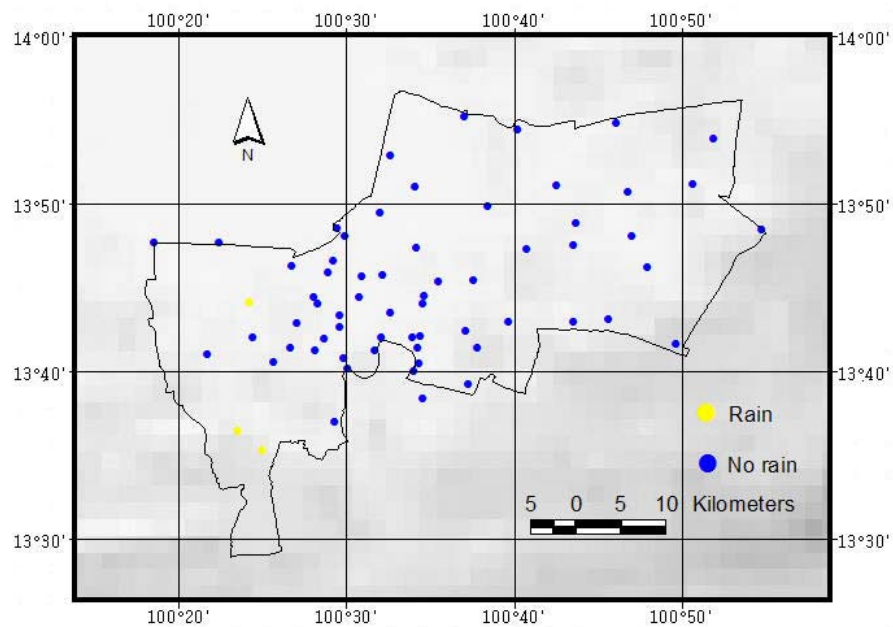


Figure K.3 Rainfall measurement stations showing raining on 03/06/2008, 22:00.

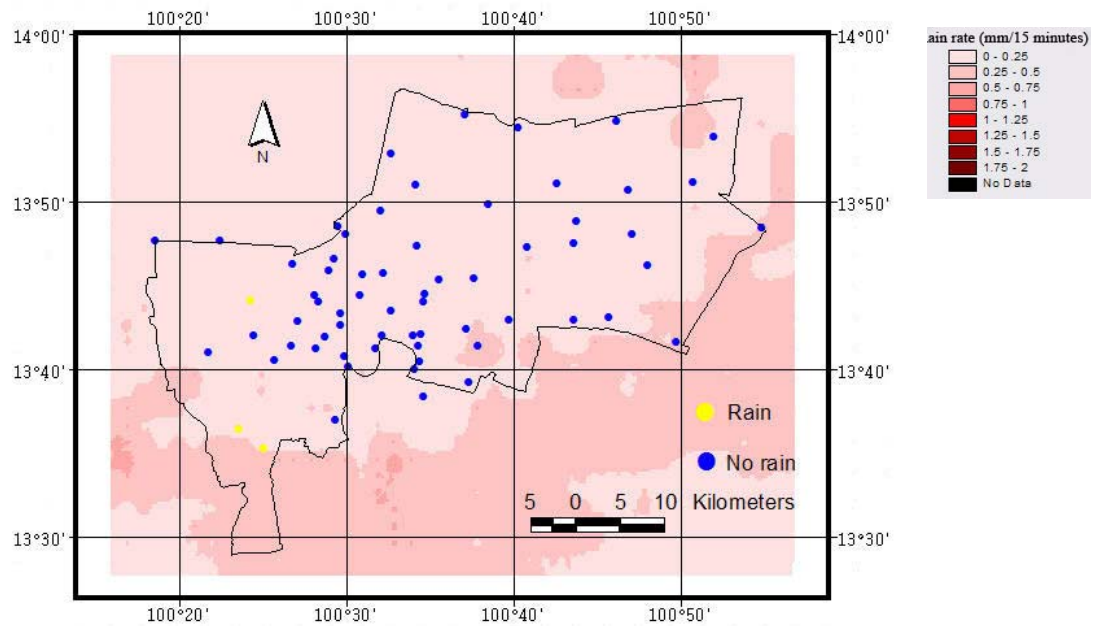


Figure K.4 Near-real time rainfall estimated result from APT image, date 03/06/2008.

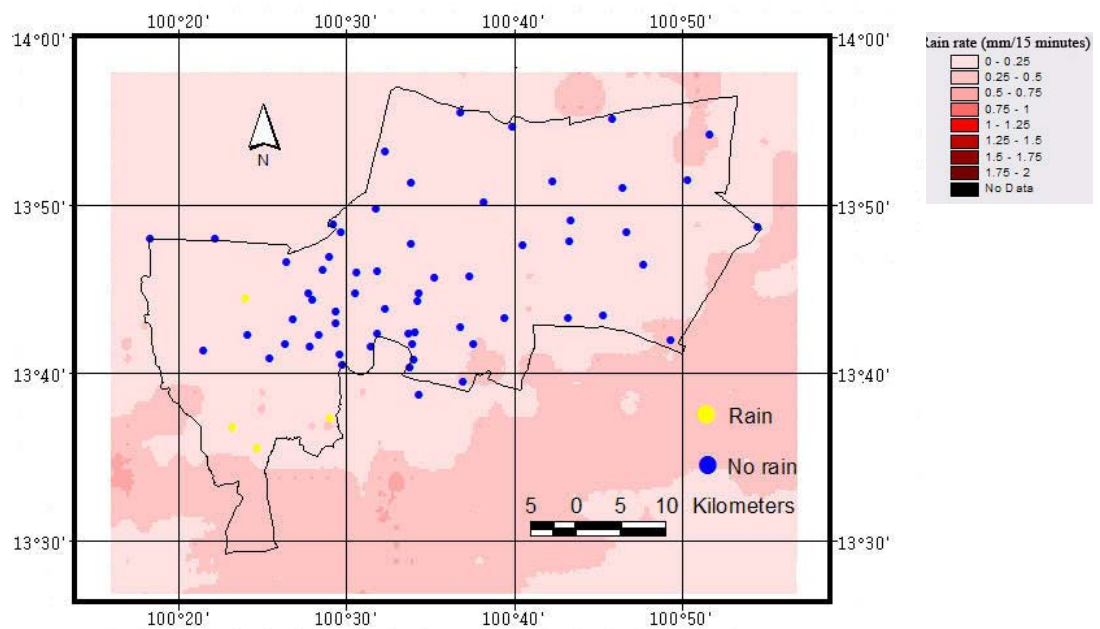


Figure K.5 After 15 minutes received, rainfall estimated result from APT image, date 03/06/2008.

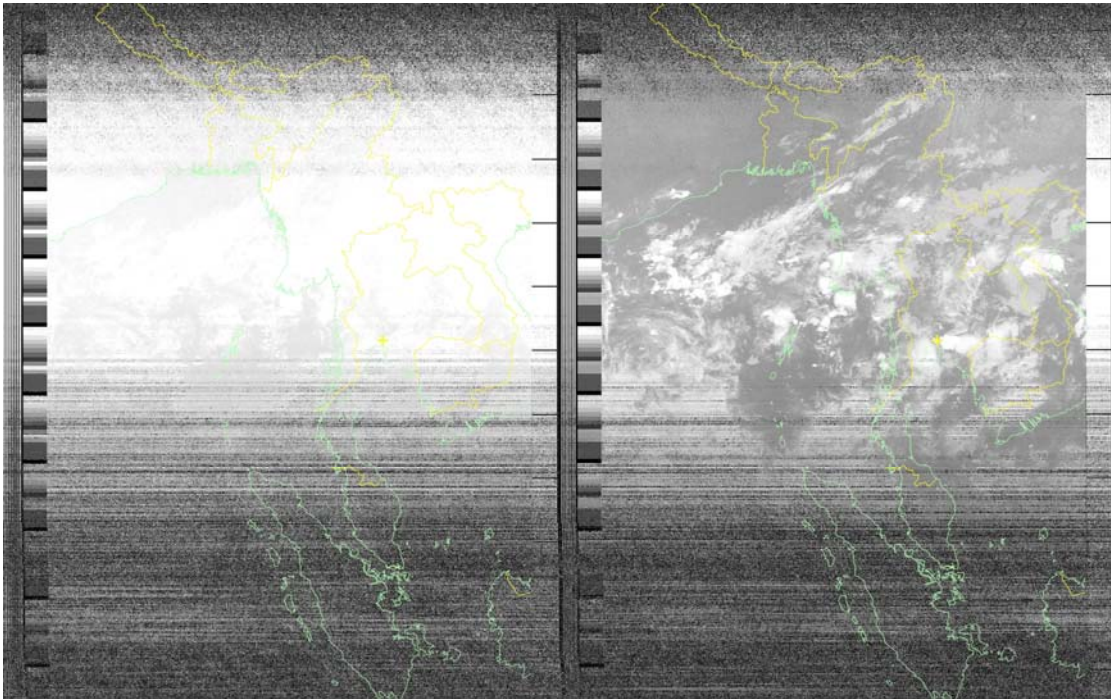


Figure K.6 APT image of NOAA 17, date 19/10/2008, 22:08 form APT receiving system.

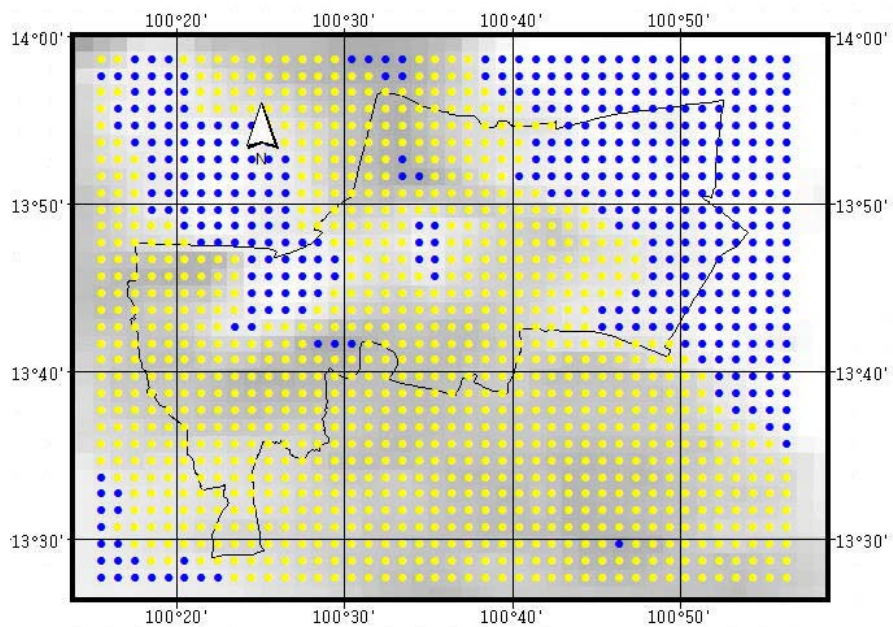


Figure K.7 Grid point data result from APT image, date 19/10/2008 showing raining (yellow) and no-raining (blue).

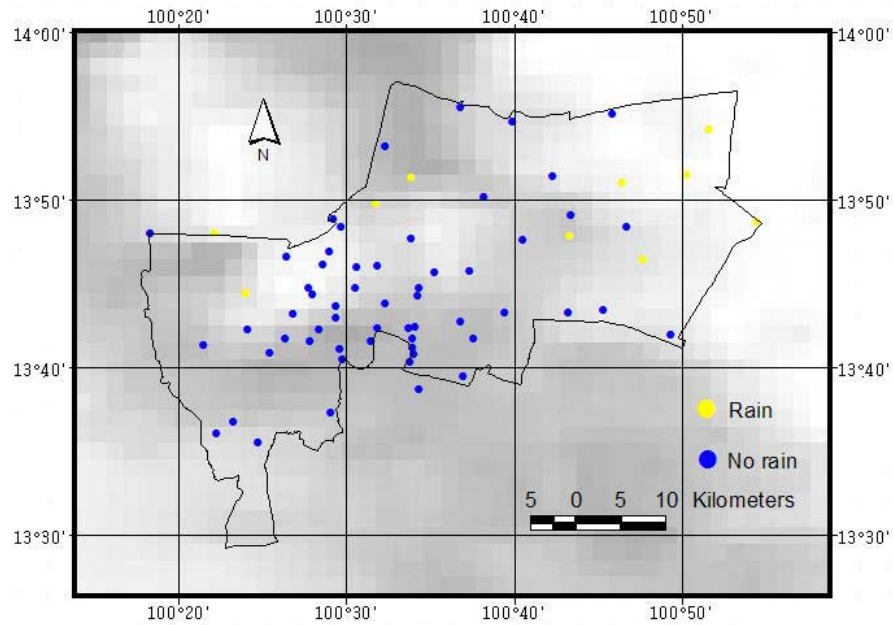


Figure K.8 Rainfall measurement stations showing raining on 19/10/2008, 22:00.

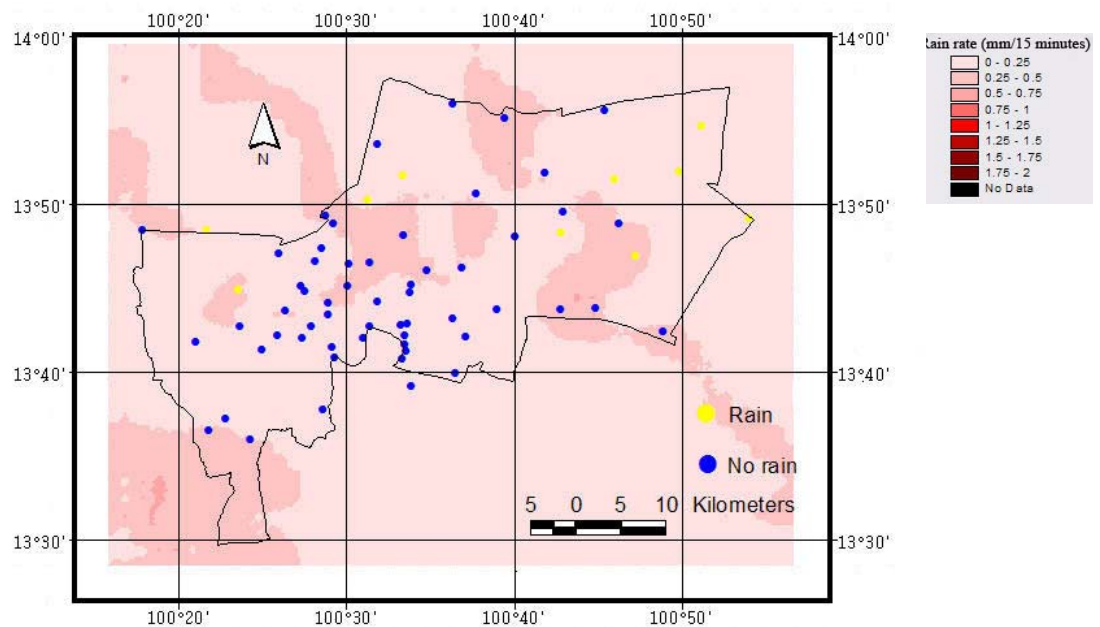


Figure K.9 Near-real time rainfall estimated result from APT image, date 19/10/2008.

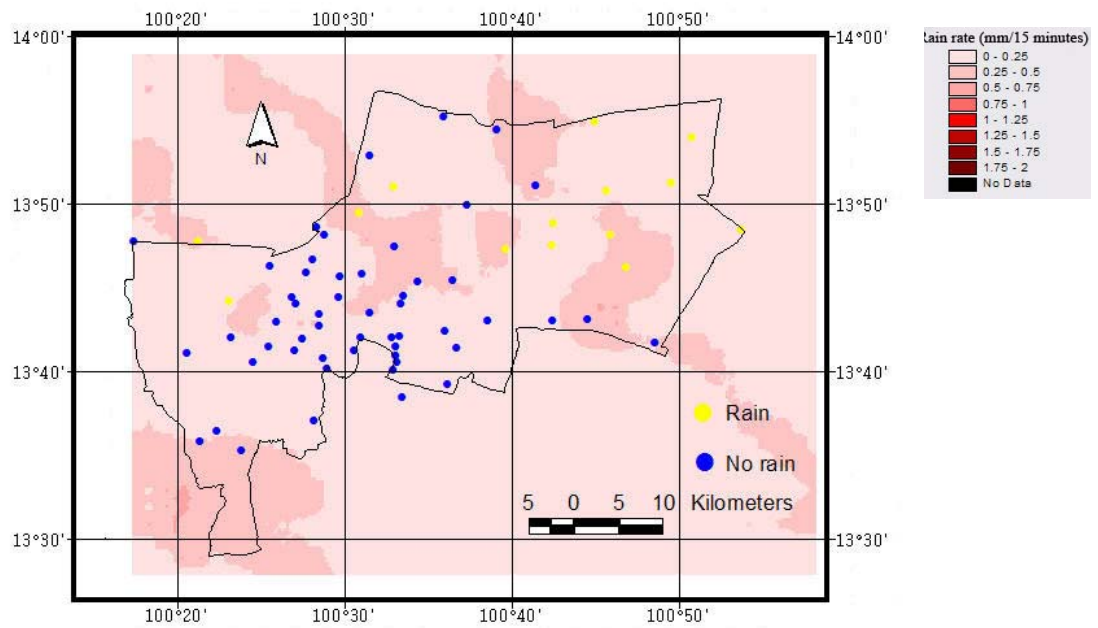


Figure K.10 After 15 minutes received, rainfall estimated result from APT image, date 19/10/2008.

APPENDIX L

LIST OF 71 STATIONS OF DEPARTMENT OF DRAINAGE AND SEWERAGE IN BANGKOK

Table L.1 The position of 71 stations of Department of Drainage and Sewerage, Bangkok Metropolitan.

Station code	Station name	Latitude	Longitude
E00	Flood Control Center	13° 46' 06.66" N	100° 33' 31.72" E
E01	WG. K. Song	13° 35' 32.61" N	100° 38' 27.03" E
E02	WG. K. Phraya Surane	13° 55' 45.31" N	100° 41' 35.37" E
E03	WG. K. Samwa	13° 51' 26.27" N	100° 43' 56.71" E
E04	HS. K. Bang Bua	13° 51' 20.59" N	100° 35' 31.06" E
E05	WG. K. Ta Oot	13° 51' 12.39" N	100° 34' 00.07" E
E06	HS. K. Lumchala	13° 50' 14.75" N	100° 39' 51.39" E
E07	WG. K. Pracha Ruamjai	13° 49' 09.77" N	100° 45' 04.30" E
E08	PS. K. Bang Khen Mai	13° 48' 53.65" N	100° 30' 49.64" E
E09	WG. K. Bueng Khwang	13° 47' 52.36" N	100° 44' 59.06" E
E10	PS. K. Bang Sue	13° 48' 27.44" N	100° 31' 17.78" E
E11	WG. K. San Saeb-Bang Chan	13° 47' 37.59" N	100° 42' 11.79" E
E12	WG. K. Lat Phrao	13° 47' 43.52" N	100° 35' 32.25" E
E13	PS. K. Sam Sen	13° 46' 58.20" N	100° 30' 35.58" E
E14	HS. K. Chao Khun Sing	13° 45' 41.00" N	100° 36' 55.00" E
E15	PS. K. Thavate	13° 46' 12.76" N	100° 30' 15.31" E
E16	HS. Anusawarichai	13° 46' 00.62" N	100° 32' 16.77" E
E17	HS. Khet Bangkok	13° 45' 46.62" N	100° 38' 59.55" E
E18	PS. K. Samsen-Soonvijai	13° 44' 49.22" N	100° 36' 01.03" E
E19	PS. K. Saen Saep-Klong Ton	13° 44' 21.60" N	100° 35' 55.85" E
E20	PS. K. Krung Kasem	13° 43' 42.78" N	100° 31' 00.96" E
E21	WG. Lat Krabang	13° 43' 19.36" N	100° 44' 56.36" E
E22	WG. Wat Kratum Sua Pla	13° 43' 19.33" N	100° 41' 06.68" E
E23	PS. K. Sathorn	13° 43' 00.47" N	100° 31' 00.69" E

Table L.1 (Continued).

Station code	Station name	Latitude	Longitude
E24	HS. Wat Kachornsiri	13° 42' 44.58" N	100° 38' 29.98" E
E25	PS. RAMA 4	13° 42' 20.49" N	100° 33' 30.23" E
E26	PS. K. Phrakanong	13° 42' 26.13" N	100° 35' 46.75" E
E27	PS. K. Toei	13° 42' 21.42" N	100° 35' 20.08" E
E28	PS. K. Jek	13° 41' 47.14" N	100° 35' 36.50" E
E29	PS. K. Wat Sai	13° 41' 06.49" N	100° 31' 13.27" E
E30	PS. K. Bang Oa	13° 40' 50.16" N	100° 35' 41.10" E
E31	PS. K. Bang Na	13° 40' 22.60" N	100° 35' 25.94" E
E32	HS. K. Bang Na-Srinakarin	13° 39' 32.52" N	100° 38' 38.63" E
E33	PS. K. Sam Rong	13° 38' 44.76" N	100° 35' 58.56" E
E34	WG. K. San Saeb-Nong Chok	13° 51' 17.00" N	100° 25' 18.00" E
E35	PS. K. Chong Non See	13° 41' 03.00" N	100° 31' 08.00" E
E36	PS. K. Bang Chark	13° 41' 35.00" N	100° 33' 07.00" E
E37	WG. K. Wat Darn	13° 41' 15.00" N	100° 35' 37.00" E
E38	PS. Ratchada-Wipawadee	13° 49' 48.72" N	100° 33' 25.20" E
E39	WG. K. Orachorn	13° 44' 45.24" N	100° 32' 08.88" E
E40	HS. Suan Benchasiri	13° 43' 49.08" N	100° 33' 59.76" E
E41	HS. K. Kao-Watsrisuksathaporn	13° 55' 12.72" N	100° 47' 33.00" E
E42	HS. K. Sibsong-Phachasamran Rd.	13° 54' 15.12" N	100° 53' 20.40" E
E43	WG. K. Sibsam	13° 51' 32.04" N	100° 52' 04.08" E
E44	HS. K. Sansab-Wat Sub Samosorn Nikorn	13° 51' 04.32" N	100° 48' 10.78" E
E45	WG. K. Luang Pang	13° 48' 46.78" N	100° 56' 14.64" E
E46	HS. K. Bung Yai-Wat Thong Sum Rit	13° 48' 25.92" N	100° 48' 25.56" E
E47	HS. K. Lum Puk She-Lum Puk She School	13° 46' 46.20" N	100° 49' 22.44" E
E48	HS. K. Pravet Bureerom-Khet Ladkrabang	13° 43' 26.04" N	100° 47' 02.04" E
E49	HS. K. Pravet Bureerom-Wat Rajkosa	13° 42' 00.36" N	100° 51' 04.32" E
E50	WG. K. Bung Born-Bung Born Station	13° 41' 43.44" N	100° 39' 12.60" E
W01	WG. K. Thawi Watthana	13° 48' 02.12" N	100° 19' 53.24" E
W02	WG. K. Buac	13° 48' 02.45" N	100° 23' 46.37" E
W03	PS. K. Chuck Phrac	13° 46' 37.95" N	100° 28' 05.61" E
W04	PS. K. Mon	13° 44' 45.20" N	100° 29' 24.81" E
W05	HS. K. Bang Chuak Nang	13° 44' 30.26" N	100° 25' 39.98" E
W06	PS. K. BangkokYai	13° 44' 22.34" N	100° 29' 37.98" E

Table L.1 (Continued).

Station code	Station name	Latitude	Longitude
W07	WG. K. Phasi Charoen	13° 43' 14.44" N	100° 28' 24.31" E
W08	HS. Wat Nimmarn Norradee	13° 42' 20.04" N	100° 25' 45.85" E
W09	PS. K. Sam Rae	13° 42' 16.90" N	100° 30' 02.25" E
W10	HS. K. Sanamchai	13° 41' 46.71" N	100° 28' 00.46" E
W11	PS. K. Dao Khanong	13° 41' 34.78" N	100° 29' 30.26" E
W12	HS. K Thawee-Phasi Charoen	13° 41' 24.00" N	100° 23' 04.06" E
W13	PS. K. See Bath	13° 40' 53.70" N	100° 27' 02.57" E
W14	PS. K. Chaeng Ron	13° 40' 28.98" N	100° 31' 26.34" E
W15	WG. K. Rang Chark	13° 37' 20.50" N	100° 30' 41.87" E
W16	PS. K. Laen Paen	13° 36' 46.98" N	100° 24' 55.05" E
W17	PS. K. Raharn	13° 36' 06.41" N	100° 23' 52.13" E
W18	PS. K. Praya Ratchamontri	13° 37' 35.00" N	100° 26' 23.00" E
W19	PS. K. Bang Yee Khan	13° 45' 54.00" N	100° 29' 51.00" E
W20	PS. K. Bang Sai Kai	13° 42' 18.00" N	100° 30' 02.00" E

Source: Department of Drainage and Sewerage, Bangkok Metropolitan

Where: K is Klong

HS is Water Height Measurement Station

PS is Water Pump Station

WG is Water Gate

APPENDIX M

FM RECEIVER



Figure M.1 FM receiver kits.

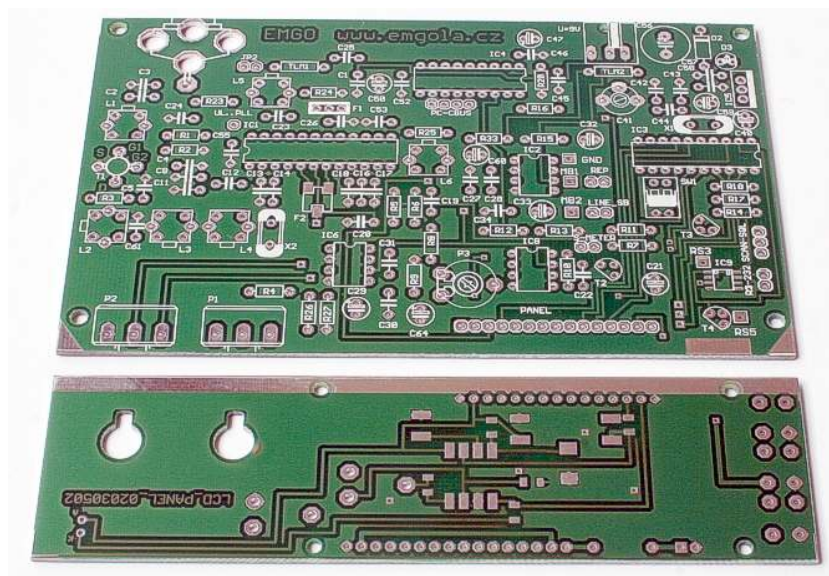


Figure M.2 FM receiver print circuit board kits.

RX137-141-567 - LIST OF THE ASSEMBLING COMPONENTS (06.03.2004)
Resistors, Trimmers and Potenciometers

Value	Position	Type	Quantity
2R2	R20		1
47R	R3		1
120R	R10 (assembly only when is Backlight LCD displ.)	For display with Backlight LED	0
120R	R26		1
180R	R14		1
1K	R28		1
2K2	R21, R23, R29		3
3K3	R8, R9		2
3K3	R11	22K when IC4= Philips!, otherwise R11=3K3	1 (0)
4K7	R18		1
8K2	R24		1
10K	R16	SMD 1206	1
10K	R5, R7, R19, R22		4
10K	R25 (setting of PLL 2400 Hz - LED display)	trimmer PIHER PT6VK100	1
15K	R17		1
22K	R4, (R11)	22K when IC4= Philips!, otherwise R11=3K3	1 (2)
39K	R6		1
47K	R12, R13		2
100K	R1, R2,		2
100K	P3 (adjust the display contrast)	trimmer PIHER PT6VK100	1
120K	R27		1
180K	R15	SMD 1206	1
5M1	R30 (assembly only alternatively)	SMD 1206	0
50K	P2	potentiometr TP160/G-spindle 4mm	1
100K	P1	potentiometr TP160/N-spindle 4mm	1

Capacitors

Value	Position	Type	Quantity
1 pF	C6, C7, C9, C10	SMD 1206	4
3,5-22 pF	C21	trimmer Philips	1
5,6 pF	C2, C5	ceramic	2
8,2 pF	C8, C12, C33	ceramic	3
12 pF	C58	SMD 1206	1
27 pF	C22	ceramic (22-47pF)	1
33 pF	C3, C11, C23, C24	ceramic (27-33pF)	4
47 pF	C14	ceramic	1
47 pF	C19 (assembly only alternatively if in L6 no capacitors)	ceramic	1
150 pF	C13	ceramic	1
2,2 nF	C25	foil WIMA spacing 5mm	1
4,7 nF	C37, C42	foil WIMA spacing 5mm	2
10 nF	C26, C49	foil WIMA spacing 5mm	2
10 nF	C35	ceramic	1
33 nF	C55	foil WIMA spacing 5mm	1
47 nF	C4, C30, C32, C36, C39	ceramic	5
47 nF	C38	foil WIMA spacing 5mm	1
100 nF	C1, C15, C16, C17, C18, C34, C43, C44, C47	ceramic	9
100 nF	C28, C56	SMD 1206	2
100 nF	C57 (no-assembly, only alternatively)	SMD 1206	0
100 nF	C61 (assembly only alternatively)	SMD 1206	0
100 nF	C51	foil WIMA spacing 5mm	1
330-470 nF	C50	foil WIMA spacing 5mm	1
470 nF	C31 (no-assembly, only alternatively)	SMD 1206	0
1 uF	C20	radial electrolytic capacitor 16V	1

Figure M.3 List of FM receiver assembling components.

4,7 uF	C54	radial electrolytic capacitor 16V	1
10 uF	C41, C45, C52, C53	radial electrolytic capacitor 16V	4
47 uF	C27, C29	radial electrolytic capacitor 16V	2
100 uF	C46	radial electrolytic capacitor 10V	1
100 uF	C40, C59	radial electrolytic capacitor 16V	2
100 uF	C60 (assembly as far as up termination setting RX)	radial electrolytic capacitor 16V	1
1000 uF	C48	radial electrolytic capacitor 16-25V	1

Notes: Foil capacitors WIMA spacing outlet 5mm

Integrated Circuits ...

Value	Position	Type	Quantity
MC3362P	IC1	DIL22-RX FM 2x MF	1
LM386	IC2, IC6	DIP8-LF amplifier	2
AT89C2051	IC3	DIL20-With program RX137141LCD_DIP4	1
SAA1057	IC4	DIL18-PLL up to 160 MHz	1
LM7805	IC5	Stabiliser +5V	1
LM567	IC7	DIP8-Tone decoder IC7	1
BF982	T1	2 GATE MOS FET (BF981)	1
BC547	T2, T3	NPN universal TO-92	2
LED 3mm	D1	Any LED diode, red colours	1
1N4001-7	D2	Rectifier diode	1
LCD display	Single line display LCD1	CM1610 and equivalent	1

Coils

Value	Position	Type	Quantity
100nH	L1, L2, L3, L4, L5	7x7mm - 0,5 mm above surface PCB	5
L455kHz	L6	7x7mm - 0,5 mm above surface PCB	1
1uH	TI1, TI2	Chooke Axial 7,5mm	2

Others

Value	Position	Type	Quantity
4,000 MHz	Quartz X1	asembling 1 mm above surface PCB	1
10,245 MHz	Quartz X2	asembling 1 mm above surface PCB	1
10,7MHz	F1	Ceramic filter muRata	1
455kHz	F2	Ceramic filter muRata	1
Up	TI1	Push button	1
Down	TI2	Push button	1
Jumper	JP1 (napájení předzesilovače)	2 pin	1
Jumper	JP2 (propojení desek DPS1 + DPS2)	11 pin /úhel 90 stupňů	1
Jumper	JP3 (Volba squelch/scan 2400 Hz)	3 pin	1
Jumper	LCD connect (connecting DPS2+LCD displej)	16 pin	1
Patice 20	Integrated circuit socket DIL 20 (AT89C2051)		1
Patice 18	Integrated circuit socket DIL 18 (SAA1057)		1
Lines-SB	Output on Sound Blaster		1
REP_jmp	Output on loudspeaker		1
REP_cinch	Output on loudspeaker	(assembly only alternatively)	1
REP	Loudspeaker 8 - 25 Ohm		0
U=12V	Power supply socked+plug 12V-2,5mm	To be connected to the adapter's cable (observe the polarity)	1
BNC-F	BNC connector - female		1
Dist_08	Distance column RX motherboard		4
Nut	Nut M3x5 Fe/Cd		4
SW1	Switch DIP 4x	at the position DIP1	1
Button	For the shaft 4mm	plast	2
DPS1	Printed circuit RX motherboard 138x84mm	PCB - material FR4/1,6mm	1
DPS2	Printed circuit Display 138x37mm	PCB - material FR4/1,6mm	1

Figure M.3 (Continued).

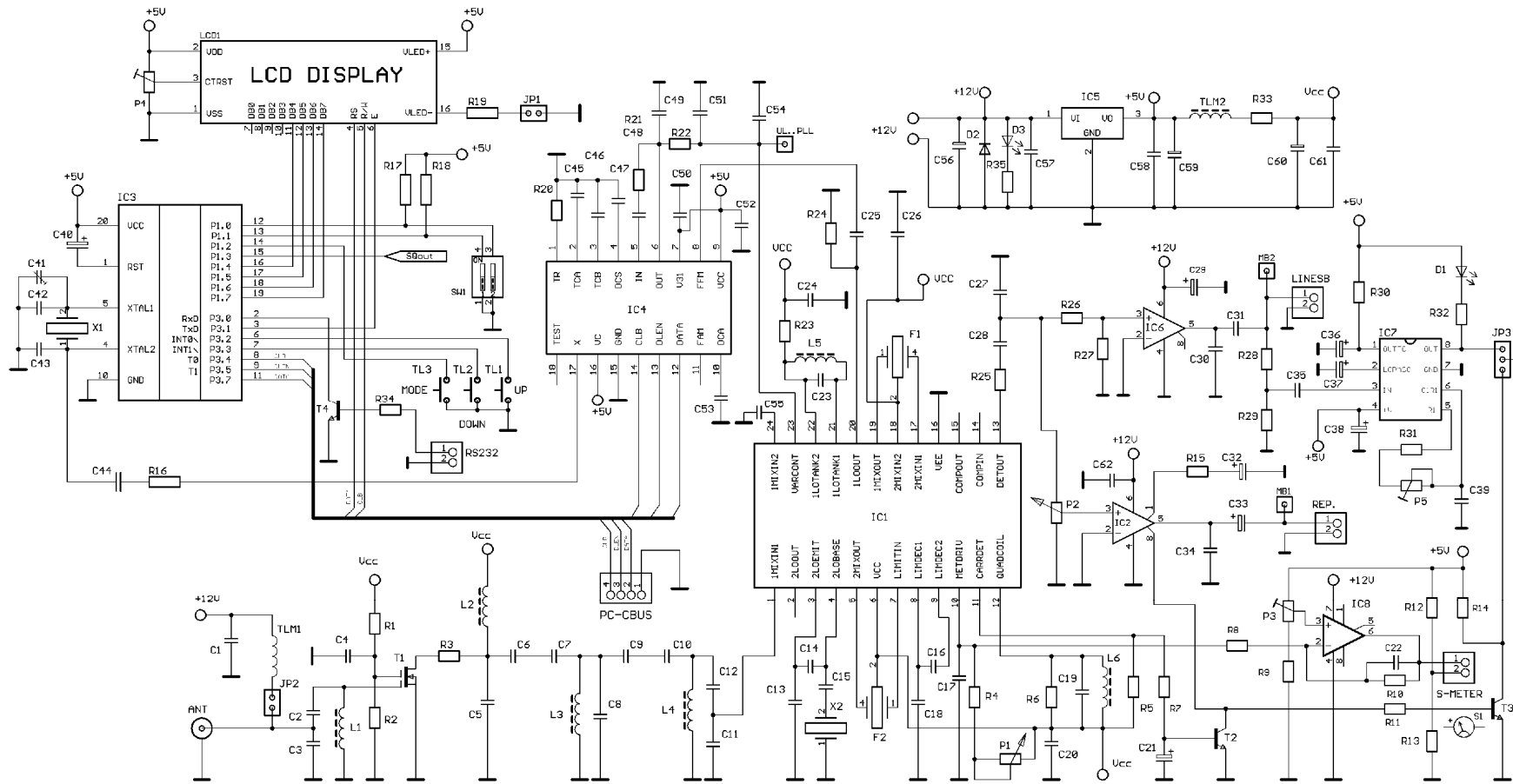


Figure M.4 FM receiver schematic.

FM Receiver For 134-137 - 141MHz

A double conversion superhetrodyne with pll
(8 interface WXtoIMG · RS/232)

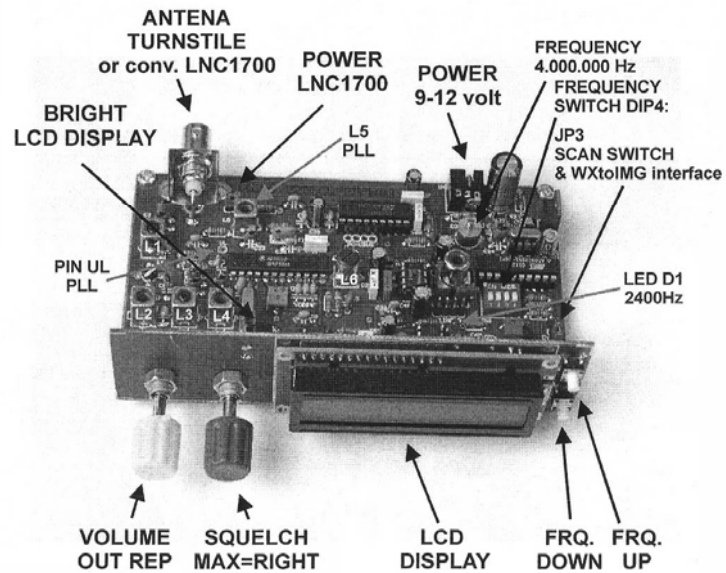


Figure M.6 FM receiver connecting and control button layout.

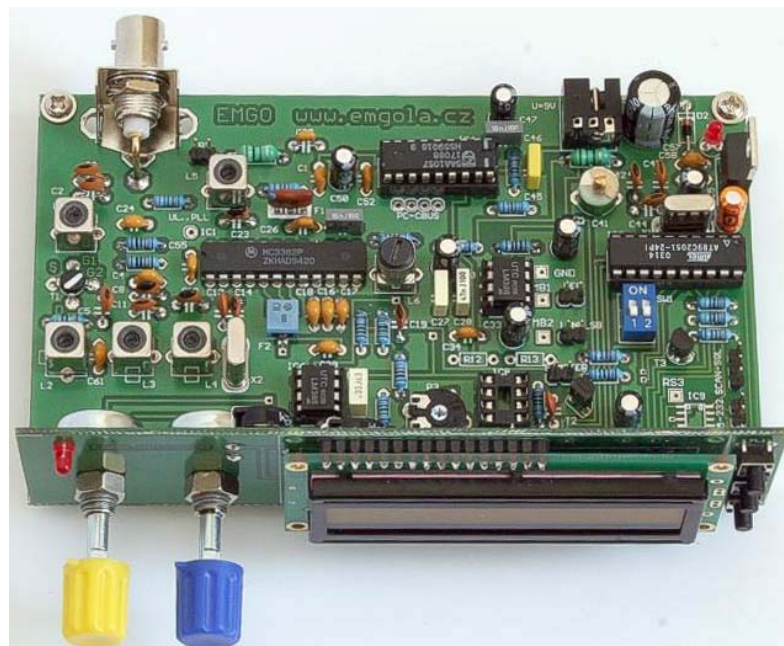


Figure M.7 FM receiver assembled.

CURRICULUM VITAE

Name : Chonmapat Torasa (Mr.)

Date of Birth : March 16, 1970

Place of Birth : Saraburi, Thailand

Education Background :

1990-1994

B. Tech. Ed. (Electrical Engineering)

King Mongkut's Institute of Technology North Bangkok, Bangkok,
Thailand

1995-2000

M.S. Tech. Ed. (Electrical Technology)

King Mongkut's Institute of Technology North Bangkok, Bangkok,
Thailand

Conference : APT Signal Receiving System Construction and Data Reformat
Process, Annual National Conference on Mapping and Geoinformatics,
28 November-1 December 2007, Ambassder Hotel, Bangkok,
Thailand.

Journal : APT Signal Receiving System Construction and Data Reformat
Process, Journal of Remote Sensing and GIS Association of Thailand
(RESGAT) 2007 Vol. 8 No. 3